



Norwegian University of  
Science and Technology

# Reliability Assessment of Long Span Suspension Bridges Subjected to Dead Loads

**Kristin Antonsen**

Civil and Environmental Engineering

Submission date: June 2016

Supervisor: Ole Andre Øiseth, KT

Co-supervisor: Øyvind Wiig Petersen, KT  
Aksel Fenerci, KT

Norwegian University of Science and Technology  
Department of Structural Engineering



## **MASTEROPPGAVE 2016**

for

*Kristin Antonsen*

### **Vurdering av sikkerhetsnivået til lange hengebruer utsatt for egenlast**

*Reliability assessment of long span suspension bridges subjected to dead loads*

I forbindelse med prosjektet ferjefri E39 planlegges det en rekke grensesprengende brokonstruksjoner. I dimensjonering av alle typer konstruksjoner benyttes partialkoeffisienter i kapasitetskontrollene for å ta hensyn i usikkerhetene til lastene og til materialegenskapene. Partialkoeffisientene har blitt kalibrert slik at et tilfredsstillende sikkerhetsnivå oppnås, men det er usikkert i hvilken grad denne kalibreringen vil gi et hensiktsmessig sikkerhetsnivå for veldig store konstruksjoner der egenlasten er en dominerende lastvirkning. Denne oppgaven dreier seg om beregning av påliteligheten til lange hengebruer utsatt for egenlast.

Opgaven bør inneholde følgende temaer:

- Grunnleggende metoder for beregning av konstruksjonspålitelighet
- Analyse av variasjon av de ulike komponentene i egenlastene til en hengebru.
- Beregning av sviktsannsynligheten til Hardangerbrua.
- Grundig analyse av usikkerheter.

Studentene velger selv hva de ønsker å legge vekt på

Besvarelsen organiseres i henhold til gjeldende retningslinjer.

*Veileder(e)*: Ole Andre Øiseth, Øyvind Wiig Petersen, Aksel Fenerci,

NTNU, 24.01.2015

Ole Andre Øiseth  
faglærer



# Preface

This master thesis completes the M.Sc. degree at the Department of Structural Engineering at the Norwegian University of Science and Technology (NTNU). The thesis has been carried out during the spring 2016. Supervisors have been Ole Andre Øiseth, Øyvind Wiig Petersen and Aksel Fenerci.

My motivation for this thesis arises a few years ago, when my dad made me aware of the excessively use of safety factors in structural engineering. In a world with limited amount of resources, I would like to make people aware of the inefficient use of materials as follows from oversized structures.

I would like to give thanks to Øyvind Wiig Petersen for all good advice and help during the master period, my results would not have been present without him. In addition, I would like to thank my friends and family for being so understanding in a time where little attention has been aimed to them. In the end, I would also like to give thanks to my wonderful roommates for their support during a long and demanding master period.

*Kristin Antonsen*

Trondheim, June 1, 2016



# Summary

In the present study the influence of standardized safety factors in large and heavy structures, where the major loading arises from self-weight of the structure itself, is considered. For this purpose, a reliability analysis of the Hardanger Bridge is performed. The loading is assumed to originate from the self-weight of the bridge deck, hangers and main cables only, i.e. all other loads are neglected.

The reliability analysis is performed by comparing axial loading and resistance capacity in the main cables and hangers. The loading is calibrated by interpolation between a simulated influence surface and estimated values of the self-weight and its location. Calibrations and estimations of the axial loading are performed by taking advantage of a data simulation tools and programs, such as MATLAB and ABAQUS. The resistance capacities are estimated from obtained test data performed by the manufacturer, along with tabulated values in codes and manuals.

Notice, simplifications and assumptions are made in this thesis in order to estimate input variables in the analysis and to be able to perform the analysis itself. It is assumed that uncertainties related to these simplifications and assumptions are negligible.

Use of ordinary numerical simulations for the reliability analysis is not possible due to low failure probability. Hence, an Enhanced Monte Carlo method (developed at NTNU) is applied. The method consists of parameterization of the limit state function  $M = R - S$ , thus true probability of failure is found by extrapolation of the obtained failure probability data from the parameterized limit state function. Results from the method give values for the reliability index  $\beta$  in the range of  $\{12.5 - 14.6\}$ , corresponding values for the probability of failure per year is equal to  $\{1 \cdot 10^{-48} - 5 \cdot 10^{-36}\}$ . However, it is important to notice the inherent uncertainties in this results, due to the lack of available information in the extrapolation work, along with uncertainties related to the portion of subjective assumptions and simplifications. More simulations  $n$  should be performed in order to reduce the amount of uncertainties. Despite the uncertainties, the results show significant higher safety level than required in codes.

In order to strengthen the results, code calibration of partial safety factors corresponding to axial loading and resistance capacity are carried out. The calibration process is performed by using an iterative *second-moment* reliability method, along with a *load and resistance factor design* format (LRFD). The calibration process was performed by taking advantage of the useful data tools MATLAB and Excel. Results for the partial safety factors calibration are compared to standardized safety factors from codes. By inserting standardized safety factors, value for the reliability index  $\beta = 12.64$  is obtained. This gives a probability of failure equal to  $p_f = 6.76 \cdot 10^{-37}$ , which is in agreement with the result from Enhanced Monte Carlo method.





# Sammendrag

I denne masteroppgaven er det sett på virkningen av standardiserte sikkerhetsfaktorer i konstruksjoner hvor den største delen av belastningen kommer fra egenvekten til konstruksjonen selv. Til dette formål er det gjennomført en pålitelighetsanalyse av Hardangerbrua hvor all annen belastning enn egenvekten er neglisjert.

Pålitelighetsanalysen er gjennomført ved å sammenligne aksial belastning og kapasitet i hoved- og hengerkablene. Belastningen som påføres konstruksjonen som følger av egenvekten er beregnet ved å modellere en «innflytelses flate», som estimerer aksial belastning i kablene ut ifra påførte krefter og deres posisjon. De påførte kreftene, som fører til belastning i kablene, er antatt å stamme kun fra egenvekten til brodekket og kablene. Datasimulering og programmering er benyttet til å estimere de aksiale belastningene. Kapasitetene til kablene er beregnet ut ifra tester og målinger gjort hos fabrikanten, samt standardiserte verdier gitt i Eurokode og håndbøker.

Det er også grunn til å nevne at forenklinger og subjektive antagelser er gjort i arbeidet med å estimere verdiene til variablene, samt i gjennomføringen av analysen. Det er dog antatt at disse antagelsene vil gi holdbare resultater.

På grunn av lave sviktsannsynligheter var det ikke mulig å gjennomføre analysen ved bruk av vanlige numeriske metoder. Det ble derfor benyttet en forbedret Monte Carlo metode, utviklet ved NTNU. Metoden består i å parametrisere grensetilstandsfunksjonen  $M = R - S$ , noe som gjør det mulig finne sviktsannsynligheter ved å bruke færre simulering. Sann sviktsannsynlighet finnes ved ekstrapolering av fremstilte sviktsannsynligheter fra den parametriserte grensetilstandsfunksjonen. Metoden gir resultater for pålitelighetsindeksen i intervallet  $\{12.5 - 14.6\}$ . Dette tilsvarer sviktsannsynlighet per år på  $\{1 \cdot 10^{-48} - 5 \cdot 10^{-36}\}$ . Det er viktig å være klar over at det er stor usikkerhet knyttet til disse verdiene, både på grunn av usikkerhet i ekstrapoleringsarbeidet, men også som følger av mange subjektive antagelser. Flere simuleringer  $n$  burde benyttes for å redusere usikkerheten. På tross av stor usikkerhet, indikerer størrelsen på resultatene et mye høyere sikkerhetsnivået enn hva som kreves i Eurokode.

For å styrke resultatene er det også gjennomført en kalibrering av sikkerhetsfaktorer knyttet til påført belastning og kapasitet. Kalibreringen er gjennomført ved å benytte et *last og resistans faktor utformings* format (LRFD) og en «*Second-Moment*» pålitelighetsmetode for estimering av sviktsannsynlighet. Resultatene fra kalibreringen av sikkerhetsfaktorene er deretter sammenlignet med standardiserte sikkerhetsfaktorer fra Eurokode. Ved innsetting av standardiserte sikkerhetsfaktorer beregnes pålitelighetsindeksen til 12.64, dette tilsvarer en sviktsannsynlighet per år på  $6.76 \cdot 10^{-37}$ . Resultatene fra kalibreringen samsvarer bra med resultatene fra Monte Carlo simuleringen.

I alle fasene av prosjektet, det vil si parameterestimering av inn og ut data, samt Monte Carlo simuleringen i seg selv, er verktøyet MATLAB benyttet. Til kalibrering av sikkerhetsfaktorer er Excel benyttet. I tillegg er dataprogrammet ABAQUS benyttet til å simulere Hardangerbroen og estimere «innflytelses flaten».



# Contents

|  |     |
|--|-----|
| <b>Preface</b> .....   | i   |
| <b>Summary</b> .....   | iii |
| <b>Sammendrag</b> .....  | v   |
| <b>List of figures</b> .....                                     | xi  |
| <b>List of tables</b> .....                                      | xiv |
| <b>1 Introduction</b> .....                                      | 1   |
| 1.1 Background .....   | 1   |
| 1.2 Objective of work .....                                      | 1   |
| 1.2.1 Organization of work .....                                 | 2   |
| 1.3 Hardanger Bridge .....                                       | 2   |
| <b>2 Statistics and structural reliability</b> .....             | 7   |
| 2.1 Fundamentals of probability theory .....                     | 7   |
| 2.2 Fundamentals of statistical analysis .....                   | 8   |
| 2.2.1 Probability density function .....                         | 8   |
| 2.2.2 Cumulative distribution function .....                     | 10  |
| 2.2.3 Distribution parameters .....                              | 10  |
| 2.2.4 Jointly distributed random variables and correlation ..... | 12  |
| 2.2.5 Regression .....   | 15  |
| 2.3 Normal distribution .....                                    | 16  |
| 2.4 Lognormal distribution .....                                 | 17  |
| 2.5 Gumbel distribution .....                                    | 18  |
| 2.6 Characteristic and design values .....                       | 18  |
| 2.7 Structural reliability analysis .....                        | 19  |
| 2.7.1 Reliability, Risk and probability of failure .....         | 19  |
| 2.7.2 Structural reliability problems .....                      | 21  |
| 2.8 Direct integration .....                                     | 25  |
| 2.8.1 Example 2.1 .....  | 27  |
| 2.9 Second – Moment and Transformation Methods .....             | 28  |
| 2.9.1 The method of Hasofer and Lind .....                       | 28  |
| 2.9.2 Example 2.2 .....  | 29  |
| 2.9.3 Extensions of the Hasofer and Lind method .....            | 31  |
| 2.9.4 Example 2.3 .....  | 33  |

|          |   |           |
|----------|---|-----------|
| 2.10     | Numerical iteration .....                                 | 36        |
| 2.10.1   | Monte Carlo Methods .....                                 | 37        |
| 2.10.2   | Example 2.4 .....   | 40        |
| 2.10.3   | Enhanced Monte Carlo method.....                          | 41        |
| 2.10.5   | Example 2.5 .....   | 42        |
| 2.11     | Deriving partial safety factors .....                     | 44        |
| 2.12     | Series and parallel systems .....                         | 45        |
| <b>3</b> | <b>Self-weight estimation</b> .....                       | <b>47</b> |
| 3.1      | Characterizing load.....                                  | 47        |
| 3.2      | Self-weight.....  | 47        |
| 3.2.1    | Uncertainties.....  | 48        |
| 3.2.2    | Density .....   | 48        |
| 3.2.3    | Volume .....  | 49        |
| 3.3      | Self-weight estimation.....                               | 50        |
| 3.4      | Self-weight estimation of the Hardanger Bridge.....       | 50        |
| <b>4</b> | <b>Resistance capacity estimation</b> .....               | <b>55</b> |
| 4.1      | Material properties.....                                  | 55        |
| 4.1.1    | Variation and correlation.....                            | 56        |
| 4.1.2    | Uncertainties.....  | 57        |
| 4.2      | Resistance capacity estimation .....                      | 57        |
| 4.3      | Resistance capacity of Hardanger Bridge.....              | 58        |
| 4.3.1    | Resistance capacity of main cable.....                    | 59        |
| 4.3.2    | Resistance capacity of hanger .....                       | 59        |
| 4.3.3    | Uncertainties.....  | 60        |
| <b>5</b> | <b>Reliability analysis of the Hardanger Bridge</b> ..... | <b>63</b> |
| 5.1      | Short on solution strategy .....                          | 63        |
| 5.2      | Simulation in ABAQUS .....                                | 64        |
| 5.2.1    | Components.....   | 64        |
| 5.2.2    | Influence surface .....                                   | 66        |
| 5.3      | Calibration of axial loading in MATLAB .....              | 67        |
| 5.3.1    | Axial load calibration .....                              | 67        |
| 5.4      | Reliability analysis .....                                | 68        |
| 5.5      | Calibration of partial safety factors .....               | 68        |
| 5.5.1    | Parameter estimation .....                                | 68        |
| 5.5.2    | Calibration process .....                                 | 69        |

|          |  |     |
|----------|--|-----|
| <b>6</b> | <b>Results and discussion</b> .....    | 71  |
| 6.1      | Load calibration .....                 | 71  |
| 6.1.1    | Self-weight .....                      | 71  |
| 6.1.2    | Component force estimation .....       | 76  |
| 6.2      | Resistance estimation .....            | 77  |
| 6.3      | Reliability analysis .....             | 80  |
| 6.4      | Code calibration (Second-Moment) ..... | 81  |
| 6.5      | Comparisons .....                      | 82  |
| <b>7</b> | <b>Conclusion</b> .....                | 85  |
| 7.1      | Further work .....                     | 86  |
|          | <b>Bibliography</b> .....              | 89  |
|          | <b>Appendices</b> .....                | 91  |
|          | <b>Appendix A</b> .....                | 93  |
|          | <b>Appendix B</b> .....                | 101 |
|          | <b>Appendix C</b> .....                | 105 |



# List of figures

|   |    |
|---|----|
| <b>Figure 1.1:</b> Map of the location bridge [4].  | 3  |
| <b>Figure 1.2:</b> Cross-section of the steel box girder [4].   | 4  |
| <b>Figure 1.3:</b> Complete picture of the entire bridge with pylons, cables and steel box girder [4].  | 4  |
| <b>Figure 2.1:</b> Example of a probability density function for normal distributed variable with zero mean and unit variance.  | 9  |
| <b>Figure 2.2:</b> Example of a cumulative distribution function for normal distributed variable with zero mean value and unit variance.  | 10 |
| <b>Figure 2.3:</b> Plot of each pair of observations $(x_i, y_i)$ as a point in the corresponding coordinate system and an isometric representation of the respective 2D histogram [6].                       | 12 |
| <b>Figure 2.4:</b> Joint, marginal and conditional probability density functions [8].   | 13 |
| <b>Figure 2.5:</b> Plots for different values of the correlation coefficient.   | 14 |
| <b>Figure 2.6:</b> Linear regression line that best fit the obtained data point.  | 15 |
| <b>Figure 2.7:</b> Plot of normal (green) and standard normal (blue) probability density function.  | 17 |
| <b>Figure 2.8:</b> Two random variable joint density function $f_{RS}(r, s)$ marginal density functions $f_R$ and $f_S$ and failure domain D [8].   | 22 |
| <b>Figure 2.9:</b> Basic R-S problem: $F_R \cdot f_S$ representation [8].   | 23 |
| <b>Figure 2.10:</b> Shows the problem with its variables R, S and M [6].  | 26 |
| <b>Figure 2.11:</b> Simple supported beam with length L, loaded by a concentrated load S.   | 27 |
| <b>Figure 2.12:</b> Shows plot of the marginal and bivariate pdf, along with limit state function in standard normal space [6].   | 30 |
| <b>Figure 2.13:</b> Rigidly clamped beam loaded by concentrated load P.   | 34 |
| <b>Figure 2.14:</b> Excel script from the iterative calculation.  | 36 |
| <b>Figure 2.15:</b> Generation of random variables. The cdf fits the lognormal distributed variable R of the example 2.4 in section 2.10.1  | 39 |
| <b>Figure 2.16:</b> Cdf for normal distributed variable X, with different variances (steep and gentle slope).   | 40 |
| <b>Figure 2.17:</b> Simply supported beam with concentrated load S and length L.  | 40 |
| <b>Figure 2.18:</b> The extrapolation curve of the enhanced method, when $\rho = 0.3$ . Blue dots are $p_f(\lambda)$ , black and red curves estimate failure probability and confidence limits, respectively. | 44 |

|   |    |
|---|----|
| <b>Figure 3.1:</b> Curve for correlation coefficient for densities and dimensions for steel and asphalt deck. ....  | 49 |
| <b>Figure 3.2:</b> Simulated mesh of the bridge deck. Yellow numbers indicate element numbers. Red arrows indicate self-weight of element and location. Black numbers indicate dimensions. ....   | 51 |
| <b>Figure 4.1:</b> Stress-strain curve.....   | 56 |
| <b>Figure 4.2:</b> Pdf for the normal distributed variables R and S. Blue curve is load variable, red and green curves are resistance variables in hangers and main cables, respectively. Red and blue curve have a much greater area of intersection than blue and green curve, hence probability of failure for the hangers will dominate. .... | 61 |
| <b>Figure 5.1:</b> Flow-chart of the solution strategy for the reliability analysis and partial safety factor calibration. ....   | 64 |
| <b>Figure 5.2:</b> Simulated Hardanger Bridge in ABAQUS.....  | 65 |
| <b>Figure 5.3:</b> Illustration of the components. Drawings of the bridge are obtained from Norwegian Public Roads Administration [4]. Numbering done in accordance with the simulation. ....   | 66 |
| <b>Figure 5.4:</b> Influence surface with node numbers (red) and dimensions (black).....  | 67 |
| <b>Figure 6.1:</b> Probability density plot for (a) steel cross-section (b) asphalt thickness for element 1 (according to figure 3.2). ....   | 72 |
| <b>Figure 6.2:</b> Joint pdf for (a) steel deck $\Delta r = 10m$ , (b) asphalt deck $\Delta r = 10m$ , (c) steel deck $\Delta r = 1310m$ , (d) asphalt deck $\Delta r = 1310m$ .....  | 73 |
| <b>Figure 6.3:</b> Probability density plot of the density for element 1 (see figure 3.2) for (a) steel deck, (b) asphalt deck.....   | 74 |
| <b>Figure 6.4:</b> Joint pdf of the densities for (a) steel deck $\Delta r = 10m$ , (b) asphalt deck $\Delta r = 10m$ , (c) steel deck $\Delta r = 1310m$ , (d) asphalt deck $\Delta r = 1310m$ . ....  | 74 |
| <b>Figure 6.5:</b> Probability density plot for the self-weight of (a) steel deck, (b) asphalt deck. For element 1 (see figure 3.2). ....   | 75 |
| <b>Figure 6.6:</b> Probability density plot for the entire bridge deck. For element 1 (see figure 3.2). ....  | 75 |
| <b>Figure 6.7:</b> Probability density plots for the axial loading forces in component (a) 1000 (main cable), (b) 5002 (hanger). Figure 5.3 illustrate the components. ....   | 76 |
| <b>Figure 6.8:</b> Joint pdf for the axial loading forces in components (a) 1000 and 1001 (main cable), (b) 5002 and 5003 (hanger), (c) 1000 and 2067 (main cable), (d) 5002 and 6066 (hanger). Figure 5.3 illustrates the components. ....   | 77 |



|   |     |
|---|-----|
| <b>Figure 6.9:</b> Probability density plot of the resistance capacity for component (a) 1000 (main cable), (b) 5002 (hanger).....  | 78  |
| <b>Figure 6.10:</b> Curves for normal distributed variables with high and low variance and pdf for axial loading. Grey and yellow areas show the respective $p_f$ .....   | 79  |
| <b>Figure 6.11:</b> Joint pdf of resistance capacities between components (a) 1000 and 1001 (main cable), (b) 5002 and 5003 (hanger), (c) 1000 and 2067 (main cable), (d) 5002 and 6066 (hanger). .....                             | 79  |
| <b>Figure 6.12:</b> The extrapolation curve of enhanced method. Blue dots are obtained pf from data points. Black and red curves estimate probability and confidence limit, respectively. Number of simulations, $n = 10^5$ . ..... | 80  |
| <b>Figure 6.13:</b> Estimation of the partial safety factors by using problem solver in excel. $n = 3 \cdot 10^5$ simulations are performed. ....   | 82  |
| <b>Figure A.1:</b> Basis of calculation.....  | 94  |
| <b>Figure A.2:</b> Basis of calculation.....  | 95  |
| <b>Figure A.3:</b> Basis of calculation.....  | 96  |
| <b>Figure A.4:</b> Basis of calculation.....  | 97  |
| <b>Figure A.5:</b> Basis of calculation.....  | 98  |
| <b>Figure A.6:</b> Basis of calculation.....  | 99  |
| <b>Figure C.1:</b> Tensile test data from Bridon.....   | 106 |
| <b>Figure C.2:</b> Tensile test data from Bridon.....   | 106 |
| <b>Figure C.3:</b> Tensile test data from Bridon.....   | 106 |
| <b>Figure C.4:</b> Tensile test data from Bridon.....   | 107 |
| <b>Figure C.5:</b> Tensile test data from Bridon.....   | 107 |
| <b>Figure C.6:</b> Tensile test data from Bridon.....   | 107 |
| <b>Figure C.7:</b> Excel script of obtained tensile test data from Bridon.....  | 108 |
| <b>Figure C.8:</b> Statistical interpretation of the obtained tensile test data.....  | 108 |

# List of tables

|   |     |
|---|-----|
| <b>Table 2.1:</b> Estimated values for the sensitivity factors $\alpha_i$ .   | 36  |
| <b>Table 2.2:</b> Results for the reliability index and probability of failure from the analytical solution.  | 43  |
| <b>Table 2.3:</b> Reliability index, probability of failure and 95% confidence intervals calculated using $n = 10^8$ simulations.   | 43  |
| <b>Table 2.4:</b> Reliability index, probability of failure, 95% confidence interval calculated using $n = 10^6$ and $10^7$ .   | 43  |
| <b>Table 3.1:</b> Mean value and coefficient of variation for weight density [19].  | 48  |
| <b>Table 3.2:</b> Values for the parameters in the correlation function (3.2) [19].   | 49  |
| <b>Table 3.3:</b> Mean values and standard deviations for deviations of cross-section dimensions from their nominal values [19].  | 49  |
| <b>Table 4.1:</b> Material strength properties for different materials [21], [22], [23], [24].  | 56  |
| <b>Table 4.2:</b> Partial safety factors for the material resistance [21], [24].  | 58  |
| <b>Table 4.3:</b> Estimated and obtained tensile strength data for the components [22], [23], [24], appendix C.   | 60  |
| <b>Table 5.1:</b> Bridge components with corresponding numbering of elements.   | 65  |
| <b>Table 6.1:</b> Mean values and standard deviation for the dimension variables $A_s$ and $t$ .  | 72  |
| <b>Table 6.2:</b> Mean values and standard deviations of the density values for each deck.  | 73  |
| <b>Table 6.3:</b> Mean values of the mean values and coefficients of variation for the axial loading in the hanger and main cable components.                               | 76  |
| <b>Table 6.4:</b> Mean value, standard deviation, area of cross-section and coefficient of variation for the resistance capacity for the hanger and main cables components. | 78  |
| <b>Table 6.5:</b> Values for the reliability index, probability of failure, confidence limits for $n$ simulations.  | 80  |
| <b>Table 6.6:</b> Partial safety factors for the resistance capacity and loading. Calibrated from the reliability analysis performed and obtained from codes [20], [24].    | 81  |
| <b>Table B.1:</b> Tables of Standard Normal Probabilities for negative Z-scores.  | 102 |
| <b>Table B.2:</b> Tables of Standard Normal Probabilities for positive Z-scores.  | 103 |
| <b>Table B.3:</b> Critical values in Standard Normal distribution.  | 104 |

---

# 1 Introduction

## 1.1 Background

The main content in this master thesis relay on prediction of failure probability and partial safety factor estimation of large bridges, in order to study reliability of large civil engineering structures. Technology is constantly changing and environmental requirements rise increasingly. This causes considerations about how to improve the utilization of the resources.

Large and heavy constructions with a high self-weight relative to other loads tend to have a low variation in the loading. The reason is that the variation in self-weight is extreme low compared to other loads, as will be discussed in chapter 3 (Self-weight estimation).

Nowadays, structural calculations are based on standards and code calibrations, this involve use of standardized partial safety factors. The partial safety factors are included in calculations to handle the uncertainties related to the variability in loads and resistances. Since the codes are supposed to be a general tool, i.e. used in all kinds of structural problems, standardized partial safety factors may therefore become too conservative, consequently cost economic increases and environmental inefficiency occurs.

From the facts stated above following hypothesis can be stated and will be covered in this master thesis:

*“In structures where the loading only (or nearly only) consist of self-weight, partial safety factors from codes and standards will lead to oversizing and inefficiency, due to low variance in the self-weight.”*

The comprehensive and well-known E39 project consist of engineering and construction of several long and heavy bridges in order to achieve a ferry free road from Trondheim to Kristiansand. Structural codes of today may be limiting and lead to unnecessary large costs, as follows from the hypothesis stated above. Hence, the scope of this thesis is of high importance in current and upcoming structural projects. For more information about the project, see [1].

## 1.2 Objective of work

Operational modal analysis of the Hardanger Bridge exposed to wind loads and reliability analysis of the Hardanger Bridge with respect to flutter instability, have been considered in previous studies, see [2], [3]. This thesis takes another point of view, and investigate the effectiveness of design calculation from codes by providing reliability analysis of the Hardanger Bridge exposed to self-weight loading. Hence, estimation of safety factors for loading and the resistance capacity with respect to the bearing system are carried out and compared with standardized partial safety factors.

The analysis is divided into four main steps. Firstly, estimation of the self-weight related to the construction. Secondly, transformation of the self-weight loading into axial loading in the cables of the suspension bridge is performed. Thirdly, estimation of the resistance capacities with respect to the considered components is done. In the last part of the analysis, comparisons between the previous estimates are done in order to provide results for the reliability and effect of code based design calculations.

In the analysis, two modelling approaches are used to investigate the effect of self-weight loading and the use of standards and codes. The first method (Second-Moment) provides results and comparisons between calibrated partial safety factors and standardized safety factors, along with results for the reliability index and the probability of failure. The second method (numerical simulation) provides results for the reliability of the structure.

The thesis is organized into seven chapters, which will be described briefly in the following section.

### 1.2.1 Organization of work

Chapter 2 consists of important theory behind structural reliability analysis and code calibration. This theory is necessary for the further understanding of the aspect.

Chapter 3 consists of self-weight estimation of the Hardanger Bridge, along with important assumptions and simplifications in the self-weight estimation.

Chapter 4 consists of resistance capacity estimation based on values from codes, standards, manuals and available strength data. Important assumptions and simplifications of the capacity estimation is included in this chapter.

Chapter 5 consists of strategies and procedures for the reliability analysis implementation and code calibration process.

Chapter 6 consists of results and discussion from the previous chapters. The chapter is subdivided into several sections, where each section present results from the above chapters. Figures and plots from the analysis are included in this part of the thesis.

Chapter 7 consists of conclusion from the analysis performed in this thesis. In addition, suggestions for further work of this subject are posted.

## 1.3 Hardanger Bridge

In this subsection, a brief introduction of the Hardanger Bridge is presented, along with valuable information regarding the dimensions and costs of the project and engineering phase.

The Hardanger Bridge crosses the Eidfjord from Bu to Vallavik, and is the longest suspension bridge in Norway. The bridge has a main span of 1310 m and a total length of 1380 m. It takes place at the west coast of Norway and has the purpose of decreasing the running time by

replacing the ferry between Bruravik and Brimnes, which has been a bottleneck at the distance Odda-Voss. Figure 1.1 shows the location of the bridge.

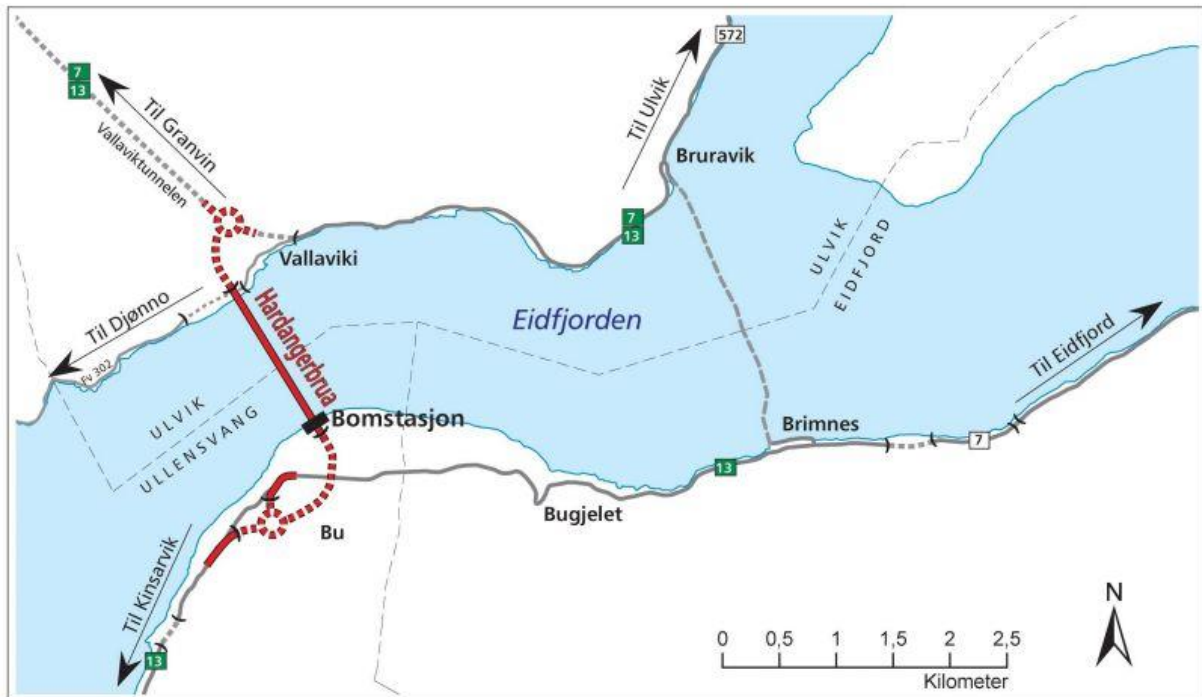


*Figure 1.1: Map of the location bridge [4].*

As can be seen from the map in figure 1.1, the bridge connects the north and south part of the west coast and makes it possible to drive from Voss to Odda without any need for ferry.

The bridge has two pylons, which consist of two concrete columns and three transverse girders called rigel. The steel box girder (part of the bridge deck) is a closed steel frame, with geometry as shown in figure 1.2. The steel box girder was produced in 12 m lengths, which were welded together in 60 m sections. The sections were installed by uplifting from a boat and then fastened with the cables.

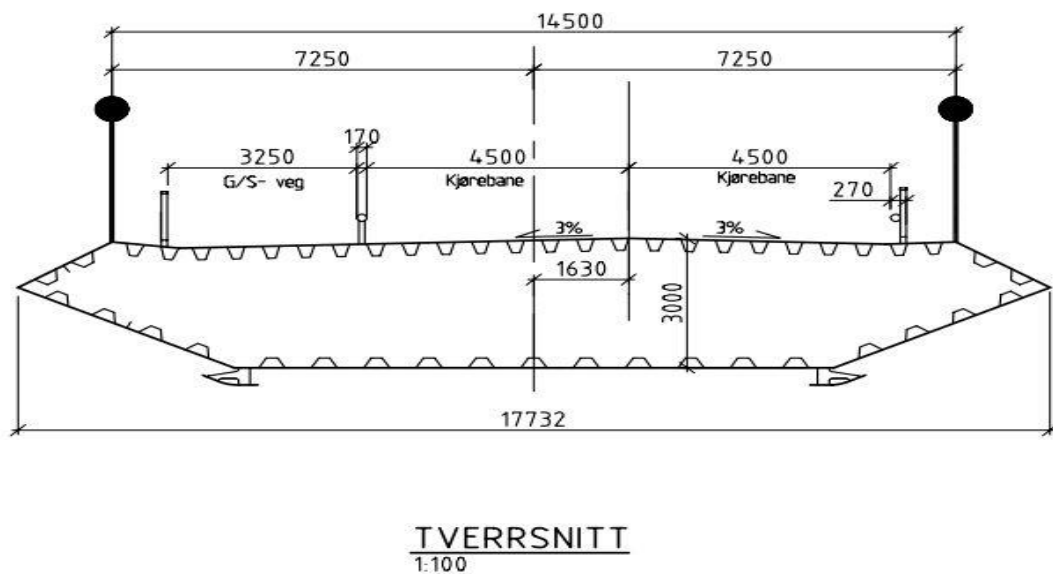


*Figure 1.2: Cross-section of the steel box girder [4].*

The main cables consist of 19 bundles of 528 wires, each wire with a diameter equal to 5,3 mm. The 19 cable bundles are compacted together in a way that gives a circular cross-section of the main cables. The main cables were installed by cable spinning from Bu to Vallavik.

130 hangers connect the steel box girder to the main cables. All the hangers are installed in the main span, with 65 hangers on each side of the steel box girder. The hangers are a “closed cable” consisting of 7 layers of wire and has a diameter of 70 mm. Notice, due to the volume of air in the hangers, effective cross-section area is obtained to be 3200 mm<sup>2</sup>, see appendix A.



*Figure 1.3: Complete picture of the entire bridge with pylons, cables and steel box girder [4].*

The construction of the bridge was carried out in three stages:

1. Work of excavating and blasting the anchorage system

2. Installing the pylons with transverse girders (concrete work)
3. Installing the main cables, hanger cables and steel box girder (steel work)

Total economic cost of the bridge was 1350 mill. NOK, where cables and steel box girder were the main cost. In addition, cost for supply routes, tunnels and client costs makes the project a total cost of 2300 mill. NOK.





---

## 2 Statistics and structural reliability

This chapter includes important statistics and probability theory, which are fundamental in structural reliability analysis. In the first sections of this chapter a brief introduction of the fundamentals of probability theory take place. Secondly, theory behind statistical analysis are presented, where main statistical concepts and formulas to determine the values of statistical variables and parameters are explained and derived. Different distribution functions are also included in this review. The latter part of the chapter contains different methods to estimate the reliability of a structure. The reliability analysis performed in this thesis rely on the methods and statistics presented in this chapter.

Examples from structural problems are used in order to give a better understanding of the different methods for calculation of structural reliability.

### 2.1 Fundamentals of probability theory

Probability theory is of high importance in order to perform a reliability analysis. Probability theory is a wide and extensive theme, which include a lot of axiom, terminology and theorem.

Important concepts for the understanding of probability theory:

- Event, which is the case considered.
- Outcome space, which is the possible outcome of an event.
- Sample space  $\Omega$ , which describe the area in where all the possible outcome of the events will occur.

The probability concept can be divided into three different parts: classical probability, frequency and subjective probability.

- **Classical probability:** the number of cases where the event occurs divided by the sample space, see (2.1).

$$P(A) = \frac{\# \text{ of outcome for event } A}{\# \text{ of possible outcome}} \quad (2.1)$$

- **Frequency:** the relative frequency in which an event will occur, given many independent recurrences under the same condition.
- **Subjective probability:** related to the degree of belief or confidence of an event to occur. This is often used in statements, where the chance of the event to occur is quantified by a subjective degree of belief.

It is important to know the differences between probability and frequency. Probability describe the inherent chance of an event to occur. Frequency probability count the amount of occurrence events given many repetitions with under the same condition(s).

Fundamental axioms of the probability theory according to *axioms of Kolmogoroff* (1933) [6]:

1. The probability of event  $A$ , denoted  $P(A)$ , is dimensionless and has an outcome between 0 and 1.
2. The probability of the sample space  $P(\Omega)$  is equal to 1, since this is the space in where all the possible outcome will occur.
3. If the events  $E_i$  do not possess any common elements, i.e. the events are mutually exclusive (disjoint), then the probability of the union of the events is equal to the sum of the probabilities of the individual events. (2.2) shows this axiom.

$$P\left(\bigcap_{i=1}^n E_i\right) = \emptyset \Leftrightarrow P\left(\bigcup_{i=1}^n E_i\right) = \sum_{i=1}^n P(E_i) \quad (2.2)$$

Two other important concepts, used in following calculations, are the degree of independence and conditional probability. The first concept states the dependency between events, i.e. the fact that the occurrence of one event influences the occurrence of another event. The latter concept is related to the influence of known information. What is the probability of an event to occur given that another event already has occurred or not? This is called conditional probability  $P(E_1|E_2)$  and is shown in (2.3).

$$P(E_1|E_2) = \frac{P(E_1 \cap E_2)}{P(E_2)} \quad (2.3)$$

For more extensive elaboration of probability rules, concepts and theories, see [6], [7], [8].

## 2.2 Fundamentals of statistical analysis

Usually the probability of an event is not a quantified value. This is the truth in most structural probability issues.

When throwing a dice, the probability for each outcome in the sample space is equal to 1/6. This is an inherent probability, because the dice has six sides and every side is as much likely to occur as another. In structural probability calculations different kind of variables need to be quantified. These variables are not always known and need to be estimated by statistical analysis.

Estimation of the variables needed in the probability calculations, is usually done by tests of specimens or by data from observations. A set of values from tests or observations are collected in a sample. Each sample is then investigated statistically, to make an assumption of the behaviour of the variable. The static may be interpreted to predict values or parameters needed in further calculations.

### 2.2.1 Probability density function

Assume a sample of values for the variable  $X$  obtained from a strength test of steel specimens. The values from the test can be collected in a diagram, which shows the values of the variables on the horizontal axis, and the number of occurrence for each values on the vertical axis. The diagram shows the probability of occurrence for each value of the variable.

If the variable can take all values within a given outcome space, the diagram can be plotted as a continuously curve. The curve is described by the probability density function (pdf), denoted  $f(x)$ . Where,  $x$  represents a given random value of the variable, while the curve represents the probability of the value to occur.

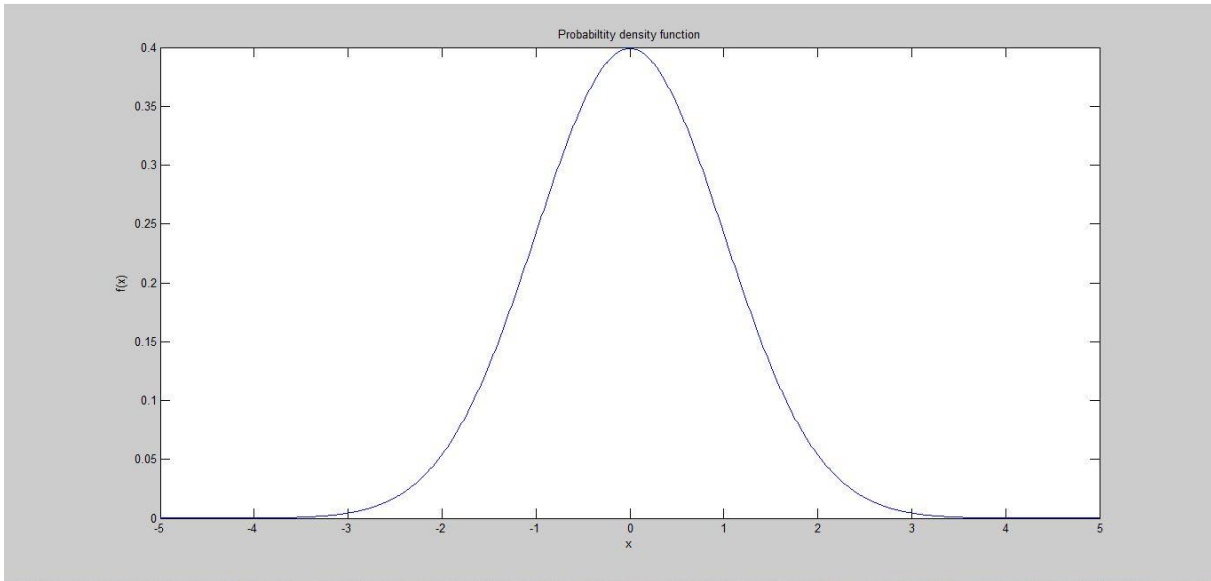


**Figure 2.1:** Example of a probability density function for normal distributed variable with zero mean and unit variance.

The probability density function predict the probability for all possible outcomes, consequently  $P(X = x) = f_X(x)$ .

When the sample space is infinite, the probability for an outcome need to be considered as the probability of  $X$  takes a value within a given interval  $\Delta x$ . Using mathematic expressions, the probability in such case can be estimated as:

$$P(a < X < b) = \int_a^b f_X(x) dx \quad (2.4)$$

The probability of  $X$  taking values on the entire sample space is equal to the probability of the entire sample space:

$$P(-\infty < X < \infty) = \int_{-\infty}^{\infty} f_X(x) dx = 1 \quad (2.5)$$

It is important to note that the density function is not equal for all kinds of variables. There exist several kinds of distributions; a couple of them are explained in following sections.

## 2.2.2 Cumulative distribution function

The area under the probability density function curve is equal to the sample space. By integrating this area, the cumulative distribution function (cdf) is found.

The cumulative distribution function,  $F(x)$ , gives the probability of  $X$  taking a value less than a certain number  $x$ , consequently  $P(X < x) = F_X(x)$ . The capital letter  $X$  is an index for a given variable, which can take a value on the entire sample space.

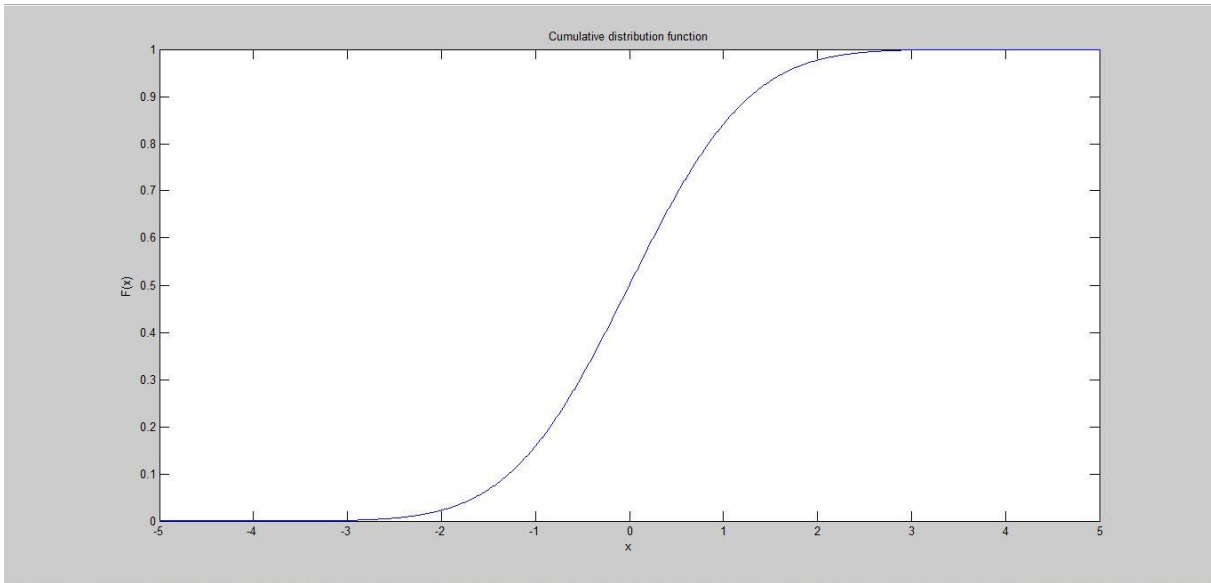


**Figure 2.2:** Example of a cumulative distribution function for normal distributed variable with zero mean value and unit variance.

Mathematically the expression for the cumulative distribution function is given as:

$$F_X(x) = P(X \leq x) = \int_{-\infty}^x f_X(t) dt \quad (2.6)$$

Where  $t$  is a dummy variable.

## 2.2.3 Distribution parameters

Random variables are usually estimated from the distribution functions and parameters. Important parameters in estimation of random variables are:

- Mean
- Variance
- Coefficient of variation

Mean is the average value of a sample and is denoted  $\mu$ . The general equation for calculating the mean value is given in (2.7).

$$\mu_X = E[X] = \int_{-\infty}^{\infty} x \cdot f_X(x) dx \quad (2.7)$$

Where  $E[X]$  is the expected value of the random variable  $X$ .

Often distributions have its own separate equation for calculating the mean value. The mean value is then found by using constants related to each distribution.

Values in a sample or a distribution often varies from the mean in one or more direction. Variance is a measure of the scatter in the values and is denoted  $\sigma^2$ . (2.8) shows the general formula for the variance.

$$\sigma_X^2 = VAR[X] = \int_{-\infty}^{\infty} (x_i - \mu_X)^2 \cdot f_X(x) dx \quad (2.8)$$

The standard deviation is a measure of the amount of variation (deviation) in the sample values. The standard deviation is found by taking the square root of the variance and is denoted  $\sigma$ .

In a random sample, where the distribution function is not known, one may use other methods to calculate the parameters. The parameters are replaced by so-called moments. The first moment is the arithmerical mean  $m_X$ , and is the middle value in the sample. The second moment, which is a measure of the scatter in the sample, is called the variance  $s_X^2$ . Formulas for the mean and the variance are given in (2.9) and (2.10), respectively.

$$m_X = \frac{1}{n} \cdot \sum_{i=1}^n x_i \quad (2.9)$$

$$s_X^2 = \frac{n}{n-1} \cdot \sum_{i=1}^n (x_i - m_X)^2 \quad (2.10)$$

Where  $n$  is the number of values in the sample.

This way of estimating parameters involves some uncertainties, because  $m_X$  and  $s_X^2$  are unbiased estimators of  $\mu_X$  and  $\sigma_X$ .

Another important parameter in statistical analysis is the coefficient of variation  $\rho$ . The parameter is the ratio between the mean value and the variance for each variable. (2.11) and (2.12) gives the formula for the parameter when the distribution function is well-known and unknown, respectively.

$$\rho_X = \frac{\sigma_X}{\mu_X} \quad (2.11)$$

$$v_X = \frac{s_X}{m_X} \quad (2.12)$$

### 2.2.4 Jointly distributed random variables and correlation

Structural reliability calculations often consist of more than one variable. Values to calibrate the variables, used in structural reliability analysis, are often collected in pairs. Example of this could be estimation of the dimensions ( $X$ ) and the dead load ( $Y$ ) of a beam. Collection of the dead load  $Y$  is dependent of the dimensions of the beam  $X$ , since the dead load  $Y$  is the product of the volume times the self-weight of the beam. The big question is whether there exists any interdependency between the two variables.

By plotting pair of values for the two variables ( $x_i, y_i$ ) in a coordinate system, it is often easier to see how the variables affect each other.

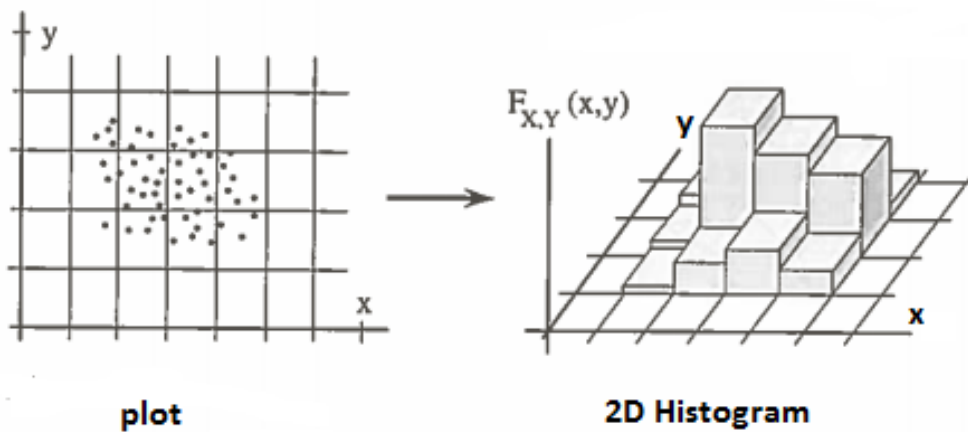


**Figure 2.3:** Plot of each pair of observations ( $x_i, y_i$ ) as a point in the corresponding coordinate system and an isometric representation of the respective 2D histogram [6].

A probability distribution function consisting of several variables  $X_i$ , is called a joint distribution function.

For an event consisting of two (or more) continuously random variables, the probabilities of occurrence given values of the variables are described by the joint cumulative distribution function:

$$F_{X,Y}(x, y) = P[(X \leq x) \cap (Y \leq y)] \geq 0 \quad (2.13)$$

“The joint (bivariate) density function  $f_{X,Y}(x, y)$  represent the probability that  $X$  takes a value between  $x$  and  $x + \Delta x$  and  $Y$  a value between  $y$  and  $y + \Delta y$  as  $\Delta x$  and  $\Delta y$  each approaches zero.” [8]

$$f_{X,Y}(x, y) = P[(x < X < x + \Delta x) \cap (y < Y < y + \Delta y)] \quad (2.14)$$

The joint density function for the two variables  $X$  and  $Y$ , consist of the marginal density functions  $f_X(x)$ ,  $f_Y(y)$  and the conditional probability distribution between the variables  $f_{X|Y}(x|y)$ .

$$f_{X,Y}(x, y) = f_{X|Y}(x|y) \cdot f_Y(y) = f_{Y|X}(y|x) \cdot f_X(x) \quad (2.15)$$

If the two variables are independent, the joint density distribution is equal to:

$$f_{X,Y}(x, y) = f_X(x) \cdot f_Y(y) \quad (2.16)$$

Figure 2.4 shows the joint, marginal and conditional probability density functions for the two variables  $X$  and  $Y$ .

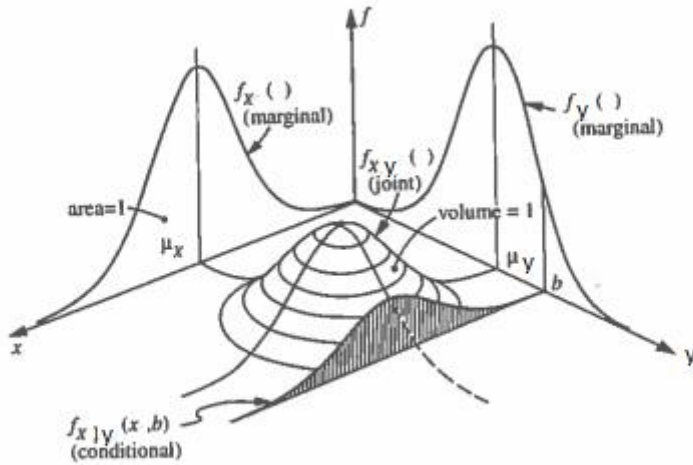


**Figure 2.4:** Joint, marginal and conditional probability density functions [8].

To measure the mutual dependence between the variables, two parameters covariance and correlation coefficient are used.

The general formula for the covariance, when the distribution is known, is shown in (2.17).

$$Cov(X, Y) = \sigma_{X,Y} = \iint_{-\infty}^{\infty} (x - \mu_X) \cdot (y - \mu_Y) \cdot f_{X,Y}(x, y) dx dy \quad (2.17)$$

An important observation is that the covariance does not have the same dimension as the standard deviation. The covariance consists of the deviation between values and the mean value, for both of the variables.

If  $f_X(\mathbf{x})$  is a  $n$ -dimensional density function of correlated variables  $\mathbf{X} = [X_1, X_2, \dots, X_n]$ . The covariance of  $\mathbf{X}$  can be written on matrix form, and is equal to:

$$\mathbf{C}_X = \begin{bmatrix} \text{Var}(X_1) & \dots & \text{Cov}(X_1, X_n) \\ \vdots & \ddots & \vdots \\ \text{Cov}(X_n, X_1) & \dots & \text{Var}(X_n) \end{bmatrix} \quad (2.18)$$

The correlation coefficient is dimensionless and is the ratio between the covariance and the product of the standard deviation for the variables:

$$\rho_{X,Y} \equiv \rho = \frac{\sigma_{X,Y}}{\sigma_X \cdot \sigma_Y} \quad (2.19)$$

The correlation coefficient varies from -1 to 1. Where 1 is perfectly correlated and -1 is perfectly negative correlated. Usually the value of correlation coefficient is somewhere between these values. Figure 2.5 shows how the correlation coefficient affect the dependency between the variables.

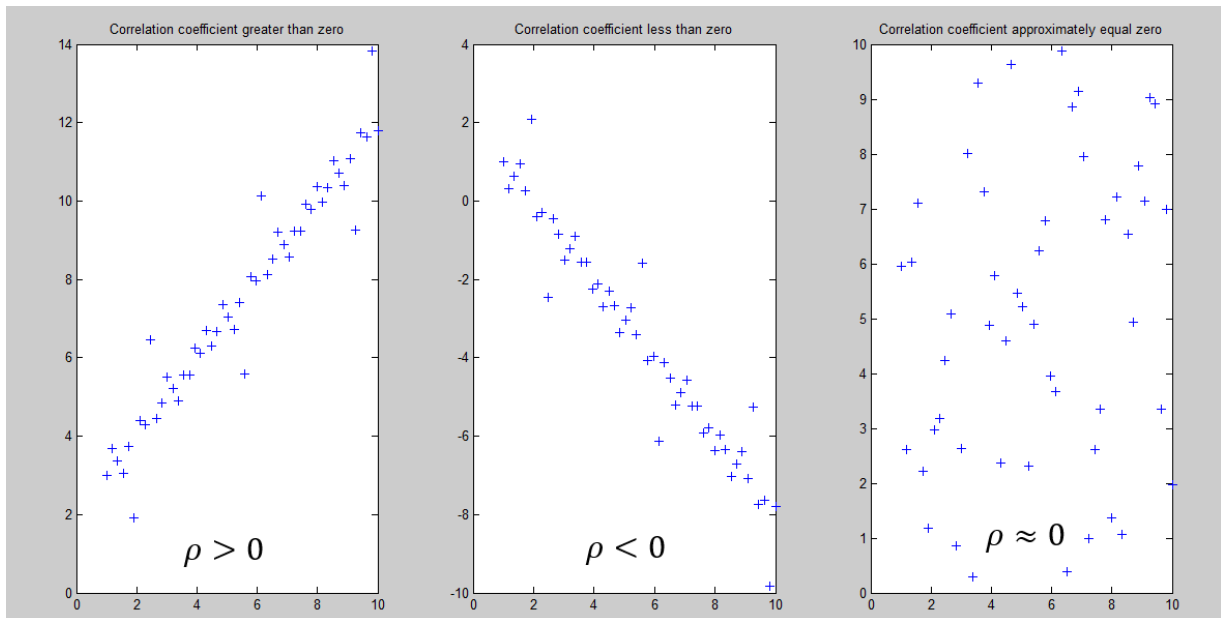


Figure 2.5: Plots for different values of the correlation coefficient.

It is important to note that even though the figure 2.5 only shows linear correlation, correlation between two variables may also have non-linear behaviour.

If  $\rho$  is equal to zero the two variables do not depend on each other, they are uncorrelated.

$$\rho_{X,Y} = 0 \Leftrightarrow f_{X,Y}(x, y) = f_X(x) \cdot f_Y(y) \quad (2.20)$$

If the values of the variables are found from random samples with unknown properties, the formulas for the covariance and the correlation coefficient is shown in (2.21) and (2.22).

$$\text{Cov}(X, Y) = s_{X,Y} = \frac{1}{n-1} \cdot \sum_{i=1}^n (x_i - m_X) \cdot (y_i - m_Y) \quad (2.21)$$



$$r_{X,Y} \equiv r = \frac{S_{X,Y}}{S_X \cdot S_Y} \quad (2.22)$$

## 2.2.5 Regression

Regression analysis is a useful tool in estimation of the correlation between two variables and makes it possible to express one variable as a function of another. From the diagram left in figure 2.5 it is possible to make a regression line between the two variables  $X$  and  $Y$ , as shown in figure 2.6.

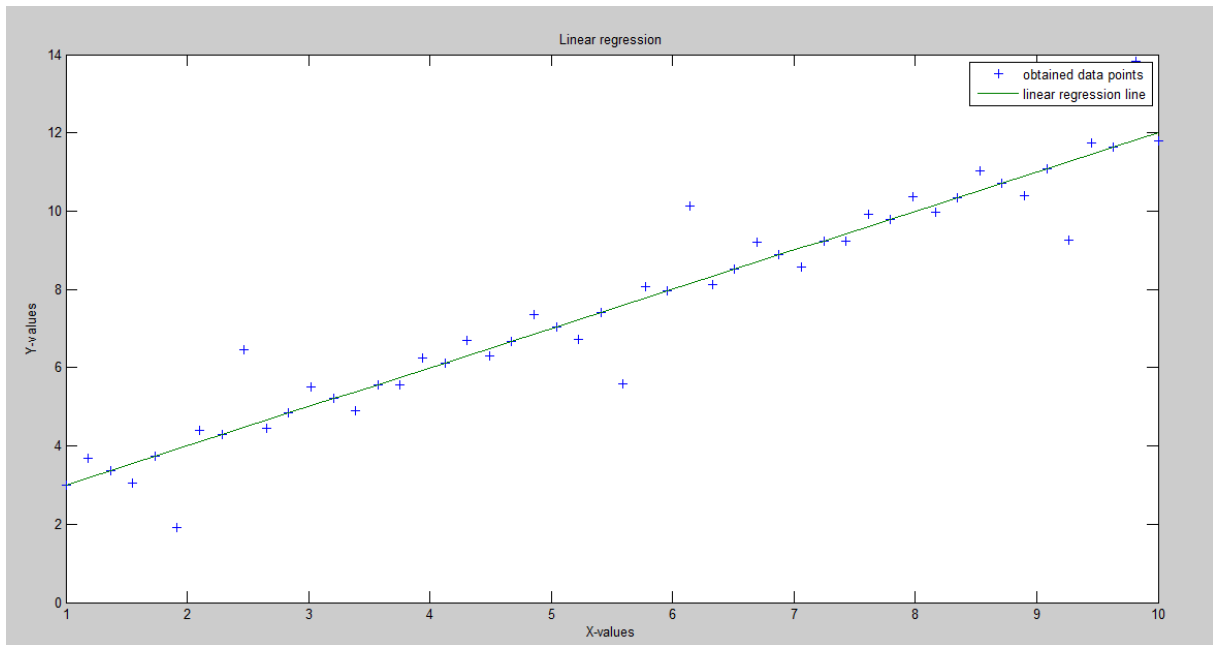


Figure 2.6: Linear regression line that best fit the obtained data point.

For every value of  $X$  it is possible to estimate the true value of  $Y$ , by using the formula:

$$Y = \alpha X + \beta + \epsilon \quad (2.23)$$

The stochastic variable  $\epsilon$ , represent the error in the model, is independent and has a constant variance for all attempt,  $\epsilon \sim N(0, \sigma^2)$ .  $\alpha$  and  $\beta$  are regression coefficients.

The true value of the regression coefficients  $\alpha$  and  $\beta$  are not possible to measure, they have to be obtained from the dataset. This is done by minimizing the error  $e_i$  between the true regression line  $y = \alpha x + \beta$ , and the estimate of the linear regression  $\hat{y} = ax + b$ .

The regression coefficients  $a$  and  $b$  are then estimated by using the method of least square:

$$SSE = \sum_{i=1}^n e_i^2 = \sum_{i=1}^n (y_i - \hat{y})^2 = \sum_{i=1}^n (y_i - a - bx_i)^2 \quad (2.24)$$

$$\Rightarrow a = \bar{y} - b\bar{x} \quad , \quad b = \frac{\sum_{i=1}^n (x_i - \bar{x})y_i}{\sum_{i=1}^n (x_i - \bar{x})^2} \quad (2.25)$$

Where,  $\bar{x}$  and  $\bar{y}$  denote the mean value of the variable  $X$  and  $Y$ , respectively.

## 2.3 Normal distribution

Normal distribution is one of the most used and important distribution function and is defined as follows:

$$f_X(x) = \frac{1}{\sigma_X \cdot \sqrt{2\pi}} \cdot e^{\left(-\frac{1}{2}\left(\frac{x-\mu}{\sigma}\right)^2\right)} \quad (2.26)$$

$$F_X(x) = \frac{1}{\sigma_X \cdot \sqrt{2\pi}} \cdot \int_{-\infty}^x e^{\left(-\frac{1}{2}\left(\frac{x-\mu}{\sigma}\right)^2\right)} dx \quad (2.27)$$

Normal probability density function is symmetric about the mean value at the horizontal axis. The distribution could be transformed into a standard normal distribution with mean value equal to zero and standard deviation equal to one. Such transformation is shown in the following equation:

$$X \sim N(\mu, \sigma) \Leftrightarrow Z = \frac{X - \mu}{\sigma} \sim N(0,1) \quad (2.28)$$

The cumulative distribution function for standard normal distribution is denoted  $\Phi(Z)$ . Values for standard normal probabilities are tabulated (see appendix B), hence is the transformation into standard normal space of high importance. The transformation is the crucial point in the Hasofer and Lind method (section 2.9.1).

The standard normal probability density function is symmetric about the horizontal axis.

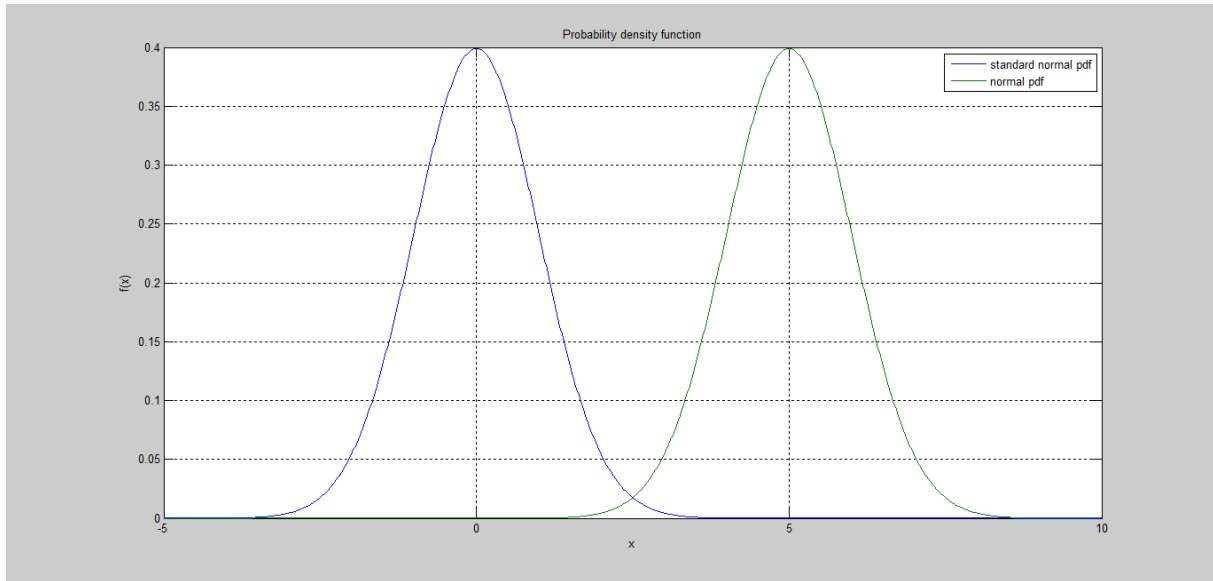


**Figure 2.7:** Plot of normal (green) and standard normal (blue) probability density function.

When a parameter consists of a mix of variables with different distributions, it is valid to assume that the distribution function for the parameter is normal distributed. This assumption is valid due to the *Central-Limit-Theorem* according to Freeman and Benjamin and Cornell [11], [12]. Therefore, the normal distribution is of high importance, both in this thesis and for general reliability analysis.

## 2.4 Lognormal distribution

The lognormal distribution is similar to the normal distribution, except it never accepts negative values.

In some cases, the needs for a distribution function which never reach negative values is required, e.g. in calibration of resistance. The strength of a structure will never reach negative values, hence gives the lognormal distribution a better estimation of the resistance than a normal distribution.

The lognormal distribution is expressed as follows:

$$f_X(x) = \frac{1}{\zeta \cdot x \cdot \sqrt{2\pi}} \cdot e^{(-\frac{1}{2}(\frac{\ln x - \lambda}{\zeta})^2)} \quad (2.29)$$

$$F_X(x) = \int_0^x \frac{1}{\zeta \cdot x \cdot \sqrt{2\pi}} \cdot e^{(-\frac{1}{2}(\frac{\ln x - \lambda}{\zeta})^2)} dx \quad (2.30)$$

Where,  $\zeta$  and  $\lambda$  are lognormal distribution parameters.

## 2.5 Gumbel distribution

Gumbel distribution is the type I extreme value distribution. The distribution takes only the largest extreme values, hence the upper tail of the distribution is the most interesting part of the distribution. The distribution is skewed as follows of the tail.

In some cases, the need for a value which has a very little possibility of exceedance, is of great importance. In structural reliability analysis the chance of a load to exceed the resistance of a structure is investigated. Such studies need a large extreme value of the load to ensure the loading not being underestimating, thus collapse of the structure.

The formulas for Gumbel distribution or extreme-value distribution are expressed in the following equations:

$$f_X(x) = \alpha \cdot e^{(-\alpha(x-u)-e^{(-\alpha(x-u))})} \quad (2.31)$$

$$F_X(x) = e^{(-e^{(-\alpha(x-u))})} \quad (2.32)$$

Where,  $\alpha$  and  $u$  are Gumbel distribution parameters.

## 2.6 Characteristic and design values

Values for the different resistance and load variables can be found from the probability distributions. The most common way to determine the values is to use the characteristic value of the variable. The characteristic value is determined on behaviour of the distribution parameters for the variables and safety aspects. (2.33) shows the formula for the characteristic value of variable  $X$ .

$$x_k = \mu_X - K_X \cdot \sigma_X \quad (2.33)$$

As the formula shows, the characteristic value consists of the two most important parameters from the distribution function: mean value and standard deviation. In addition, the characteristic value is affected by a factor  $K_X$ .  $K_X$  is estimated on behaviour of the variable influence on the reliability.

Resistance variables prevent the structure to fail, hence need for a low enough characteristic value to ensure satisfying safety is of high importance. To ensure satisfying safety, underestimation of the characteristic values for the resistance variables are performed. This is done by using a low fractile-value. For normal distributed resistance variables, NS 3490 (NS) assume 5% fractile-value [10].

The 5% fractile-value means that in 95% of the cases, the variable value falls above this limit. In other word, there are 5% chance that the value of the variable is lower than the characteristic value.

For normal distributed load variables, the same procedure as for the resistance variables is used except that a 95% fractile-value is now assumed according to NS 3490 [10]. In load cases it is important to satisfy a characteristic value with low probability of exceedance.

When the fractile-value  $p$  is clarified, the  $K_X$  factor is estimated from the inverse cumulative distribution function for a standard normal distribution.

$$K_X = \Phi^{-1}(p) = F_X^{-1}(p) \quad (2.34)$$

## Design value

The most general form of checking a structure is to include some partial safety factors  $\gamma$ . The partial safety factor takes into account the fact that there might be some uncertainties related to the variables and that there is a 5% chance that the characteristic value is being exceeded.

Another important effect related to the partial safety factor, is the ability to adjust the variables. The variables are increased or decreased by multiplied or divided by the partial safety factor. When a characteristic value is divided or multiplied by a partial safety factor it becomes a design value.

$$r_d = \frac{r_k}{\gamma_R} \quad (2.35)$$

$$s_d = \gamma_S \cdot s_k \quad (2.36)$$

## 2.7 Structural reliability analysis

Structural Engineers' main task is to construct structures within an acceptable safety level. For this purpose, codes and standards have been developed to decide whether the structure is on the safe side or not. Although the codes state whether the structure is safe or not, it says nothing about the probability of failure for the structure. To get an insight in the probability of failure of a structure, structural reliability analysis is a well-applied tool.

### 2.7.1 Reliability, Risk and probability of failure

*“Reliability is defined as the probability that an item or facility will perform its intended function for a specific period of time, under defined conditions.”* [6]

This is a broad definition of the reliability concept, which indicates that the reliability concept is a useful tool in many areas. In a structural engineering context, the following statement better explains the definition of the structural reliability concept:

*“The probability that a structure will not attain each specified limit state (ultimate or serviceability) during a specified reference period.”* [7]

The limit state is a failure mode deciding whether the structure is on the safe side or not, further explained in following sections.

The reference period refers to the interval of time the structure is affected by the load or the estimated lifetime of the structure.

The reliability of a structure is the complementary event of the probability of failure for a structure, or stated in another way the probability of failure for a structure is the opposite of the probability for a structure to maintain stable during loading. Hence, the expression for the reliability of a structure becomes:

$$r = 1 - p_f \quad (2.37)$$

Where,  $p_f$  denotes the probability of failure for a structure.

### Probability of failure

The chance for a structure to fail is called the probability of failure. The calculation of the probability of failure is explained in the following sections and can be obtained by using different methods.

(2.37) shows that the probability of failure is the complement of the reliability, i.e. the probability of failure for a structure is equal to the probability of the total outcome space  $\Omega$  minus the probability of the structure to remain stable during loading or throughout the reference period.

### Risk

Risk is a measure of the magnitude of hazard in connection with an event. The estimation of risk is a function of the probability of failure and the extent of damage:

$$R = p_f \cdot E[D] \quad (2.38)$$

Here,  $R$  represent the term risk, while  $p_f$  and  $E[D]$  denotes the probability of failure and expected damage related to the event, respectively.

The expected damage (expected costs), can be given as numbers of injured (dead) people per event or in monetary units. Since the probability of failure is dimensionless, the term risk gets the same unit as the expected damage. Another way of calculating risk is by using the frequency of failure  $h_f$  instead of the probability of failure  $p_f$ .

$$R = h_f \cdot E[D] \quad (2.39)$$

An example of this could be injured (dead) people in car accidents per year. If the number of accident on a specific road is equal to 10 per year and the expected numbers of injured (dead) persons per accident is 3, the risk related to the road is equal to:  $R = 10 \text{ accidents per year} \cdot 3 \text{ injured} = 30 \text{ injured per year}$ .

In some cases, the calculation of risk is affected by some difficulties. For example, the probability of failure for a structure is usually very small, typically in the order of magnitude  $\{10^{-7} - 10^{-20}\}$ , while the expected damage related to the failure is extreme high.

By using (2.38) this result in a “zero-times-infinite” ( $0 \cdot \infty$ ) calculation of risk. This means that the risk may have any value between zero and infinite. In such cases, an impact assessment of the measures is often necessary.

In order to satisfy the requirement of structural reliability, the structure is classified into reliability classes. The classes depend on the consequences related to a failure and required security level. Different classes make different demands about the dimensioning. This is tabulated in codes and standards, see [10], [20]. This way, the risk (related to the structure) is included in the structural calculations.

## 2.7.2 Structural reliability problems

### Basic structural problem

Basic structural reliability problem consider one load variable  $S$  resisted by one resistance variable  $R$ , both with known probability density functions  $f_S(\cdot)$  and  $f_R(\cdot)$ . Resistance is the structures ability to resist loading. Resistance can be bending capacity, stress capacity, deflection criterions, shear strength, etc. External or internal forces inflict loading on the structure. External forces can be loads cased from climatic conditions like snow, wind, rain or other loads applied from the outside. Internal forces apply to loads caused from interactions between different elements in the structure. For example, a roof beam supported by two columns, here the forces are transferred from the beam to the two columns.

Failure of a structure may be determined from different criterion related to the reliability and serviceability of the structure, such as deflection, fractures, safety aspects, requirements for vibration, etc.

In the following, failure of the structure is assuming to occur when the load  $S$  exceed the capacity  $R$  of the structure (element) considered. The probability of failure can be expressed as:

$$p_f = P(R \leq S) = P(R - S \leq 0) \quad (2.40)$$

Or in a more general way

$$p_f = P[G(R, S) \leq 0] \quad (2.41)$$

Where,  $G(\ )$  is the *limit state function*, which define the limit between the safe and failure domain of the structure considered. In the safe domain, the structure maintain stable during loading, while in the failure domain the structure exceeds the safety limit and is qualified as damaged and unstable. Consequently, probability of failure is equal to the probability of limit state violation.

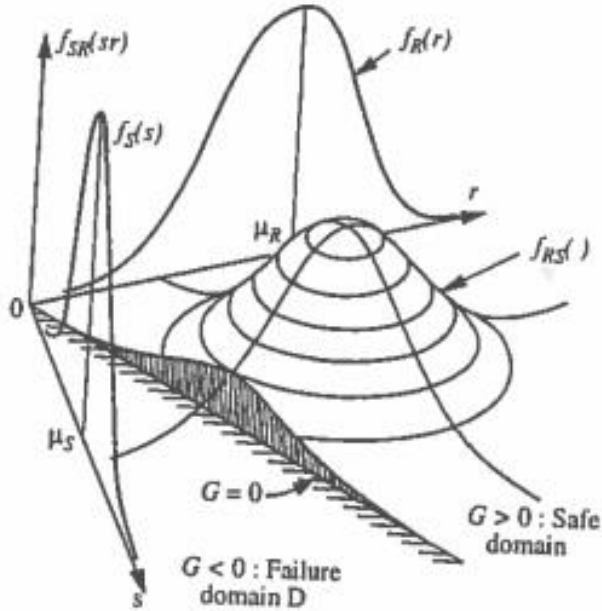


**Figure 2.8:** Two random variable joint density function  $f_{RS}(r, s)$ , marginal density functions  $f_R$  and  $f_S$  and failure domain  $D$  [8].

The probability of failure is equal to the integral of the joint density function (see sections 2.2.2 and 2.2.4) over the area where the load  $S$  exceed the resistance  $R$ , represented by the hatched failure domain  $D$  in figure 2.8. Hence, following equation for the probability of failure can be established:

$$p_f = P(R - S \leq 0) = \int_D \int f_{R,S}(r, s) dr ds \quad (2.42)$$

If  $R$  and  $S$  are independent, i.e.  $f_{R,S}(r, s) = f_R(r) \cdot f_S(s)$ , the probability of failure is equal to:

$$p_f = P(R - S \leq 0) = \int_{-\infty}^{\infty} \int_{-\infty}^{s \geq r} f_R(r) \cdot f_S(s) dr ds \quad (2.43)$$

provided  $x \geq t$ , and that the two variables  $R$  and  $S$  are independent, equation 2.43 can be further derived by using the formula of cumulative distribution function (2.6).



$$p_f = \int_{-\infty}^{\infty} F_R(x) \cdot f_S(x) dx \quad (2.44)$$

This integral is known as a convolution integral.

The best way of explaining the integral in (2.44), is to look at the failure condition of the problem. The structure will fail if the load exceeds the resistance, hence will the probability of structural failure be equal to the probability that the value of  $S$  exceeds the value of  $R$ .

Let  $x$  denote a given value of interest. If  $S$  is equal to  $x$ , then failure will occur if  $R$  is less than the given value  $x$ . The probability that  $S$  is equal to  $x$ , is explained in section 2.2.1 and found by using the probability density function. While the probability that  $R$  is less than a given value  $x$ , is found by using the cumulative distribution function as mention in section 2.2.2.

$$P(S = x) = f_S(x) \quad (2.45)$$

$$P(R < x) = F_R(x) \quad (2.46)$$

To find the total probability of failure, the product of the two probabilities need to be evaluated along the entire outcome space. If the two functions are continuously, the probability of failure is equal to the integral of the product over the total outcome space  $[-\infty, \infty]$ . Illustrated in figure 2.9.

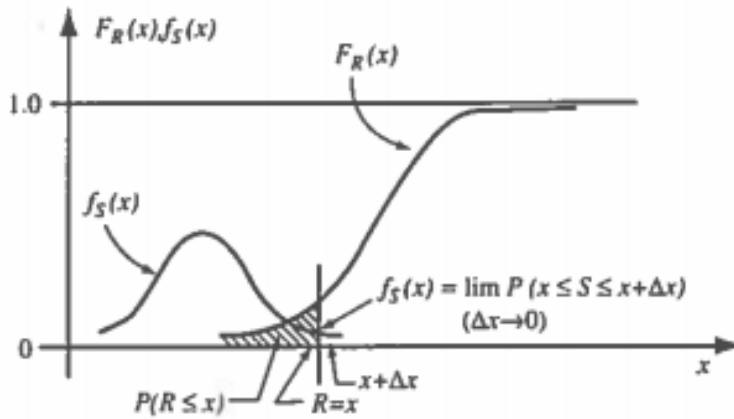


Figure 2.9: Basic R-S problem:  $F_R \cdot f_S$  representation [8].

An alternative expression for the convolution integral is by using the concept of complementary events:

$$p_f = \int_{-\infty}^{\infty} [1 - F_S(x)] \cdot f_R(x) dx \quad (2.47)$$

Which is simply :

*“the sum of the failure probabilities over all the cases of resistance for which load exceeds the resistance”*. [8]

### General structural problem

In many structural problems, this simplification of the problem is not adequate to use since it may not be possible to reduce the system into a simple one-to-one random variable problem, with one independent load  $S$  and one independent resistance  $R$  variable.

Resistance and load are often compound of more than one dependent variable. The bending capacity  $M_{Rd}$  may for instance be found by using material strength  $f_m$  and section modulus  $W$ . While the design moment  $M_{Ed}$  could follow from a uniformly distributed load  $Q$  over the length  $L$ . Both of the variables  $M_{Rd}$  and  $M_{Ed}$  depend on the dimensions of the structure, hence a dependency between the variables exists. There may also be cases where the loading or the resistance consist of more than one applied load or resistance component, e.g. the loading on a structure consist of both dead and live load.

The need for a more generalized version of the probability of failure expression is present. For this purpose, a definition of the basic variables related to the structure need to be performed.

Basic variables are fundamental variables, which define and characterize the behaviour and safety of a structure, e.g. dimensions, densities, material strength, etc. It is convenient to choose the basic variables so that they are independent, this is not always possible though.

When the basic variables are proposed, the simple  $R - S$  form of the limit state function can be replaced by a generalized expression in terms of all the basic variables. Assume a vector of all the basic variables involved in the problem  $\mathbf{X}$ , the simple variables for resistance  $R$  and load  $S$  expressed in terms of the basic variables may be established by the following equations:

$$R = G_R(\mathbf{X}) \quad (2.48)$$

$$S = G_S(\mathbf{X}) \quad (2.49)$$

Since the basic variables may be dependent, the cumulative distribution function for the variables  $R$  and  $S$  need to be obtained by a multiple integration over the relevant basic variables.

$$F_R(r) = \int_r \dots \int f_{\mathbf{X}}(x) dx \quad (2.50)$$

And similarly for the load variable.

The expression for the  $F_R$  and  $F_S$  can be used in (2.44) and (2.47), respectively.

A more convenient way of estimating the probability of failure is by generalize the limit state function  $G(R, S)$ . In order to do this, expression for the variables  $R$  and  $S$  from (2.48) and (2.49) are used.

$$G(R, S) \stackrel{X}{\Rightarrow} G(G_R(\mathbf{X}), G_S(\mathbf{X})) \Rightarrow G(\mathbf{X}) \quad (2.51)$$

Example of a general limit state function:  $G = f(Q, G, E, D, X_m, c)$ . Where, the random variables  $\mathbf{X}$  are divided into variables of loads and actions  $Q$ , permanent loads  $G$ , material properties  $E$ , geometrical parameters  $D$  and model uncertainties  $X_m$ . The variable  $c$  takes into account the influence of constants in the limit state function.

With the limit state function expressed as  $G(\mathbf{X})$ , the generalization of the expression for the probability of failure becomes:

$$p_f = P[G(\mathbf{X}) \leq 0] = \int \dots \int_{G(\mathbf{X}) \leq 0} f_{\mathbf{X}}(\mathbf{x}) d\mathbf{x} \quad (2.52)$$

Where, the joint density function  $f_{\mathbf{X}}(\mathbf{x})$ , becomes integrated over the space of limit state violation  $G(\mathbf{X}) \leq 0$ , as is equal to the failure domain  $D$  in figure 2.8.

If the basic variables are independent, the expression for the joint density function is equal to the product of the marginal density function for all the variables, see (2.16).

If the basic variables are dependent, the complexity increases and the concept of conditional probability needs to be included, see (2.15).

There are essentially three ways of solving the multi-dimensional integration in (2.52):

1. Direct integration: This is possible only for some few special cases.
2. Transformation of the integrand to establish remarkable properties to determine (approximately) the probability of failure. So-called “*First Order Second Moment*” methods.
3. Numerical integration: Simulate values to perform the integration required, such as the Monte Carlo simulation.

In the following sections, the three methods are further explained and performed by analysing structural problems.

## 2.8 Direct integration

For some special cases, the convolution integral (2.44) is possible to solve analytically. The method introduce a new parameter called the reliability index (safety index). The concept of reliability index  $\beta$ , was invented by the American Professor C. A. Cornell [13], hence the method is also named the method of Basler/Cornell (Basler invented the method in notation of Cornell). The index is a measure of the safety level for an element considered and has subsequently been improved in different ways.

## Ch. 2 Statistics and structural reliability

The main concept of the method is to establish a random variable for the safety aspects with known distribution parameters. The random variable  $M$ , called the safety margin, is assumed to be normal distributed and is equal to the limit state function:

$$M = G(X) \quad (2.53)$$

and can be seen in figure 2.10

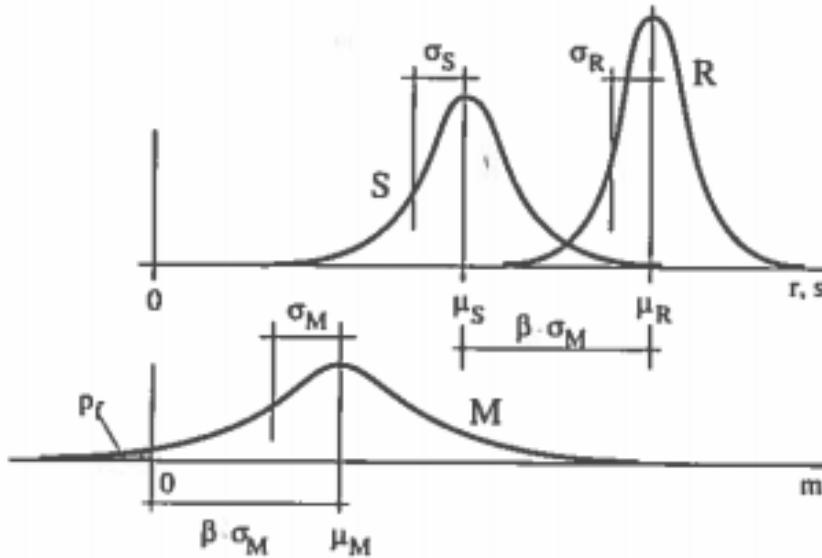


**Figure 2.10:** Shows the problem with its variables  $R$ ,  $S$  and  $M$  [6].

The reliability index  $\beta$ , is the distance between the failure domain and the mean value of the structure measured in standard deviations, as can be seen in the lower diagram in figure 2.10. From this observation following formula for the reliability index can be derived:

$$\beta = \frac{\mu_M}{\sigma_M} \quad (2.54)$$

Where  $\mu_M$  and  $\sigma_M$  are the mean values and standard deviation for the safety margin, respectively. These distribution parameters can be calculated by using computational rules and the distribution parameters for the basic variables.

$$\mu_M = \mu_R - \mu_S \quad (2.55)$$

$$\sigma_M^2 = \sigma_R^2 + \sigma_S^2 - 2\rho_{RS}\sigma_S\sigma_R \quad (2.56)$$

Where,  $\rho_{RS}$  is the correlation coefficient for the two variables.

If the random variables are uncorrelated, i.e.  $\rho_{RS} = 0$ , the variance for the safety margin is equal to:

$$\sigma_M^2 = \sigma_R^2 + \sigma_S^2 \quad (2.57)$$

From the reliability index  $\beta$ , the probability of failure can be estimated by using the following equation:

$$p_f = \Phi(-\beta) \quad (2.58)$$

Where  $\Phi(\cdot)$  is the standard normal distribution function, with zero mean and unit variance. Values for the cumulative distribution function, for different input values of  $\beta$ , are tabulated in appendix B. It is important to note that the probability of failure is obtained from the standard normal distribution, hence the results will only be exactly for normally distributed variables.

In the following, an example is performed in order to give a better understanding of the procedure of the method.

### 2.8.1 Example 2.1

Consider a simple supported beam (shown in figure 2.11), applied by one single load variable  $S$  resisted by one resistance variable  $R$ .

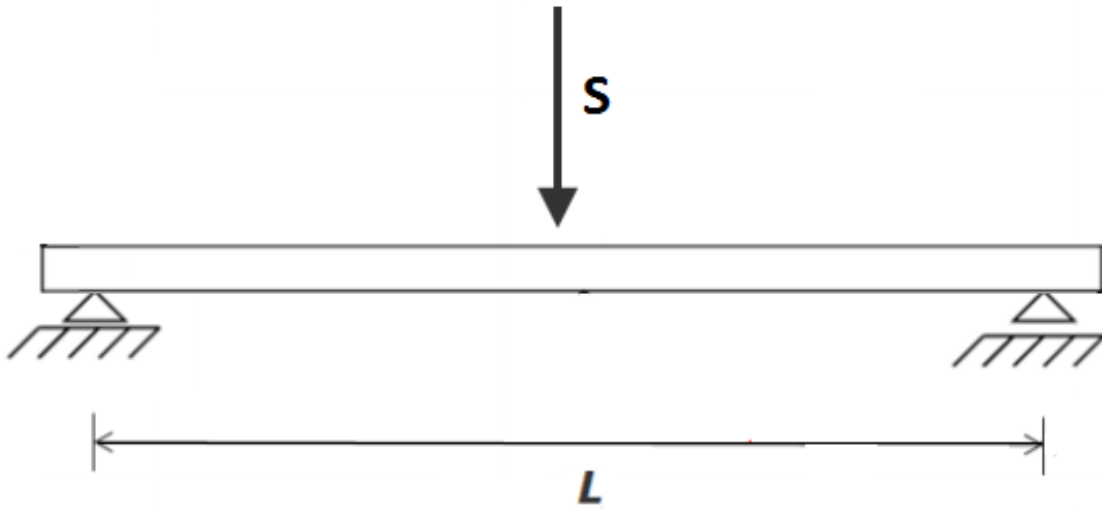


**Figure 2.11:** Simple supported beam with length  $L$ , loaded by a concentrated load  $S$ .

The random variables  $R$  and  $S$  are normally distributed, with mean value and standard deviation equal to:

$$R \sim N(10kNm, 2.25kNm)$$

$$S \sim N(3kN, 1kN)$$

The structure fails if the bending moment from the load  $S$  exceeds the bending capacity  $R$ . The applied bending moment can be estimated from following formula, see [10]:

$$M_{Ed} = \frac{S \cdot L}{4} \quad (2.59)$$

Where  $L$  is the length of the beam and is deterministic equal to 5 m.

Consequently, following failure limit state equation can be established:

$$G = R - \frac{5 \cdot S}{4} = 0 \quad (2.60)$$

The safety margin equals the limit state function, hence the safety margin equals:

$$M = R - \frac{5 \cdot S}{4} \quad (2.61)$$

With distribution parameters equal to:

$$\mu_M = \mu_R - \frac{5 \cdot \mu_S}{4} = 10 - \frac{5 \cdot 3}{4} = 6.25 \text{ kNm} \quad (2.62)$$

$$\sigma_M^2 = \sigma_R^2 + \left(\frac{5 \cdot \sigma_S}{4}\right)^2 = 2.25^2 + \frac{25}{16} \cdot 1^2 = 3.81 \text{ kNm} \quad (2.63)$$

From these distribution parameters, the safety index  $\beta$  is estimated, hence the probability of failure is determined.

$$\beta = \frac{\mu_M}{\sigma_M} = \frac{6.25}{\sqrt{3.81}} = 3.20 \quad \Leftrightarrow \quad p_f = \Phi(-3.20) = 7 \cdot 10^{-4} \quad (2.64)$$

## 2.9 Second – Moment and Transformation Methods

The integration of (2.52) cannot be solved analytically except for some special cases. In order to solve the integral, methods to simplify the integration process have developed. A dominant and well-known method is described in the following section.

The method bypassing the integration of (2.52) by transforming the integrand  $f_X(\mathbf{x})$  to a multi-normal probability density function, and then perform reliability estimations in accordance with the procedure stated in section 2.8.

The reliability estimation is carried out by combining the first two moments of each variable i.e. mean value and standard deviation, hence the name *Second-Moment* method. This way of calculating the reliability index provides only exact probability of failure if the random variables are normal distributed. When the variables have other distribution, the procedure only provide a nominal failure probability.

### 2.9.1 The method of Hasofer and Lind

The method of Hasofer and Lind is a state-of-the-art in reliability analysis, because of the wide area of application.

The method rely on the work of Basler/Cornell, i.e. the reliability index estimation (section 2.8). The main difference is that the method of Hasofer and Lind transform the limit-state function into a standard normal space before calculation of the reliability index. The transformation process is shown in (2.28). By doing the transformation, the ability to solve complex limit state functions are possible. The transformation is done by standardised the variables in the limit state function. See [14], for a more extended version of the method.

An example is performed in order to illustrate the method.

## 2.9.2 Example 2.2

Again, consider the simple supported beam in figure 2.11.

Now, assume that the limit state function consists of only two random variables  $R$  and  $S$ :

$$G = R - S \quad (2.65)$$

Where  $R$  is the resistance capacity and  $S$  is the applied loading, both measured in  $[kN]$ .

The variables  $R$  and  $S$  are transformed into standardised variables  $U_1$  and  $U_2$ , by using the following formulas:

$$U_1 = \frac{R - \mu_R}{\sigma_R} \quad \rightarrow \quad R = U_1 \cdot \sigma_R + \mu_R \quad (2.66)$$

$$U_2 = \frac{S - \mu_S}{\sigma_S} \quad \rightarrow \quad S = U_2 \cdot \sigma_S + \mu_S \quad (2.67)$$

The new variables  $U_1$  and  $U_2$  are standard normal distributed with mean value equal to zero and standard deviation equal to one. The expression for the variables  $R$  and  $S$  are inserted into the limit state function, which will lead to a limit state function consisting only of the standard normal distributed variables  $U_1$  and  $U_2$ :

$$\begin{aligned} G &= R - S \\ &= (U_1 \cdot \sigma_R + \mu_R) - (U_2 \cdot \sigma_S + \mu_S) \quad (2.68) \\ &= (\mu_R - \mu_S) + U_1 \cdot \sigma_R - U_2 \cdot \sigma_S \end{aligned}$$

The safety index  $\beta$  can now be obtained analytical or graphic.

Analytical estimation of  $\beta$  is done by using the method of Basler/Cornell, see (2.54), where the moments of the safety margin is equal to:

$$\mu_M = (\mu_R - \mu_S) + \mu_{U_1} \cdot \sigma_R - \mu_{U_2} \cdot \sigma_S \quad (2.69)$$

$$\sigma_M = \sqrt{(\sigma_{U_1} \cdot \sigma_R)^2 + (\sigma_{U_2} \cdot \sigma_S)^2} \quad (2.70)$$

Since the two random variables are independent and normal distributed and the limit state function is linear, no transformation is needed. Thus, the probability of failure can be calculated from (2.58).

Graphic estimation of  $\beta$  is best illustrated by figure 2.12.

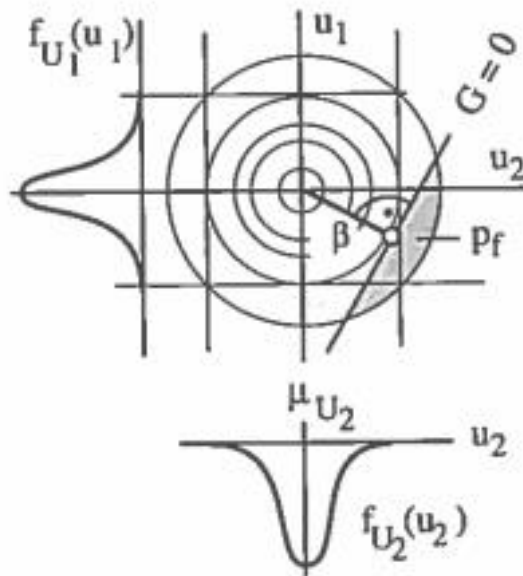


**Figure 2.12:** Shows plot of the marginal and bivariate pdf, along with limit state function in standard normal space [6].

The limit state function is transformed into the standard normal space, represented with the standardised variables  $U_1$  and  $U_2$ . The limit state equation  $G = 0$  separates the failure domain from the safety domain. The reliability index  $\beta$  is defined as the shortest way from origin to the limit state equation  $G = 0$ . Least square sentences are a helpful tool in finding the safety index  $\beta$ .

The point at the limit state equation closest to the origin is called the design point. The coordinates for the design point can be estimated from the reliability index and the sensitivity index  $\alpha$  for each normal distributed variables  $U_i$ :

$$u_i^* = \beta \cdot \alpha_i \quad (2.71)$$

Where, the sensitivity index  $\alpha$  is a measure of the contribution of each variable in the limit state function and may be established from following formula:

$$\alpha_i = \frac{c \cdot \sigma_i}{\sigma_M} \quad (2.72)$$

Notice, that the term  $c$  in the formula represent the constant variable related to the variable  $i$ .

In example 2.1,  $c = \frac{5}{4}$ .



In original coordinates, the design point is equal to:

$$x_i^* = u_i^* \cdot \sigma_i - \mu_i \quad (2.73)$$

The method explained above is only valid for linear limit state functions, with independent, normally distributed variables. For other limit-state functions, the method is just an approximation. In the upcoming sections, an extended version of the Hasofer and Lind method is presented.

### 2.9.3 Extensions of the Hasofer and Lind method

The extension of the Hasofer and Lind method includes the facts that a limit state function:

1. May contain more than two variables
2. May not be linear
3. May contain variables with any kind of distributions

#### More than two variables

When a limit state function contains more than two variables, it is generally written as:

$$G = a_0 + \sum_{i=1}^n a_i \cdot X_i \quad (2.74)$$

Where,  $a_0$  denotes the constant term, while  $a_i$  represent the factor multiplied with the random variable  $X_i$ .  $X_i$  is a given basic variable with distribution parameters  $\mu_i$  and  $\sigma_i$ .

The reliability index  $\beta$  and the failure of probability  $p_f$  are found by (2.54) and (2.58). Where  $\mu_M$  and  $\sigma_M$  are estimated from following equations:

$$\mu_M = a_0 + \sum_{i=1}^n a_i \cdot \mu_i \quad (2.75)$$

$$\sigma_M = \sqrt{\sum_{i=1}^n (a_i \cdot \sigma_i)^2} \quad (2.76)$$

#### Non-linear limit state function

For non-linear limit state functions, the concept of Taylor series and iteration are used. The limit state function is approximate as a Taylor series.

$$G \approx G(x_i^*) + \sum_{i=1}^n (X_i - x_i^*) \cdot \left. \frac{\partial G}{\partial X_i} \right|_* + \dots$$

$$\approx G(x_i^*) - \sum_{i=1}^n x_i^* \cdot \frac{\partial G}{\partial X_i} \Big|_* + \sum_{i=1}^n X_i \cdot \frac{\partial G}{\partial X_i} \Big|_* \quad (2.77)$$

Further simplification of the equation leads to:

$$G \approx a_0 + \sum_{i=1}^n a_i \cdot X_i \quad (2.78)$$

Where the terms  $a_0$  and  $a_i$  are expressed in the following equations:

$$a_0 = G(x_i^*) - \sum_{i=1}^n a_i \cdot x_i^* \quad (2.79)$$

$$a_i = \frac{\partial G}{\partial X_i} \Big|_* \quad (2.80)$$

Approximation of this kind, using only the first order term of the Taylor series, is called the First Order Reliability Method (FORM). Consequently, if approximation including the second order term as well, the method is known as the Second Order Reliability Method (SORM).

The sensitivity factor  $\alpha$  can be found by using the terms  $a_i$  from the Taylor approximation and the standard deviations of the variable  $i$ . The safety margin  $M = G$ :

$$\alpha_i = \frac{a_i \cdot \sigma_i}{\sigma_M} \quad (2.81)$$

The sensitivity factor  $\alpha$  and the reliability index  $\beta$  determine the fractile-value for the variable. Consequently, (together with the distribution parameters for the variable) design point values for the variables can be estimated by the following formula:

$$x^* = \mu_X - \alpha_X \cdot \beta \cdot \sigma_X \quad (2.82)$$

Notice, the sensitivity index is positive for load variables, while it is negative for resistance variables.

After approximation of the non-linear limit state function, the iteration process in order to obtain the optimal design point starts. First the design point  $X^*$  or the starting point for the iteration process is chosen. The mean or characteristic values of the variables are often used.

From the design point it is possible to calculate the mean value and standard deviation of the safety margin, reliability index, sensitivity index, and hence a new design point from the formulas mention above. The iteration process becomes as follows:

1. Determine design point ( $X^*$ ). Starting point values in first iteration.

2. Calculate the values of  $a_0$  and  $a_i$  by inserting values from step 1 into (2.79) and (2.80).
3. Estimate  $\mu_M$  and  $\sigma_M$  from (2.75) and (2.76)
4. Calculate  $\beta$  from estimates in step 3 and (2.54).
5. Calculate  $\alpha_i$  from (2.81) and previously estimates of the parameters  $\sigma_M$ ,  $\sigma_i$  and  $a_i$ .
6. Calculate a new design point from (2.82).

The iteration process goes on until the deviation between prior and posterior reliability index  $\beta$  convergence against zero. When this is done the failure of probability is found from (2.58).

### Non-normally distributed variables

Non-normally distributed variables are often entering in structural reliability analysis. There are two main approaches for estimating the reliability index, when the variables are non-normally distributed:

1. Tail approximation
2. Transformation into standard-normal space

The latter approach consists of a transformation of all variables into the standard normal space. This transformation is mentioned earlier in this section (2.9.1 and 2.9.2). Such transformation often results in complex non-linear limit state functions.

The tail approximation replaces the original distribution by an equivalent normal distribution at the design point. To make the approximation valid, the equivalent normal density and distribution function needs to be equal to the origin distribution functions at the design point.

$$F_X(x^*) = F_X^N(x^*) \quad (2.83)$$

$$f_X(x^*) = f_X^N(x^*) \quad (2.84)$$

The equivalent normal distribution parameters are obtained from the following formulas:

$$\mu_X^N(x^*) = x^* - \sigma_X^N(x^*) \cdot \Phi^{-1}(F_X(x^*)) \quad (2.85)$$

$$\sigma_X^N(x^*) = \frac{1}{f_X(x^*)} \cdot \varphi(\Phi^{-1}(F_X(x^*))) \quad (2.86)$$

These normal distribution parameters are used in further calculation of the reliability index and failure probability. Such calculations are performed by using equations as mentioned previously in this section.

### 2.9.4 Example 2.3

Consider a beam loaded by a concentrated force  $P$  as shown in figure 2.13.

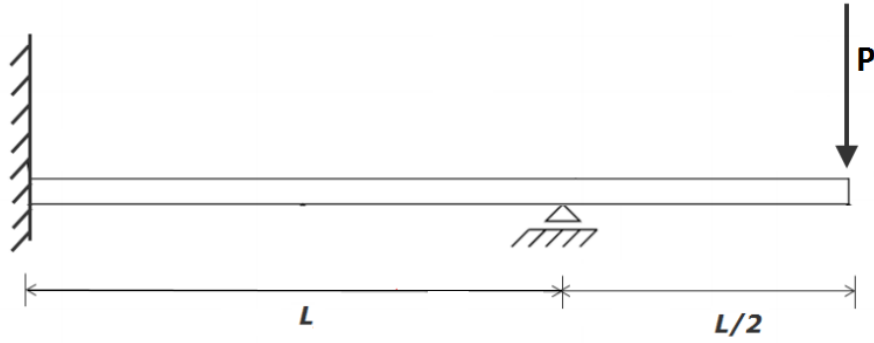


Figure 2.13: Rigidly clamped beam loaded by concentrated load  $P$ .

The beam fails if the maximum deflection  $u_{max}$  from  $P$  exceeds the deflection failure criterion [7]:

$$u_{max} \geq \frac{1}{30}l \quad (2.87)$$

The maximum deflection of the beam can be found from following formula, see [10]:

$$u_{max} = \frac{5 Pl^3}{48 EI} \quad (2.88)$$

Where,  $P$  is the concentrated load,  $l$  is the length of the span,  $E$  is the modulus of elasticity and  $I$  is the relevant moment of inertia.

Assume that  $P, I$  and  $E$  are uncorrelated random variables with mean values and standard deviations equal to:

$$\begin{aligned} P &\sim \text{Gumbel}(4 \text{ kN}, 1 \text{ kN}) \\ E &\sim \text{Normal}\left(2 \cdot 10^7 \frac{\text{kN}}{\text{m}^2}, 0.5 \cdot 10^7 \frac{\text{kN}}{\text{m}^2}\right) \\ I &\sim \text{Normal}(10^{-4} \text{ m}^4, 0.2 \cdot 10^{-4} \text{ m}^4) \end{aligned}$$

The length of the beam is deterministic and equal to  $l = 5\text{m}$ . By inserting the length into (2.87) and (2.88), the limit state equation of the beam becomes:

$$G = EI - 78.12P \leq 0 \quad (2.89)$$

The basic variables are then standardized by using Hasofer/Lind transformation as in example 2.2. This lead to following limit state function:

$$G = (10^{-4} + 0.2 \cdot 10^{-4}U_1)(2 \cdot 10^7 + 0.5 \cdot 10^7U_2) - 78.12(\mu_P^N + \sigma_P^N U_3) = 0 \quad (2.90)$$

Where the standard normal distributed variables  $U_1, U_2$  and  $U_3$  represent the basic variables  $I, E$  and  $P$ , respectively.

The safety margin equals the limit state function obtained in (2.90), hence:

$$M = (10^{-4} + 0.2 \cdot 10^{-4}U_1)(2 \cdot 10^7 + 0.5 \cdot 10^7U_2) - 78.12(\mu_P^N + \sigma_P^N U_3) \quad (2.91)$$

Distribution parameters of the safety margin, i.e. mean value and standard deviation, provides values of the reliability index according to (2.54).

The basic variable  $P$  is Gumbel distributed, thus a transformation into a normal distributed variable with mean value  $\mu_P^N$  and standard deviation  $\sigma_P^N$  is needed. The parameters are found by using the formula (2.85), (2.86) and value for the design point. Design point corresponding to the Gumbel distribution is estimated by inverting the formula in (2.32):

$$u_3^G = F_P^{-1}(F_N(u_3)) = F_P^{-1}(\Phi(u_3)) \quad (2.92)$$

and inserting the design point value for the standard normal distributed variable  $u_3$ .

96% and 4% fractile values are assumed to be the starting point for the standardized variables. This corresponding to starting point values equal to  $\mathbf{u} = \pm 1.74$  (negative value for resistance variables, positive value for the load variable). From this starting point following parameter values for the normal distributed variable  $P$  are obtained:

$$\begin{aligned} u_3^G &= F_P^{-1}(1.74) = 6.03 \\ \mu_P^N &= 3.05 \\ \sigma_P^N &= 1.71 \end{aligned} \quad (2.93)$$

Since the problem consist of a non-linear limit state function an iterative process, with steps as stated in **non-linear limit state function**, it needs to be performed in order to estimate the reliability index. Values from the iteration process is shown in figure 2.14.

| Iteration    | 1     | 2     | 3     | 4     | 5     | 6     |
|--------------|-------|-------|-------|-------|-------|-------|
| $u_1$        | -1,74 | -1,88 | -1,25 | -0,81 | -0,66 | -0,61 |
| $u_2$        | -1,74 | -2,71 | -3,02 | -3,13 | -3,18 | -3,20 |
| $u_3$        | 1,74  | 1,11  | 1,03  | 0,85  | 0,73  | 0,67  |
| $\Phi(u_3)$  | 0,96  | 0,87  | 0,85  | 0,80  | 0,77  | 0,75  |
| $u_3^G$      | 6,03  | 5,07  | 4,95  | 4,73  | 4,58  | 4,52  |
| $F_N(u_3^G)$ | 0,96  | 0,87  | 0,85  | 0,80  | 0,77  | 0,75  |
| $f_N(u_3^G)$ | 0,05  | 0,16  | 0,18  | 0,23  | 0,26  | 0,28  |
| $\sigma_P^N$ | 1,71  | 1,35  | 1,31  | 1,23  | 1,17  | 1,15  |
| $\mu_P^N$    | 3,05  | 3,56  | 3,61  | 3,69  | 3,73  | 3,75  |
| $\mu_M$      | 0,73  | 0,61  | 0,67  | 0,73  | 0,75  | 0,76  |
| $\sigma_M$   | 0,21  | 0,18  | 0,20  | 0,22  | 0,23  | 0,23  |
| $\beta$      | 3,49  | 3,43  | 3,34  | 3,33  | 3,32  | 3,32  |
| $\alpha_1$   | -0,54 | -0,36 | -0,24 | -0,20 | -0,18 | -0,18 |
| $\alpha_2$   | -0,78 | -0,88 | -0,94 | -0,96 | -0,96 | -0,96 |
| $\alpha_3$   | 0,32  | 0,30  | 0,26  | 0,22  | 0,20  | 0,20  |

Figure 2.14: Excel script from the iterative calculation.

The values tend to converge against a solution after approximately 6 iterations, as can be seen in figure 2.14. The reliability index becomes equal to approximately 3.32, which give a probability of failure of:

$$\beta = 3.32 \rightarrow p_f = \Phi(-\beta) = 4.5 \cdot 10^{-4} \quad (2.94)$$

Further, values of the sensitivity index  $\alpha_i$  becomes:

| Random variable            | Sensitivity factor $\alpha_i$ |
|----------------------------|-------------------------------|
| Moment of inertia, $I$     | -0.18                         |
| Modulus of elasticity, $E$ | -0.96                         |
| Concentrated load, $P$     | 0.20                          |

Table 2.1: Estimated values for the sensitivity factors  $\alpha_i$ .

The values of the sensitivity factors indicate that modulus of elasticity has a significant contribution of impact in the limit state function, while the relevant moment of inertia and the concentrated load have less contribution in the limit state function, provided values for the variables given in this example.

## 2.10 Numerical iteration

Numerical iteration may solve complex problems where more than two variables are involved and/or dependency between the variables exists. Still there is some cons related to the

numerical solution tool. Growth of round-off errors and excessive computation times when the dimensions of the integration increases.

Since limit state functions tend to be more general than a linear function and that the variables rarely are normal distributed, methods to deal with this problem are developed. Because of the increase in dimensions causes increasing computational effort, numerical methods to deal with large integration problems are developed. These methods are simulations or Monte Carlo methods. In the following section, different Monte Carlo methods are explained.

### 2.10.1 Monte Carlo Methods

Monte Carlo methods are used in cases where the complexity makes the use of other methods too difficult and time-consuming. By using a high number of samples, the accuracy may increase as the estimation of failure of probability occurs.

The Monte Carlo method is based on measurements of the limit state violation, i.e. when  $G(\mathbf{X} \leq 0)$ . In order to estimate the probability of failure, values for the basic variables are generated and inserted into the limit state function. An index  $I$  is made to count for every violation of the limit state function.

The probability of failure is found from the following equation.

$$p_f = \frac{\# \text{ of failure}}{\# \text{ of tests}} = \frac{I}{n} \quad (2.95)$$

Where,  $n$  is the number of simulations conducted.

This way of estimating the probability of failure is called Crude Monte Carlo simulation and is the most familiar of the Monte Carlo methods. The method strongly depends on the computational effort of the computer programs in order to get accurate results (high number of simulations). Because of this, extensions of the method have been developed in order to get acceptable results with reduce computational effort.

#### Important sampling

Important sampling is a more efficient approach of the Monte Carlo method, which can bring enormous gains by reducing the number of simulations needed for an acceptable result. The essence of the method:

*“... take draws from an alternative distribution whose support is concentrated in the truncation region.”*[15]

Principle is to drawn values from specific intervals that are more valuable than others are (they give greater function values), which result in a more accurate result. A probability curve  $p(x)$  may be established to indicate the intervals of greater impact. The principle is:

$$I = \int_F x \cdot f(x) dx = \int_P \frac{f(x)}{p(x)} \cdot p(x) dx \quad (2.96)$$

Where  $\int p(x) dx = 1$ .

### Confidence interval

Deviations of the obtained failure probability might occur, because of the inherent uncertainty related to the simulation method. The variation in the results, however, decreases as the number of simulations increases. In order to obtain result within acceptable limits confidence intervals for the estimator  $p_f$  are applied.

Confidence interval gives an upper and lower limit for the estimated parameter. An approximated  $(1 - \alpha) \cdot 100\%$  confidence interval for  $p_f$  can be estimated from:

$$C^- \leq p_f \leq C^+ \quad (2.97)$$

The limits  $C^\pm$  are established from:

$$C^\pm = p_f \pm z_{\frac{\alpha}{2}} \sigma_{p_f} \quad (2.98)$$

Where,  $z_{\frac{\alpha}{2}}$  is a critical value in the standard normal distribution, values for the parameter is tabulated in appendix B.

The standard deviation of the estimated probability of failure  $\sigma_{p_f}$  can be found from:

$$\sigma_{p_f} = \sqrt{\frac{p_f(1 - p_f)}{n}} \quad (2.99)$$

The number of simulations  $n$ , needed in order to achieve acceptable results, might be obtained by taking advantage of the concept coefficient of variation (2.11) and rewrite the formula above:

$$n = \frac{1 - p_f}{p_f \cdot COV^2} \quad (2.100)$$

It is assumed that the mean value of the probability of failure is equal to the estimated probability of failure, i.e.  $\mu_{p_f} = p_f$ . In almost every large and complex structures, probability of failure is small enough to assume:  $1 - p_f \approx 1$ .

Consider a beam similar to figure 2.13. Assume that the estimated probability of failure is approximately equal to  $p_f \approx 10^{-7}$ , and the coefficient of variation is equal to  $\rho_{p_f} = 0.1$ . By using the formula in (2.100),  $n \approx 10^9$  simulations are needed in order to achieve acceptable results of the standard deviation  $\sigma_{p_f}$ .

### Generation of basic variables

The number generation described in this section is only valid for a single variable with known probability distribution and distribution parameters.



Values of the basic variable are generated by using a computer program with a random number generator, e.g. MATLAB or Excel. The random number generator produce random numbers  $n_i$  between zero and one. Values for the variable are estimated by invert the cumulative distribution function  $F_X(x)$  for the variable and make use of the produced random number  $n_i$ :

$$x_i = F_X^{-1}(n_i) \quad (2.101)$$

Figure 2.15 shows this.

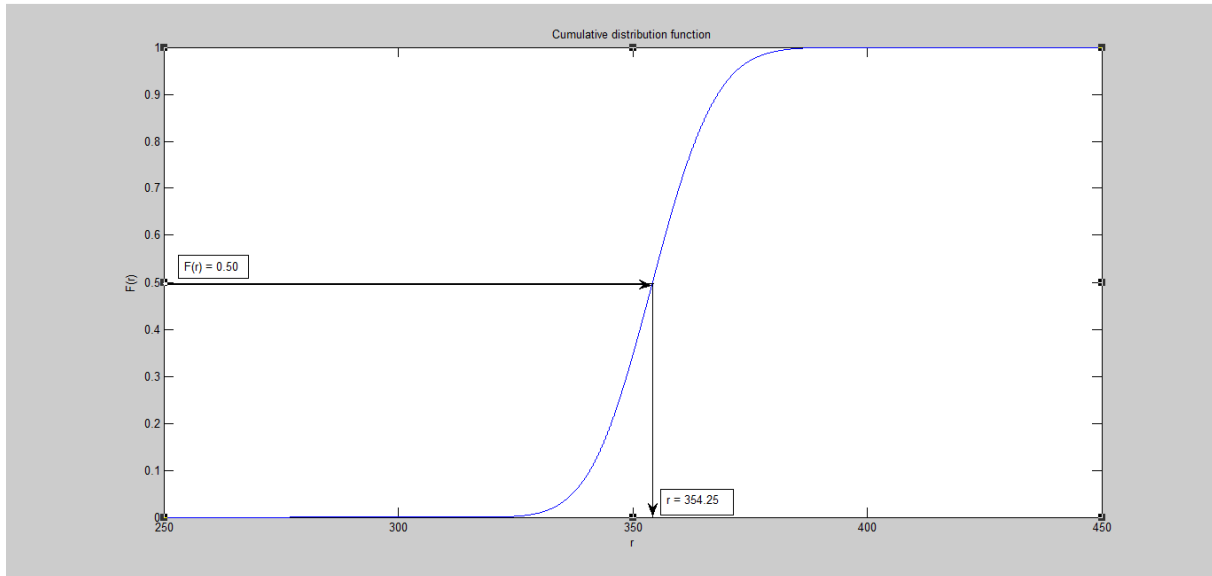


**Figure 2.15:** Generation of random variables. The cdf fits the lognormal distributed variable  $R$  of the example 2.4 in section 2.10.1

The distribution function related to the variable account for the characteristics about the distribution, i.e. generated values for a normal distributed variable, with mean equal to zero, tend to be around zero. The reason for this is that the cumulative distribution function decide the outcome of the variable value. If the slope is steep at an interval  $[a, b]$  at the vertical axis, all generated numbers within the interval will cause approximately the same values for the variable. Figure 2.16 shows the variation in values from the same generated number for two different distributions.

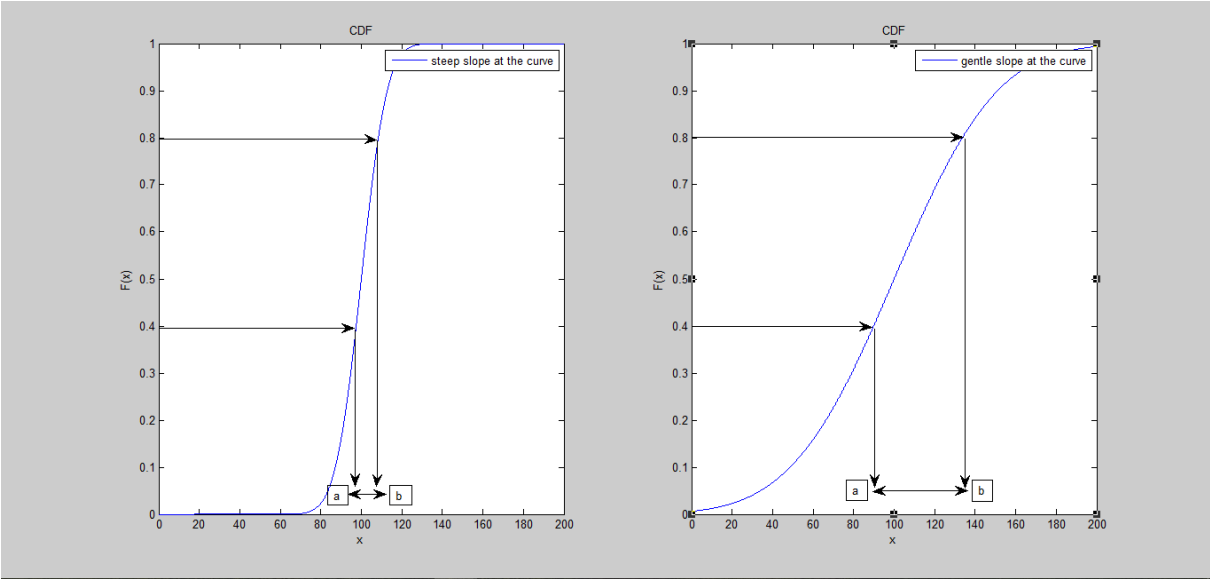


Figure 2.16: Cdf for normal distributed variable X, with different variances (steep and gentle slope).

2.10.2 Example 2.4

Once more, a simply supported beam with load effect S and resistance capacity R is considered.

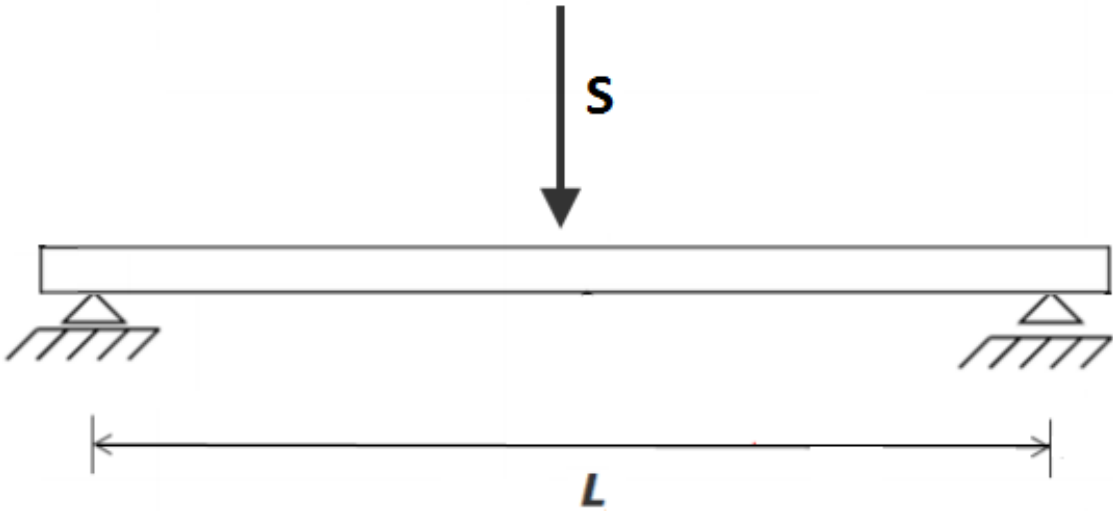


Figure 2.17: Simply supported beam with concentrated load S and length L.

Now assume that the resistance R is Log Normal distributed and the load effect S is Gumbel distributed, with following distribution parameters:

$$R \sim \text{Log } N(5.87, 0.03) \text{ [MPa]}$$

$$S \sim \text{Gumbel}(100, 10) \text{ [kN]}$$

The beam is assumed to fail if the moment from the applies load  $P$  exceeds the resistance capacity, see [10]:

$$G(R, S) = R \cdot W - \frac{SL}{4} \leq 0 \quad (2.102)$$

Where  $W$  is the section modulus and  $L$  is the length of the beam and is deterministic  $L = 5m$ .

Values for the variables  $R$  and  $S$  are generated by using the method stated above (section 2.10.1 generation of basic variables). The generalizations  $r$  and  $s$  are thus inserted in the limit state function:

$$G(r, s) = r_i \cdot W - \frac{s_i \cdot L}{4} \quad (2.103)$$

This procedure is repeated  $10^6$  times. In 139 cases failure occur, hence the probability of failure becomes:

$$p_f = \frac{139}{10^6} = 1.39 \cdot 10^{-4} \quad (2.104)$$

### 2.10.3 Enhanced Monte Carlo method

The method was presented by Næss et al. at Department of Mathematical Sciences, NTNU.

*“The aim of this method is to reduce computational cost while maintaining the advantages of crude MC simulation...”* [17]

The main idea behind the method is to enable prediction of the probability of failure by utilizing available results, i.e. making a function in order to predict the probability of failure. A brief presentation of the method is presented in the this section.

Probability of failure is equal to the probability of limit state violation,  $p_f = P(M \leq 0)$ . In order to obtain the probability of failure, when large number of simulation is required, a “reduced” limit state function is created:

$$M(\lambda) = M - \mu_M(1 - \lambda) \quad (2.105)$$

Where  $\lambda$  is a scaling factor between zero and one. Consequently, the probability of failure for the new limit state function is equal to:

$$p_f(\lambda) = P[M(\lambda) \leq 0] \quad (2.106)$$

As can be seen from (2.105),  $M(1) = M$ , hence  $p_f(\lambda \neq 1) > p_f$ . This indicate that less simulations  $n$  is needed in order to obtain failure probabilities for the reduced limit state function, provided that  $\lambda < 1$ .

Crude Monte Carlo method often requires large number of simulations  $n$  in order to achieve acceptable results, when the probability of failure are approaching zero (small values). This

makes the method time-consuming and comprehensive, hence Enhanced Monte Carlo method is preferred used.

The probability of failure is assumed to behave as follows:

$$p_f(\lambda) \approx q \cdot \exp\{-a(\lambda - b)^c\} \quad (2.107)$$

When  $\lambda \rightarrow 1$ , the probability of failure converge against the true solution.  $q, a, b, c$  are unknown parameters, which can be estimated by using a number  $i \in \{1, \dots, m\}$  of known data point for different values of  $\lambda$ , i.e.  $(\lambda_i, p_f(\lambda_i))$ . The parameters are optimized by minimizing the mean square error function on the log level, i.e. minimizing the sum of following function for all data point  $m$ .

$$F(q, a, b, c) = \sum_{i=1}^m w_i (\log(p_f(\lambda_i)) - \log(q) + (a(\lambda_i - b)^c)^2 \quad (2.108)$$

$w_i$  is a weighting factor, which emphasis more reliable data point and prevents the heteroscedasticity of the estimation problem at hand. In the following calculations, the weighting factor is assumed to be calculated by following equation:

$$w_i = (\log C^+(\lambda_i) - \log C^-(\lambda_i))^{-2} \quad (2.109)$$

$C^\pm(\lambda_i)$  is the upper and lower limit related to the confidence interval for the estimator  $p_f$ . Formula for the confidence interval is given in (2.98).

As follows from the mean square error function, if  $p_f(\lambda_i) = 0$  the minimizing process will stop. Thus, lower values of  $\lambda$  need to be chosen. The minimization of the mean square error function is performed with a Levenberg–Marquardt least squares optimization method included in the MATLAB function *lsqnonlin* [18]. For a more extensive presentation of the Enhanced Monte Carlo method, see [16].

### 2.10.5 Example 2.5

Assume a simply supported beam, as seen in figure 2.17, exposed to a concentrated force  $S \sim N(50,5)$ . The beam has a resistance capacity  $R \sim N(100,10)$  and a correlation coefficient  $\rho_{RS} \in \{0, 0.3\}$ .

In order to obtain the reliability index and the probability of failure of the beam, an analytical solution as well as a Crude Monte Carlo simulation and an Enhanced Monte Carlo simulation are performed.

#### **Analytical solution**

Since the two random variables are normally distributed, an analytical solution of the convolution integral in (2.44) is possible in order to obtain the probability of failure. The calculation is straightforward according to the procedure stated in section 2.8. Result from the calculation is given in table 2.2.

| $\rho_{RS}$ | 0                    | 0.3                  |
|-------------|----------------------|----------------------|
| $\beta$     | 4.47                 | 5.13                 |
| $p_f$       | $3.85 \cdot 10^{-6}$ | $1.45 \cdot 10^{-7}$ |

**Table 2.2:** Results for the reliability index and probability of failure from the analytical solution.

The result shows that the probability of failure decrease with increasing positive correlation between the variables. With other words positive correlation reduces the chance of load  $S$  exceed the resistance  $R$ .

### Crude Monte Carlo

Crude Monte Carlo simulation is performed according to section 2.10.1, by using a simple MATLAB script. MATLAB possess a random number generation tool, which generate values for the basic variables in the limit state function.  $10^8$  simulations are used and table 2.3 shows the results.

| $\rho_{RS}$ | 0                    | 0.3                 |
|-------------|----------------------|---------------------|
| $\beta$     | 4.48                 | 5.09                |
| $p_f$       | $3.75 \cdot 10^{-6}$ | $1.8 \cdot 10^{-7}$ |
| $CI_{95\%}$ | $\pm 10.1\%$         | $\pm 46.2\%$        |

**Table 2.3:** Reliability index, probability of failure and 95% confidence intervals calculated using  $n = 10^8$  simulations.

The results from the Crude Monte Carlo simulations are consistent with the theoretical results, but  $\rho_{RS} = 0.3$  give some deviations in the confidence interval.

### Enhanced Monte Carlo

Enhanced Monte Carlo simulation is performed according to the procedure stated in section 2.10.3.  $10^6 - 10^7$  simulations are performed in order to obtain result in accordance with theoretical and Crude Monte Carlo simulation. Accuracy might have been improved by increasing the number of simulations, but shows the advantages of computational effort related to the method. Results from the simulation are shown in table 2.4.

| $\rho_{RS}$ | 0                    | 0.3                  |
|-------------|----------------------|----------------------|
| $\beta$     | 4.47                 | 5.15                 |
| $p_f$       | $3.85 \cdot 10^{-6}$ | $1.31 \cdot 10^{-7}$ |
| $CI_{95\%}$ | $\pm 99.8\%$         | $> \pm 100\%$        |
| $N_{sim}$   | $10^6$               | $10^7$               |

**Table 2.4:** Reliability index, probability of failure, 95% confidence interval calculated using  $n = 10^6$  and  $10^7$ .

The result clearly shows that the method provide result within acceptable limits with a smaller number of simulation than the Crude Monte Carlo simulation. When complex problems are

considered, this is a valuable property in order to obtain acceptable result without spending too much effort in computational work.

The confidence interval, however, are much larger for the Enhanced Monte Carlo Method compared to the Crude Monte Carlo method. The reason for this is that the confidence intervals for the Enhanced Monte Carlo is not centred around the probability of failure, it is extrapolated in the same way as for the extrapolation curve. First confidence intervals for the different values of  $\lambda_i, i \in \{1, \dots, m\}$  are estimated in order to calculate the weighting factor  $w_i$  used in estimation of the parameters  $q, a, b, c$ . Then new confidence interval for the obtained extrapolation curve  $F(q, a, b, c, \lambda)$  are estimated for calibration of new extrapolation curves for the confidence intervals. Because of these repetitive procedures, values of the confidence intervals often become greater than the ordinary confidence intervals related to Crude Monte Carlo simulation.

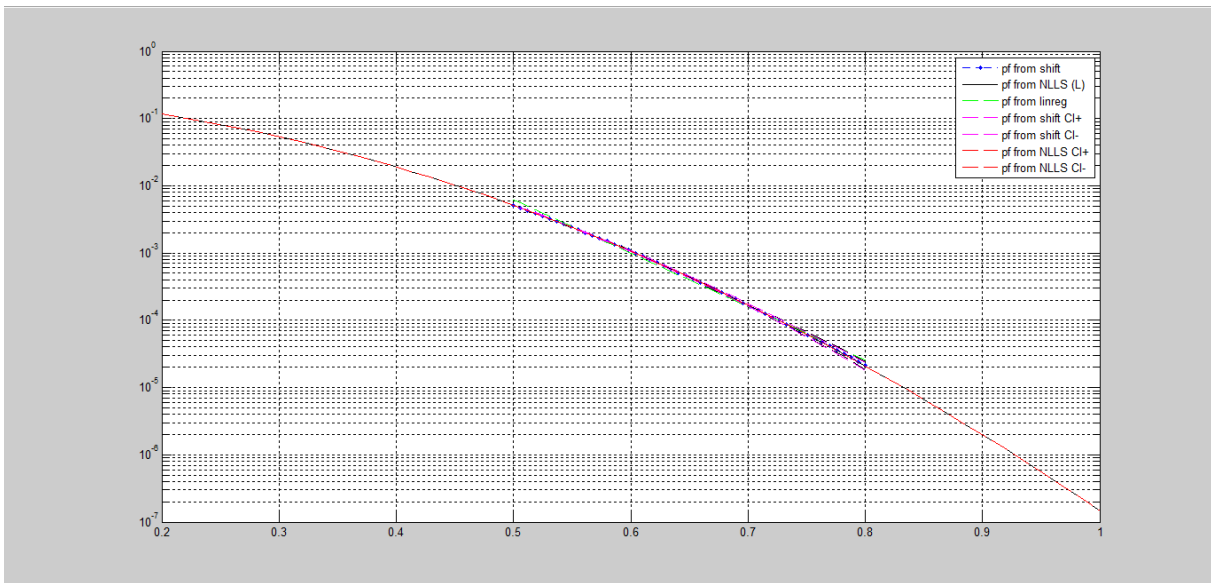


Figure 2.18: The extrapolation curve of the enhanced method, when  $\rho = 0.3$ . Blue dots are  $p_f(\lambda)$ , black and red curves estimate failure probability and confidence limits, respectively.

## 2.11 Deriving partial safety factors

Structural reliability analysis involves many uncertainties and constraints. The safety factors consider these uncertainties when deriving reliability index or dimensions. Partial safety factors are denoted  $\gamma$  in reliability analysis, and is a tool to adjust the limit state function in a wanted direction.

Partial safety factors are standardized in structural codes. The factors are derived from investigations and calculation, to make the structures satisfy the requirements related to the safety aspects. The partial safety factors are conservative, which may result in an ineffective use of resources by overestimating the necessary resistance of the structures.

The safety factors are included in the limit state function by using the design values of the variables. Design value is mentioned in section 2.6. Using the limit state function in (2.65) as an example, following limit state function can be obtained:

$$G = R - S \rightarrow g = r_d - s_d = \frac{r_k}{\gamma_R} - s_k \cdot \gamma_S \quad (2.110)$$

The partial safety factors can be derived in different ways. The estimation of the factors often depends on the method used in solving the reliability problem.

By using the method of Hasofer/Lind, the factors are estimated from the values related to the design point  $x^*$ . The design point is supposed to converge against the right solution, hence the design value. This leads to following expressions for the partial safety factors:

$$\begin{aligned} x_d &= x_i^* \\ \gamma_S \cdot x_k &= \mu_i - \alpha_i \cdot \beta \cdot \sigma_i \\ \gamma_S &= \frac{\mu_i - \alpha_i \cdot \beta \cdot \sigma_i}{x_k} \end{aligned} \quad (2.111)$$

The expression above is for load/action variables. For a resistance variable, the partial safety factor is found by flipping the expression, i.e.  $\gamma_R = \gamma_S^{-1}$ .

Sensitivity factors  $\alpha_i = \pm\{0.7 - 1\}$  are assumed recommended by The Nordic Committee on Building Regulations (NKB, 1978) [9]. This, however, provides a 5% fractile value for the resistance variable when  $\beta = \{1.645 - 2.35\}$ .

Another way of estimating the partial safety factors is by using a “safety level”. The “safety level” is consistent with a given level of failure probability or more precisely a target reliability index  $\beta_t$ . Iteration process are needed in order to obtain estimates of  $\beta$  equal to  $\beta_t$ . The partial safety factors are continuously updated with new values to make the reliability index  $\beta$  converges toward  $\beta_t$ .

Values for the  $\beta_t$  is stated in codes and standards, see [20].

Optimization algorithms may be used for this purpose.

## 2.12 Series and parallel systems

Structures are often simplified as systems or combination of systems, to make the reliability calculations possible. A system is a pairing of several elements. An element is a part of the entire construction, which is capable of existing as a single unit. To investigate the entire system as a combination of several elements, the probability of failure for each element is necessary to know. There are two types of system: series and parallel system.

### Series system

If the entire system fails if one element fails, the system is a series system. The probability of failure for the entire system is equal to the probability of the union of elements in the system. By using the law of de Morgan [7], the expression for the system probability of failure is obtained from following equations:

$$\begin{aligned} P_f &= P(E_1 \cup E_2 \cup \dots \cup E_i \cup \dots \cup E_n) \\ &= 1 - P(\bar{E}_1 \cap \bar{E}_2 \cap \dots \cap \bar{E}_i \cap \dots \cap \bar{E}_n) \\ &= 1 - \prod_{i=1}^n (1 - p_{fi}) \end{aligned} \quad (2.112)$$

Where  $p_{fi}$  is the probability of failure for the element  $i$ , while capital  $P_f$  is the probability of failure for the entire system.

Notice, this expression is only valid if the elements are statistical independent.

If the elements are perfectly correlated, the probability of failure for the entire system is equal to:

$$P_f = \max[p_{fi}] \quad (2.113)$$

### Parallel system

If the entire system fails when all the elements in the system have failed, the system is a parallel system. When the elements are statistical independent, the probability of failure for the entire system is equal to the intersection of the probability of failure for all elements.

$$P_f = P(E_1 \cap E_2 \cap \dots \cap E_i \cap \dots \cap E_n) = \prod_{i=1}^n p_{fi} \quad (2.114)$$

When the elements are perfectly correlated, the probability of failure for the entire system is equal to:

$$P_f = \min[p_{fi}] \quad (2.115)$$

### Upper and lower bounds

From the above expressions for the system probability of failure, following upper and lower bounds for series and parallel system are obtained, respectively:

$$\begin{aligned} \max[p_{fi}] &\leq P_f \leq 1 - \prod_{i=1}^n p_{fi} \\ \prod_{i=1}^n p_{fi} &\leq P_f \leq \min[p_{fi}] \end{aligned} \quad (2.116)$$

In practice, constructions are usually combination of several series and parallel systems.



---

## 3 Self-weight estimation

All structures are exposed to some kinds of actions. Actions are “forces”, which affect the structure in a way that causes internal or external effects, such as deformations, stresses, material deterioration, etc. Forces arise from the surrounding environment and can be of natural character: wind, snow, rain, earthquake, temperature, etc. or it can be associated with human activities.

In structural calculations, it is more common to use the term load instead of action. The reason for this is that action is a rather general concept, while the expression load is related to structural concerns. Since this thesis is of structural affair, the term load is preferred.

This thesis will include estimations connected to structural components exposed to self-weight loading. In order to obtain reliable data for the self-weight, simplifications of the structures are made. A more detailed description of the simplification is presented latter in this chapter.

### 3.1 Characterizing load

Loads can be categorized in many different ways. In structural context, the loads are often divided into classes of durability:

- Permanent loads: loads that occur during the entire (or nearly entire) reference period.
- Variable loads: loads that variate with a high frequency in time.
- Accidental loads: loads that occur very rarely at time. (Earthquake, fire, hurricane, etc.)

### 3.2 Self-weight

The self-weight of a structure is the weight of the structure itself and is characterized by the following three statements:

- The probability of the load to occur at an arbitrary point-in-time is close or equal to one.
- The uncertainties related to the magnitude of the load is negligible.
- The variability over time is negligible.

Since the variability over time is negligible, the self-weight is considered as being a permanent load. Because of the small variation in magnitude and occurrence, the self-weight can be estimated as a normal distributed load.

The self-weight of a given component (structure) is estimated from following equation [19]:

$$G = \int_V \rho \cdot g \, dV \quad (3.1)$$

Where  $G$ ,  $\rho$  and  $V$  is the self-weight (measured in force [N]), density and volume of the component, respectively.

### 3.2.1 Uncertainties

Even though the variations of the magnitude of the load are negligible at one point of the structure, uncertainties related to the self-weight over the entire structure (or several structures) may arise. These uncertainties concern about following variations:

- Variation inside one component
- Variation between different components in the same structure
- Variation between different structures

A component is a part of the entire structure in this context, for example a floor in an office building.

### 3.2.2 Density

The density of a component is found by doing investigations of the material in the component.

| Material        | Mean value [kN/m <sup>3</sup> ] | Coefficient of variation |
|-----------------|---------------------------------|--------------------------|
| Steel           | 77                              | 0.01                     |
| Concrete        | 25                              | 0.03                     |
| Timber (pine)   | 5.1                             | 0.1                      |
| Timber (spruce) | 4.4                             | 0.1                      |

*Table 3.1: Mean value and coefficient of variation for weight density [19].*

Densities in different points within a component or structure might vary. The correlation between two points in a structure or a component is in this thesis estimated from the following formula [19]:

$$\rho(\Delta r) = \rho_0 + (1 - \rho_0) \cdot e^{-\left(\frac{\Delta r}{d}\right)^2} \quad (3.2)$$

Where  $\rho_0$ ,  $\Delta r$  and  $d$  is correlation between two points far away from each other (in the same member), distance between the two points and correlation length, i.e. measure of the correlation structure, respectively.

Due to the difficulties related to the estimation process of correlation within a component (element), general formulas for the correlation are invented, as shown in (3.2). By using this method of estimating the correlation between points within a component uncertainties arise.

Parameters, i.e. correlation between two points far away  $\rho_0$  and correlation length  $d$ , in the formula need to be assumed either from judgement or obtained data, e.g. from tests,

investigation, codes and standards, etc. Hence, the results rely on the accuracy in the judgements of the parameter estimations.

In addition, uncertainties arise as follows from the assumption of the general formula itself. The correlation estimated from (3.2) is assumed to behave exponential, which may not be the case in every considered component.

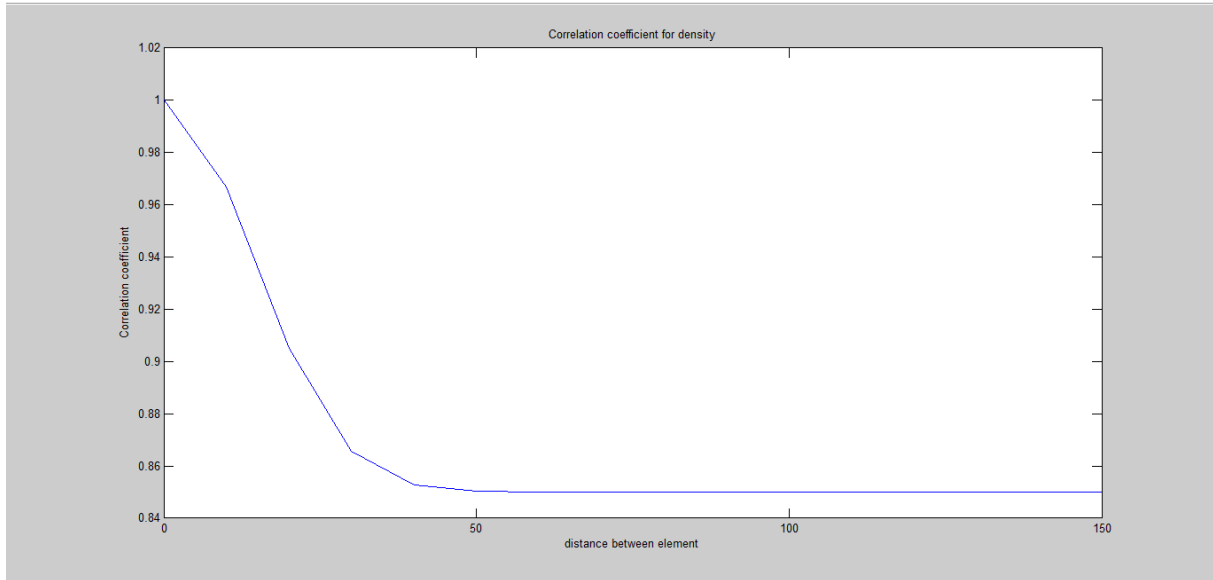


**Figure 3.1:** Curve for correlation coefficient for densities and dimensions for steel and asphalt deck.

In absence of information related to the parameters following values for the correlation between two points far away from each other  $\rho_0$  and the correlation length  $d$  can be used:

| Parameter | Value  |
|-----------|--|
| $d$       | 10 m (beam or column)<br>6 m (plate)<br>3 m (volume) |
| $\rho_0$  | 0.85   |

**Table 3.2:** Values for the parameters in the correlation function (3.2) [19].

### 3.2.3 Volume

The volume of the component is determined from the dimensions. The mean values for the volume are assumed to be equal to the nominal values of the dimensions, while the standard deviations are a function of the values of the deviation in dimensions.

| Material                               | Mean value        | Standard deviation    |
|--|-------------------|-----------------------|
| Steel                                  | $0.01 * A_{nom}$  | $0.04 * A_{nom}$      |
| Concrete ( $a_{nom} > 1000\text{mm}$ ) | 3 mm              | 10 mm                 |
| Concrete ( $a_{nom} < 1000\text{mm}$ ) | $0.003 * a_{nom}$ | $4 + 0.006 * a_{nom}$ |

**Table 3.3:** Mean values and standard deviations for deviations of cross-section dimensions from their nominal values [19].

$A_{nom}$  and  $a_{nom}$  represent the nominal values of the cross-section area and dimensions, respectively.

Deviation in dimensions at one point in the member might affect the dimensions in another. Correlation between two points in a member can be calculated by using (3.2), according to JCSS [19].

## 3.3 Self-weight estimation

Structural calculations of today are carried out in accordance with structural codes and standards, supplemented by a National Annexes. The basis of calculations in codes and standard should be able to fit every purpose of design calculations and still remain within satisfactory safety limits. Because of the large size of application area, codes and standards have to take into account the uncertainties related to the applied load, e.g. the size of surface exposed to loading, load duration, variation in magnitude in load. For this purpose, different load coefficients are invented and developed.

Deviations, however, in the magnitude of applied load may arise as follows discrepancies in expected values or unforeseen events and circumstances. Due to this fact, a factor  $\gamma$  is invented to ensure a safety level within acceptable limits. The safety factor is related to the loading case only, which lead to a partial safety factor for the loading  $\gamma_S$ , where the capital letter  $S$  represent the loading case.

Partial safety factors for loading are determined to be 1.35, in the Norwegian Annex [20]. Consequently, following requirement for self-weight estimation based on structural codes is present:

$$\begin{aligned} W_D &= \gamma_S \cdot W_{Ch} \\ W_D &= 1.35W_{Ch} \end{aligned} \quad (3.3)$$

Where,  $W_D$  and  $W_{Ch}$  represent the design and characteristic self-weight, respectively. Design values are used in every design calculation, except for a few special cases.

In the present work, self-weight estimation of the Hardanger Bridge is done in order to conduct a reliability analysis of the construction. The estimation is carried out based on formulas and values stated in this chapter, in addition to some simplification and measurements from the *basis of calculation* paper for the structure, see appendix A.

## 3.4 Self-weight estimation of the Hardanger Bridge

Self-weight is the only load considered in this thesis, and it is assumed that the self-weight of the Hardanger Bridge consist of the weight of the bridge deck, hangers and main cables only. The reason for this assumption is to reduce the complexity of the problem. In addition, these components constitute the major part of the self-weight loading of the structure, i.e. self-

weight loading of the pylons is assumed to be carried by the pylon itself. Hence, the simplification is assumed to give a high enough accuracy.

The self-weight of the main cables and hangers are applied to the components directly by including gravity and densities of the components in the simulation of the bridge.

In order to obtain the self-weight of the bridge deck, a rectangular plate ( $1320 \cdot 14.5 \text{ m}^2$ ) equal to the bridge deck is simulated. Figure 3.2 illustrate this.

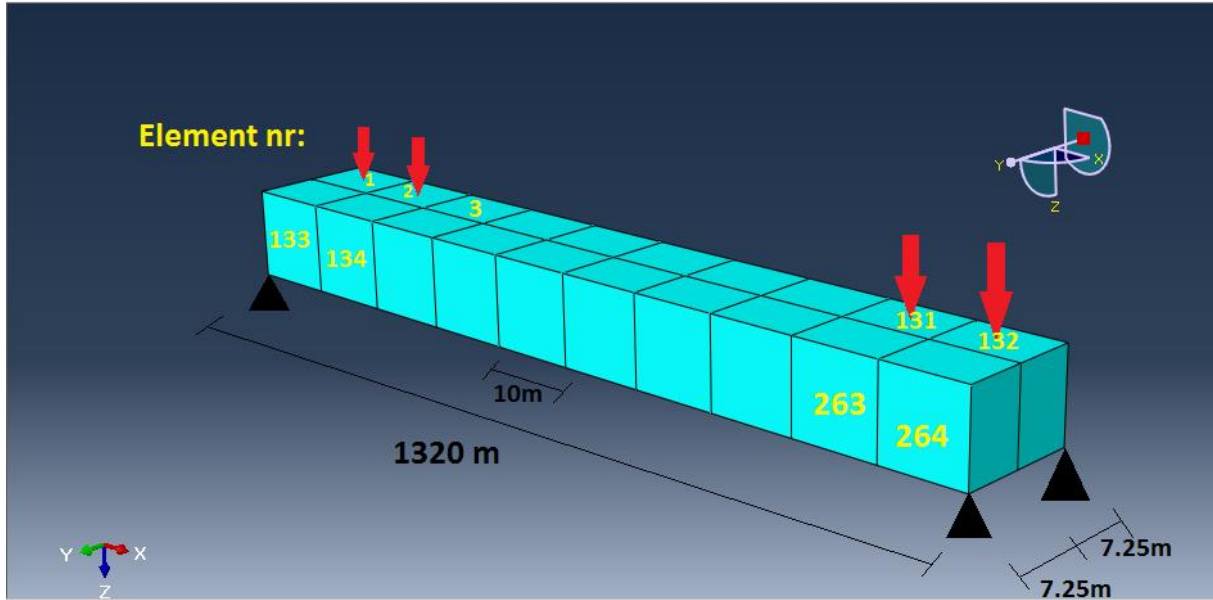


*Figure 3.2: Simulated mesh of the bridge deck. Yellow numbers indicate element numbers. Red arrows indicate self-weight of element and location. Black numbers indicate dimensions.*

This plate is meshed into 264 elements, where each element ( $10 \cdot 7.25 \text{ m}^2$ ) gives a force contribution to the self-weight by the formula:

$$F_{gi} = \rho_i \cdot g \cdot V_i \quad (3.4)$$

Where  $V_i$  and  $\rho_i$  is the volume and density of the element, respectively.

For simplicity, the bridge deck is assumed to consist of an asphalt deck on top of the steel box girder. The steel box girder and the asphalt deck are simulated with a squared cross-section in order to reduce the complexity. Both of these assumptions are considered to give small enough uncertainties.

For the asphalt deck thickness is assumed to variate along the cross-section and length of the bridge deck, while for the steel deck the cross-section is assumed to variate. Consequently, estimation of volume  $V_i$  is assumed to consist of the random variables thickness  $t$  and cross-section  $A_s$  for the asphalt and steel deck, respectively.

The self-weight estimation of the simulated bridge deck is performed by using a MATLAB script. Embedded normal and multivariable distribution functions along with a random number generator are used in order to obtain characteristic values for the density and dimensions.

## Ch. 3 Self-weight estimation

---

Both the density and dimension variables in the self-weight estimation are assumed to be normal distributed. This assumption may cause some uncertainties, but due to the *Central-Limit-Theorem*, it is qualified as good enough, according to Freeman and Benjamin and Cornell [11], [12].

### Density correlation

Correlation coefficients of the densities for the steel and asphalt deck are obtained from codes, according to (3.2) [19]. Values for the far away correlation and correlation length are assumed appropriate:

$$\begin{aligned}\rho_0 &= 0.85 \\ d &= 20m\end{aligned}\tag{3.5}$$

Value of the far away correlation  $\rho_0$  is obtained from table 3.2. Value for the correlation length  $d$  is assumed higher than the standardized values in table 3.2, hence  $d = 20\text{ m}$  is a good estimate for both deck. These assumptions are assumed to give uncertainties of little importance.

### Dimension

Mean values and standard deviations of the deviation in the dimensions (see table 3.3), complicate the calculations. Consequently, calibration of the dimensions needs to be done in the following steps:

#### For steel deck:

1. Calculate the mean value and standard deviation of the deviation in the cross-section by inserting value for  $A_{nom}$  in table 3.3.
2. Estimate the deviation of the cross-section from the calculated values in step 1, by using a 90% fractile-value.
3. Use the value from step 2 and nominal value (mean value) to calibrate the cross-section dimension. Assume normal distribution and correlation coefficient between the different cross-sections.

90% fractile-value for standard deviation of the cross-section is assumed conservative, due to the fact that the elements are precast sections made by one manufacture. The fractile-value is found according to (2.34).

#### For asphalt deck:

1. Estimate the standard deviation of the deviation in the thickness, by assuming coefficient of variation equal to 10%.
2. Obtain mean values for the deviation in thickness from manuals [27].
3. Use values from step 1 and 2 to calculate thickness dimensions by assuming normal distribution. Include correlation between the different thickness dimensions.

According to table 3.3, coefficient of variation for dimensions of the concrete deck is assumed to be equal to 5%, when the dimensions are less than  $1000\text{mm}$  ( $t = 80\text{mm}$ ). Since the variation in asphalt is assumed to be greater than a cast in situ concrete, a coefficient of variation equal to 10% is assumed to give values within an acceptable limit. Variation in

asphalt is assumed greater than variation in cast in situ concrete, because the formwork corresponding to cast in situ concrete provides a lower variance. Asphalting do not require any kind of formwork, thus greater variance.

Values for the nominal dimensions (thickness and cross-section) are stated in the basis of calculation (see appendix A) and in manuals from Norwegian Public Roads Administration [27]:

$$A_{nom} = A_s = 0.5813m^2 \quad (3.6)$$

$$a_{nom} = t = 0.08m \quad (3.7)$$

### **Dimension correlation**

Characteristic values for the dimensions are assumed correlated with correlation coefficients in accordance with the correlation coefficient for the densities (3.2) and table 3.2 [19].

### **Location of the self-weight loading**

The self-weight is assumed uniformly distributed over the entire bridge deck, since the bridge deck is assumed double symmetrical the coordinates for the resultant force for each element is set in the middle of each element.





---

## 4 Resistance capacity estimation

The ability of a structure to withstand loading, is the resistance capacity of the structure. The magnitude of the resistance capacity for a structure depends on material properties and dimensions of the structure.

Material properties determine whether the structure is ductile or brittle, have a high or low strength, the magnitude of strain due to increasing stresses, corrodes or not, etc. Dimensions of the structure determine how much of these material properties are available. In other words, to ensure a specific level of resistance capacity in a structure, the elements of the structure must consist of a material with satisfactory properties as well as right dimensions.

This chapter comprises important comments and concepts related to the estimation process of resistance capacity. In the latter part, procedure for capacity estimation of the Hardanger Bridge along with assumptions and uncertainties are presented.

### 4.1 Material properties

Material properties are defined from test specimens, which have been investigated in laboratory by carefully exposure of increasing loads. Tests of specimens need to be carried out in a certain way in order to get reliable results, strict (standardized) rules and requirements for the implementation of the tests are therefore determined.

Main characteristics of the mechanical behaviour of a material, such as modulus of elasticity and material strength, are described by a two dimensional stress-strain curve, as shown in figure 4.1. In addition, useful properties such as yield stress, limit of proportionality, strain at rupture and maximum stress, can be found from the diagram.

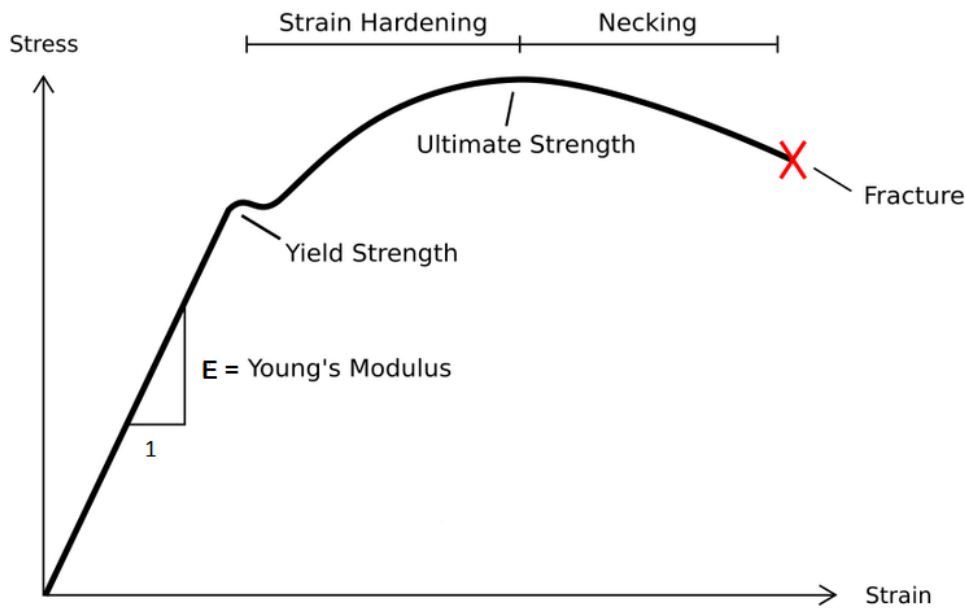


Figure 4.1: Stress-strain curve.

Materials might possess different kind of properties, which may be used in various areas. Concrete for instance has low tensile strength because of brittleness in the material thus are concrete elements used in columns, where the major loading occurs in compression. Prestressed steel has a high tensile strength and is therefore very suitable for use as main cables in suspension bridges. Consequently, carefully selections of materials are of high importance in order to gain maximum resistance capacity.

| Materiale             | Strength properties         | Coefficient of variation |
|-----------------------|-----------------------------|--------------------------|
| Prestressing steel    | $f_{pk} = 1570 \text{ MPa}$ | 0.025                    |
| Structural steel S355 | $f_{yk} = 355 \text{ MPa}$  | 0.07                     |

Table 4.1: Material strength properties for different materials [21], [22], [23], [24].

Where  $f_{pk}$  and  $f_{yk}$  are characteristic values for the tensile strength and yield strength, respectively.

### 4.1.1 Variation and correlation

Material properties might vary both in time and space. The variation of the material properties can be divided into three levels:

1. Global (macro): variations primarily result of production technology or strategy, e.g. different manufactures. Global variations might also arise from statistical uncertainty.
2. Local (meso): spatial correlation within the system, not too large distance between the considered points.
3. Micro: rapidly fluctuating variations and inhomogeneity. Variation in pore size in the material might be an example.

Spatial correlation within the system (local variation) is of high impact when resistance capacity is estimated. Discrepancies in material properties for different element of the system, may cause under- or oversizing of the resistance capacity.

Consider a suspension bridge with main cables consisting of a thousand wires. If several wires are damaged at same location, the resistance capacity of the main cable is lower in the area close to the damage than points far away. The reduction of the resistance may lead to lack of capacity (or in worst case collapse) when loading. Therefore, it is necessary to include correlation in resistance capacity estimation.

Correlation between points in the material is not always defined in codes and standards or other manuals, due to the fact that investigations and tests of correlation within an element (component) of the same material are conducted in a very small extent. Use of information about the correlation for a given structure (or element) may also result in uncertainties when used in other structures, because of the differences between the structures.

Because of the absence of information regarding the correlation coefficients, an exponential function (similar to the self-weight correlation function (3.2)) are used in the following calculations. This is only an assumption though.

### 4.1.2 Uncertainties

Spatial variation in strength from one point to another may occur. Variations in material give rise to uncertainties due to the fact that the material might behave different than expected.

Uncertainties may also occur due to discrepancies between the measured properties in specimens and real structures. These uncertainties need to be accounted for:

- Deviations in properties between observed structural properties and predicted properties
- Deviations as follow variations in workmanship when incorporating the material in structures and laboratory
- Deviations due to scaling
- Uncertainties due to alterations in time

There may also be other uncertainties related to the determination of material properties and behaviour (not mentioned here), which might have greater impact than the listed ones, that should be accounted for.

## 4.2 Resistance capacity estimation

Resistance capacity estimation of today is based on standardized construction calculation and tabulated data. Codes and standards are used to decide dimensions of structure elements in order to obtain a required safety level of the construction. For this purpose, different material and dimensions coefficients are developed and derived.

## Ch. 4 Resistance capacity estimation

---

To ensure, however, an acceptable safety level within the elements, safety factors to deal with the occurrence of unexpected events within the material, such as bursts, ruptures, cracks, are developed. Similar to the partial safety factor for loading in section 3.3, the safety factor is related to estimation of the resistance capacity only. Hence, partial safety factor for resistance capacity  $\gamma_R$  are developed.

Values for the partial safety factors differ for various kinds of materials. Table 4.2 gives Norwegian values of the safety factors for different materials.

| Material         | $\gamma_R$ |
|------------------|------------|
| Structural steel | 1.05       |
| Wires and cables | 1.20       |

*Table 4.2: Partial safety factors for the material resistance [21], [24].*

As can be seen from the table, nominal values for the resistance need to be divided by the partial safety factor, in order to account for uncertainties related to unexpected events. Hence, following equation for resistance capacity estimation can be obtained, see [10]:

$$R_D = \frac{R_k}{\gamma_R} \quad (4.1)$$

Where  $R_D$  and  $R_k$  are the design and characteristic resistance capacity, respectively. Design values are further used in almost every design calculation.

In the following section, procedures and assumptions for estimation of the resistance capacity for the Hardanger Bridge are presented. In the latter part some important notes regarding the uncertainties involved are mentioned.

### 4.3 Resistance capacity of Hardanger Bridge

In the reliability analysis of the Hardanger bridge (considered in this thesis) resistance capacities are expressed in terms of characteristics values and distribution parameters, i.e. mean value and standard deviation.

The Hardanger Bridge is a rather big and complex construction, with many components sharing the load. Because of the complexity, simplifications of the structure are assumed in order to quantify the resistance capacity more easily.

The reliability analysis performed in this thesis includes comparisons of the axial loading and resistance capacity in the hangers and main cables. Consequently, calculation of the resistance capacity of the structure correspond to capacity estimation of the hangers and main cables only.

The hangers and main cables are part of the entire bearing system of the bridge and are assumed to carry the loading obtained from the self-weight of the bridge deck, hangers and main cables (see section 3.4). The hangers and main cables are divided into 266 components (further explained in sections 5.2.1), thus resistance capacities and axial loading in each of the 266 components are estimated in order to perform the reliability analysis.

### 4.3.1 Resistance capacity of main cable

The main cables consist of 528 parallel wires tied together in 19 bundles. Resistance capacity of the main cable consist of strength contribution from these 10032 wires. Even though the wire appears as a unitary element, variation along the wire may arise. Variation of this kind causes reduction in strength capacity due to length effect. The length effect is assumed to reduce the strength capacity by 10% [25], [26].

The main cable, however, consist of several wires in parallel. The interaction between these wires are assumed to reduce the strength capacity due to the Daniel's effect. The Daniel's effect is assumed to reduce the strength capacity by 8% [25], [26].

The resistance (strength) capacity of the wires is calculated from obtained tensile strength data from the manufacturer, see [5] and appendix C. The data is interpreted by using statistical tools to calculate mean values and standard deviation (see section 2.2.3). The tensile strength data is measured as stress, with units MPa.

In order to obtain resistance capacity of the main cables, values from the obtained strength data multiplied with the cross-section area of the main cable are performed.

The cross-section area of the main cable can be estimated from following formula and obtained data for the cross-section dimension:

$$A_{main} = A_{wire} \cdot n_{wire} = \frac{d^2}{4} \cdot \pi \cdot n_{wire} \quad (4.2)$$

Where  $d$  and  $n_{wire}$  is the diameter and number of wires in the main cable, respectively.

Hence, following formula for the resistance (strength) capacity of the main cables are found:

$$R_{Main} = A_{main} \cdot f_{pk_{wire}} \cdot 0.9 \cdot 0.92 \quad (4.3)$$

Where  $f_{pk_{wire}}$  is nominal value for tensile strength of the wires.

Correlation between the components (or element of the main cable) are assumed to be exponential (similar to (3.2)), with variables equal to:

$$\begin{aligned} \rho_0 &= 0.9 \\ d &= 50m \end{aligned} \quad (4.4)$$

The reasons for this assumptions are due to the fact that each elements of the main cable consist of the same wires. In addition, all of the wires are produced by the same manufacture [5].

### 4.3.2 Resistance capacity of hanger

## Ch. 4 Resistance capacity estimation

Estimation of the resistance capacity in the hanger elements are rather difficult to obtain since there is no tensile strength data from tests available. Tabulated strength values from codes and manuals, therefore, are used.

The hangers are assumed to consist of prestressed steel, similar to the main cables. Table 4.1 states nominal values and coefficient of variation for prestressed steel.

The capacity values are multiplied with the cross-section of the hangers, in order to estimate the resistance capacity.

Cross-section of the hangers  $A_{hanger} = 3200mm^2$ , see appendix A. This is lower than the expected area calculated from dimensions, due to the fact that the cable is coiled.

Following equation for hanger capacity can be obtained:

$$R_{Hanger} = A_{Hanger} \cdot f_{pk} \quad (4.5)$$

Where  $f_{pk}$  is nominal value for tensile strength of prestressing steel.

Values for the correlation coefficient between the different hangers are not stated in the basis of calculation or other manuals/codes. Hence, an exponential curve for the correlation coefficient (similar to (3.2)), along with conservative assumptions for the variables are used.

$$\begin{aligned} \rho_0 &= 0.5 \\ d &= 30m \end{aligned} \quad (4.6)$$

Reasons for these assumptions are based on lower correlation between the hangers, due to separately production by different manufactures [5]. This might lead to a lower correlation coefficient than obtained by investigation, but it is assumed to be conservative.

### 4.3.3 Uncertainties

Tabulated resistance values from codes and standards are usually intended for use in code calibration and design calculations, therefore the values are often conservative. This means that the values are undersized in order to meet the safety margin.

Tensile strength data from tests tend to shows a much greater resistance capacity than the tabulated values, as can be shown in the table 4.3. Provided similar tabulated values for the main cables as for the hangers.

| components             | Mean values | Coefficient of variation |
|------------------------|-------------|--------------------------|
| Hangers (tabulated)    | 1570 MPa    | 0,025                    |
| Main cables (measured) | 1686 MPa    | 0,01                     |

*Table 4.3: Estimated and obtained tensile strength data for the components [22], [23], [24], appendix C.*

Because of the deviations in main cables (measured) and hanger (tabulated data) strength data, uncertainties will arise. Measured data with low variation have a much smaller overlap area with the loading than the tabulated data with greater variation. Hence, probability of

failure for the hangers (tabulated data) tend to be larger than for the main cables (measured data). Low probability of failure is difficult to estimate, hence larger probability of failure will dominate in the reliability analysis. Figure 4.2 illustrates this.

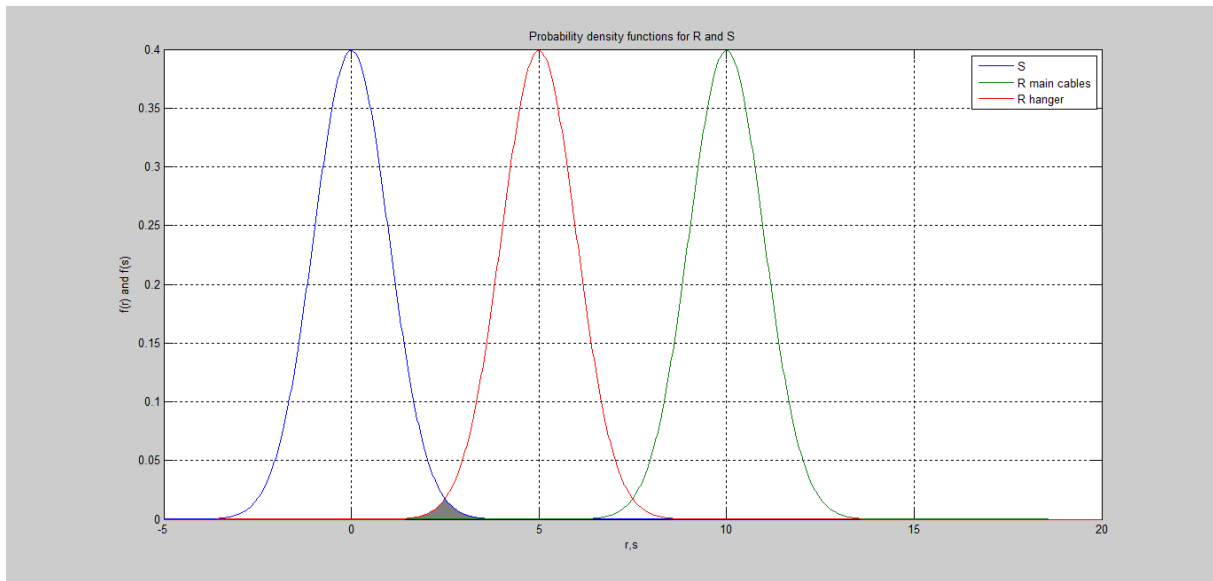


**Figure 4.2:** Pdf for the normal distributed variables  $R$  and  $S$ . Blue curve is load variable, red and green curves are resistance variables in hangers and main cables, respectively. Red and blue curve have a much greater area of intersection than blue and green curve, hence probability of failure for the hangers will dominate.





---

# 5 Reliability analysis of the Hardanger Bridge

Review the hypothesis stated in the introduction: *structures, where self-weight constitutes the major part of the loading, tend to be oversized as a result of the standardized design calculation.*

In order to test the validity of the hypothesis, a reliability analysis of the Hardanger Bridge, along with calibration of partial safety factors, are carried out. Strategies and procedures for implementation of the reliability analysis and the partial safety factor calibration are presented in the following sections.

The reliability analysis and calibration process are carried out by taking advantage of the computer programs MATLAB, Excel and ABAQUS. In addition, simplifications of the problem are assumed to make the calculations more easily feasible and still maintain reliable accuracy.

## 5.1 Short on solution strategy

A brief review of the solution strategy for reliability analysis and partial safety factor calibration is presented in the following steps:

1. Simulation of the bridge in ABAQUS with respect to force estimation.
2. Estimation of the self-weight of the construction (stated in chapter 3)
3. Calibration of the component force due to self-weight loading (MATLAB)
4. Estimation of the resistance capacity of the structure (stated in chapter 4)
5. Reliability analysis of the structure and partial safety factor calibration (MATLAB and Excel)

Notice, the reliability analysis and the partial safety factor calibration are performed by simply analysing the reliability in the main cables and hanger components only. This simplification is stated in section 4.3, as well as in the following sections.

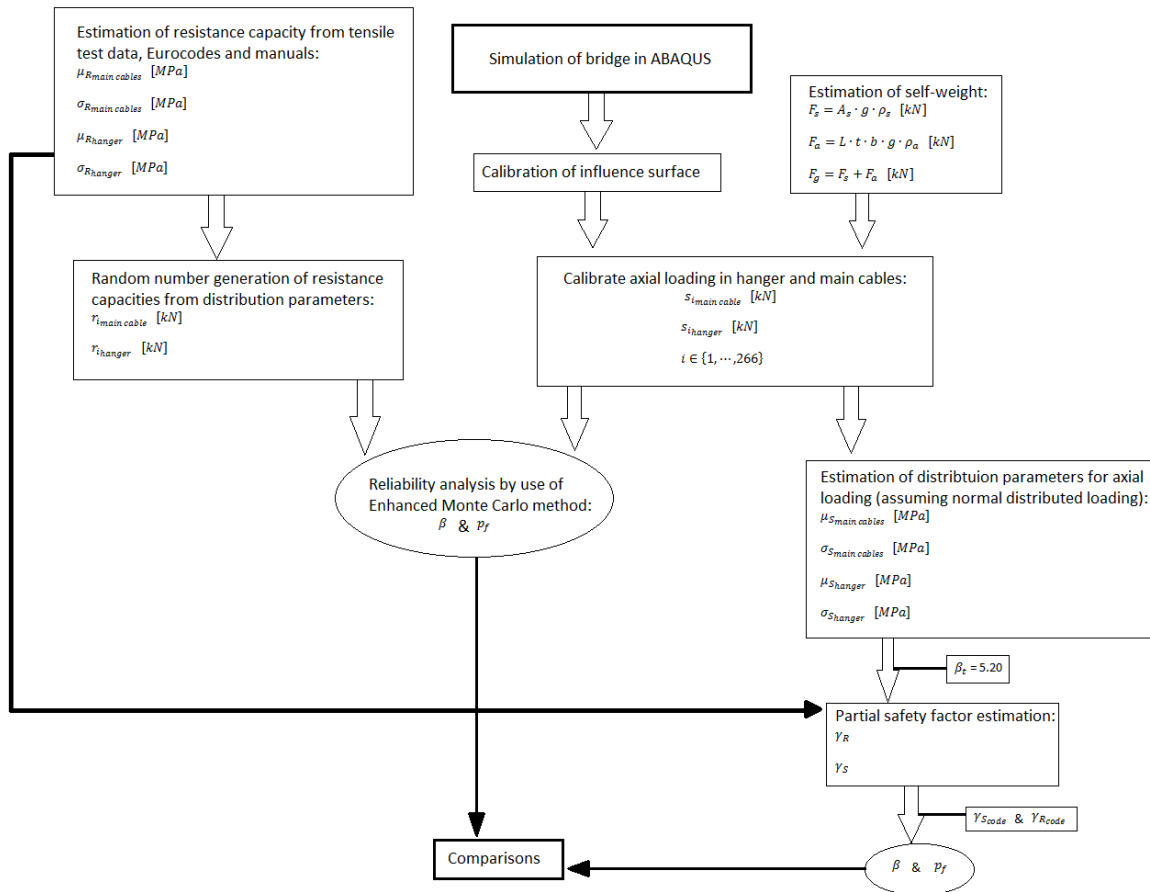


Figure 5.1: Flow-chart of the solution strategy for the reliability analysis and partial safety factor calibration.

## 5.2 Simulation in ABAQUS

ABAQUS CAE is a simulation tool, to solve complex problem and FEM analysis with reduced running time at low costs. ABAQUS makes it possible to simulate complex and difficult systems and models for all kinds of industrial applications, see [28], [29] for more information.

In this thesis, ABAQUS is used to simulate the Hardanger Bridge and its applications. The Hardanger Bridge is, as can be seen in section 1.3, a complex structure with many important components of high impact. In order to solve this kind of problems by using the method described in section 5.1, several simplifications are made.

### 5.2.1 Components

The bridge is simulated by using solid elements of the main components, i.e. pylons, cables, hangers and steel box girder. The table 5.1 gives the number of element and numbering of the elements of each component:

| Structural element | Number of element  | Numbering  |
|--------------------|--|--|
| Pylon              | 145 elements at each pylon   | At Vallavik: 20 000-series<br>At Bu: 30 000-series   |
| Main cable         | 66 elements in main span at each cable<br>2 element in side span at each cable | North side: 1000-1067<br>(1000 and 1067 in side span)<br>South side: 2000-2067<br>(2000 and 2067 in side span) |
| Hanger             | 65 elements at each side   | North side: 5002-5066<br>South side: 6002-6066   |
| Box girder         | 328 elements   | 1-328  |

Table 5.1: Bridge components with corresponding numbering of elements.

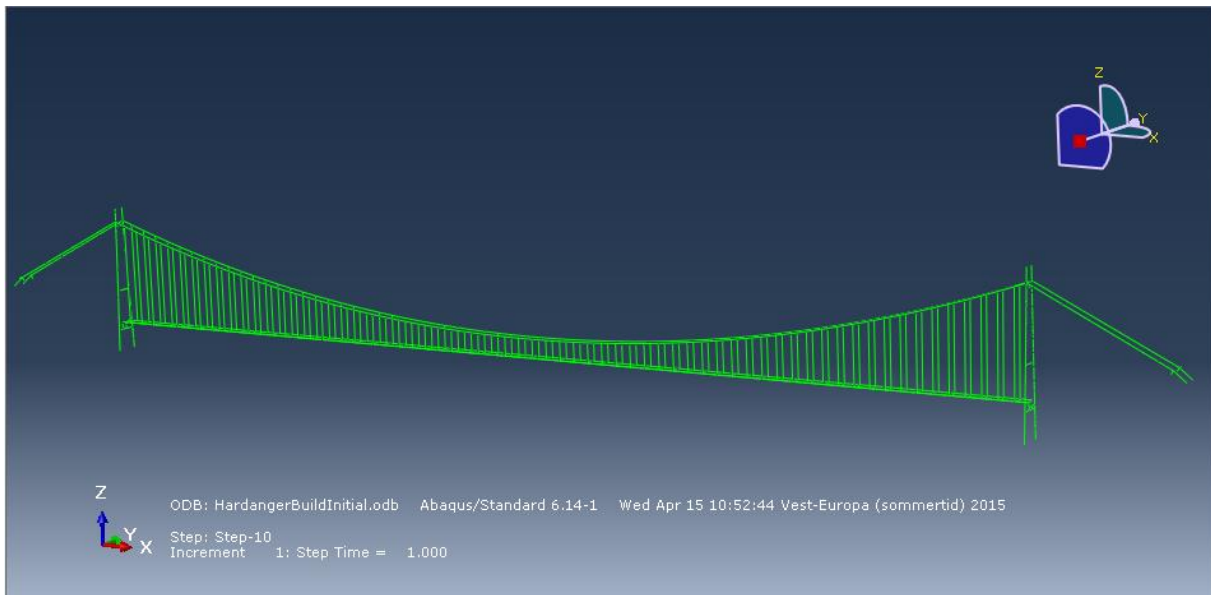


Figure 5.2: Simulated Hardanger Bridge in ABAQUS.

The bridge deck (steel box girder) is simulated as a simple beam, with simplified geometry. Assumptions of the geometry are done in order to obtain the effect from the applied loading only. Equipment and tools such as lifts, construction machinery, workers, lightning, railing, signs, etc., (used under and after construction) are not included in this simulation.

The hanger cables are simulated as 65 equally spaced elements along each sides of the bridge deck between the pylons, 130 elements in total. The cross section of the hangers is modelled in accordance with the information given in section 1.3 and *basis of calculation* (appendix A).

The main cables are divided into 134 elements. 132 elements are simulated in the main span, with length equal to the distance between the hangers, while 4 elements are simulated in the side span (between the pylons and the anchoring at Vallavik/Bu). As for the hangers, the cables are modelled in accordance with the specification given in appendix A and in section 1.3.

## Ch. 5 Reliability analysis of the Hardanger Bridge

In further calculation, the concept *component* comprises the considered components only, i.e. the hangers and main cables. In all 266 components are considered in the analysis.

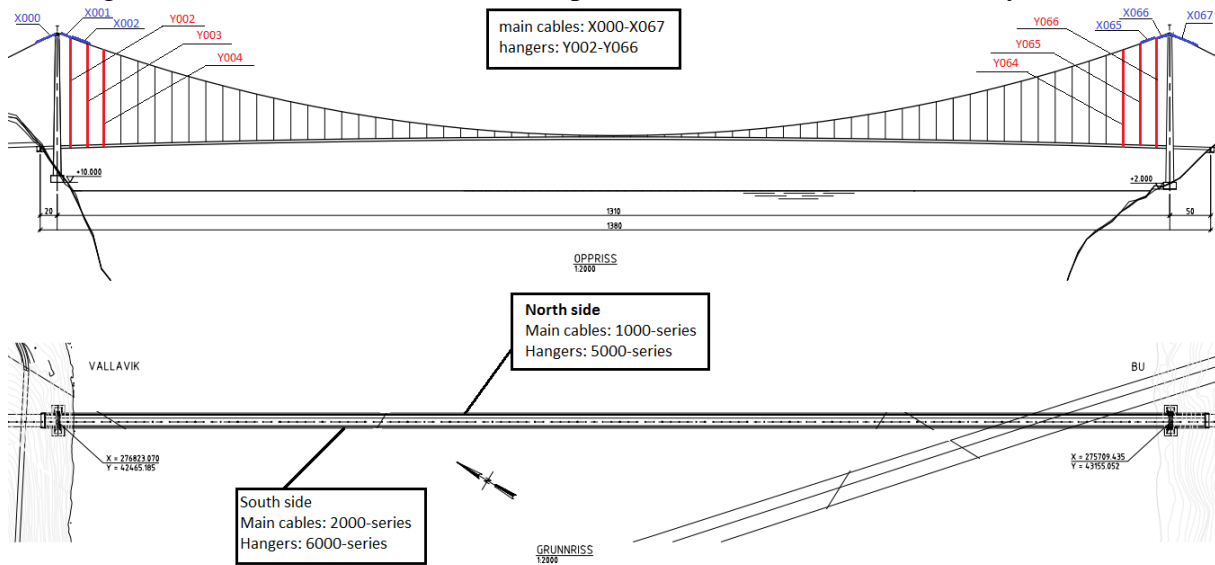


**Figure 5.3:** Illustration of the components. Drawings of the bridge are obtained from Norwegian Public Roads Administration [4]. Numbering done in accordance with the simulation.

The bridge deck is assumed to be a part of the loading carried by the components, while the pylons are assumed to only carry its own self-weight. These assumptions may lead to uncertainties, but the accuracy is assumed to be high enough.

Notice, the bridge deck may also achieve failure due to the fact that the bridge deck is carrying the self-weight loading between the hangers, but this is not included in this thesis.

The bridge, however, is assumed linear behaviour after construction.

### 5.2.2 Influence surface

In order to include the loading in the simulation, an influence surface is modelled. Since this thesis concern about the self-weight loading only, it is assumed that the loading take place at the bridge deck. Hence, the influence surface is modelled as an approximation of the bridge deck.

As a simplification, the loading is assumed to be applied only at the top of the bridge deck. This simplification may involve uncertainties due to the fact that loads may be applied at several other locations, but since the self-weight of the bride deck, which is high compared with others loads, takes place at the bridge deck discrepancies are assumed negligible.

The influence surface is modelled by a  $1320 \times 14,5 \text{ m}^2$  rectangular plate with 67 nodes equally spaced at each long side, as shown in figure 5.4.

One at a time, a unit load is placed in each of the 134 nodes and the corresponding forces in the 266 components (hangers and main cables) are measured in order to obtain the influence surface.

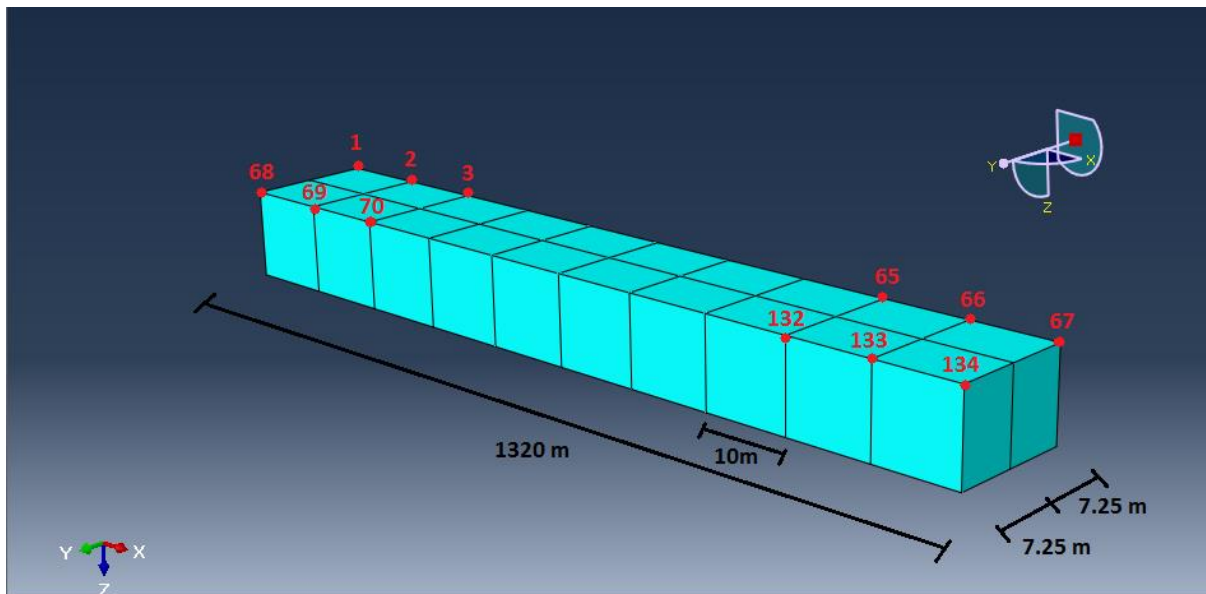


*Figure 5.4: Influence surface with node numbers (red) and dimensions (black).*

When the self-weight loading of the bridge deck is applied, corresponding axial forces in each of the 266 components are calibrated by using interpolation formulas between the loading and locations of the loading and the influence surface. For this purpose, the computer program MATLAB is used.

### 5.3 Calibration of axial loading in MATLAB

MATLAB is a programming language used in calculation of several iteration and complex mathematical problems. The program has a wide range of embedded codes, which is of high importance in more complex mathematical calculations, see [30] for more information.

In the reliability analysis and the partial safety factor calibration, MATLAB is used for four purpose:

- Self-weight estimation
- Transformation of the self-weight loading into axial forces in each component
- Estimation of distribution parameters related to the loading forces
- Estimation of the failure probability of the Hardanger bridge

#### 5.3.1 Axial load calibration

The calibration process of the axial loading in the components due to the self-weight loading of the bridge, are divided into two main parts.

Firstly, the self-weight of the Hardanger Bridge is estimated, in accordance with section 3.4.

Secondly, axial loading is calibrated by transformation of the self-weight loading into applied axial loading in each of the 266 components.

When the self-weight and its coordinates are estimated as described in sections 3.4, axial forces in the components (hangers and main cables) are obtained by interpolation between the self-weight forces and its coordinates and the influence surface.

This simulation is done  $n$  times in order to increase the accuracy, i.e.  $n$  characteristic values for the axial forces (due to the applied self-weight) are obtain. The simulations  $n$  are collected in a matrix for further calculations.

Due to high running time  $3 \cdot 10^5$  simulations of the transformation process are performed.

## 5.4 Reliability analysis

The reliability analysis of the Hardanger Bridge is performed by using the Enhanced Monte Carlo method elaborated in section 2.10.3.

The method was carried out by using a MATLAB script and estimated values for the resistance capacities and the axial loading from sections 4.3.1, 4.3.2 and 5.3.1, respectively.

It is assumed that the components work as a series system, due to the fact that redistribution of forces will cases significant deformation or in worst case collapse. Hence, if one component fail, the structure is assumed to become unstable, i.e. series system according to section 2.12.

## 5.5 Calibration of partial safety factors

Calibration of partial safety factors is performed on behaviour of estimated distribution parameters for the axial loading and the resistance capacity.

### 5.5.1 Parameter estimation

#### Loading, S

When the axial loading forces in the components are found (section 5.3.1), distribution parameters for the loading, i.e. mean value and standard deviation, are determined by assuming normal distributed loading. The self-weight loading is a sum of contributions from

all elements of the structure, which is assumed to behave normal distributed according to the *Central-Limit-Theorem*, see Freeman and Benjamin and Cornell [11], [12].

The embedded function *fitdist* (MATLAB) is used to obtain mean values and standard deviations for each of the 266 components. Because the force simulation is done  $3 \cdot 10^5$  times, the *fitdist* function will provide values within an acceptable limit.

### Resistance, R

Distribution parameters for the resistance capacities are assumed normal distributed, due to contribution of resistance capacity from all components. This assumption is valid according to the *Central-Limit-Theorem*, see Freeman and Benjamin and Cornell [11], [12].

Distribution parameters for the resistance capacity, however, are obtained from test and tabulated data as elaborated in chapter 4.3.1 and 4.3.2.

## 5.5.2 Calibration process

The calibration of the partial safety factors comprises an iterative process for minimizing deviation between a wanted reliability level  $\beta_t$  and the estimated reliability index  $\beta$ , as mentioned in the last part of section 2.11.

The minimization of the deviation is done by optimizing values of the partial safety factors ( $\gamma_S, \gamma_R$ ). The optimization process is performed by taking advantage of *problem solver*, which is an optimization tool in the computer program Excel.

Estimated reliability is found by considering the violation of the limit state function of the structure (in accordance to section 2.7.2). In the following sections equations for the limit state function and the reliability index are stated.

### Limit state function

Since the main cable and hanger components are assumed to behave as a series system, failure in each of the 266 components need to be considered. Consequently 266 limit state functions need to be developed.

Each of the components are assumed to be loaded by only one axial tensile force, related to the self-weight loading. From this assumption following limit state function for each of the 266 components can be obtained:

$$G_i = R_i - S_i \quad (5.1)$$

Where  $R_i$  and  $S_i$  are the resistance capacity and axial loading for each component, respectively.

### Reliability index

The formula for the reliability index is stated in section 2.8 and equal to:

$$\beta = \frac{\mu_R - \mu_S}{\sqrt{\sigma_R^2 + \sigma_S^2}} \quad (5.2)$$

Provided limit state function equal to (5.1).

By using the concepts of design and characteristic values, the expression can be rewritten.

$$\beta = \frac{\frac{\gamma_R \gamma_S}{1 + k_R COV_R} - \frac{1}{1 + k_S COV_S}}{\sqrt{\left(\frac{COV_S}{1 + k_S COV_S}\right)^2 + \left(\frac{COV_R \gamma_R \gamma_S}{1 + k_R COV_R}\right)^2}} \quad (5.3)$$

Where  $COV_R$  and  $COV_S$  are coefficient of variation for the resistance capacity and the loading, respectively, see (2.11).

### Target reliability index

A target reliability index of  $\beta_t = 5.2$ , is obtained in order to estimate a structure within a reasonable limit. A reference period of 1 year is assumed, this is conservative and will give a higher safety level. The target reliability is found in codes by considering the consequences related to a failure of the structure and assumption regarding the reference period, see [20].

In the optimization process, partial safety factors for the loading and the resistance will become equal. This is true based on the fact that the partial safety factors are acting together as a product in the formula (5.3), hence the problem solver would not be able to distinguish between the two partial safety factors.



---

# 6 Results and discussion

Based on estimated input parameters in chapter 3 and 4, a reliability analysis on the Hardanger Bridge is performed according to the procedure elaborated in chapter 5. In addition, partial safety factors for the loading and resistance are estimated. For this purpose, important and valuable statistical tools and methods elaborated in chapter 2 are used.

Results and discussion of the estimated input parameters are presented in the first part of this chapter. In the latter part, results and discussion of the reliability analysis and the partial safety factor calibration take place. At the end of this chapter, a comparison between the two methods of estimating reliability index and probability of failure are presented.

Notice, since the reliability analysis of the bridge is carried out by considering the main cable and hanger components only (according to previous assumptions), estimated input parameters of the applied loading and resistance capacities for the corresponding components are carried out.

Methods and procedures for the estimations and calibrations are performed in accordance to previously elaborated theory (see chapter 2).

The aim of this thesis is to show the oversizing of large structures with self-weight as the major loading. In order to state the validity of the hypothesis, comparisons of measured and tabulated values of the variables for the components are proposed.

## 6.1 Load calibration

The procedure for load calibration in this thesis (accounted for in chapter 3 and 5) rely on estimates of the considered explicit loading, namely the self-weight. The self-weight is used in calibration of the axial loading, corresponding to the main cables and hanger components of the structure.

### 6.1.1 Self-weight

The self-weight is a product of the density, gravity and the volume of the structure, see (3.1).

The self-weight of the structure is assumed to consist of the weight of the bridge deck, along with self-weight of the components. The axial loading caused by the self-weight of the components itself is included in the simulation in ABAQUS. Self-weight estimation of the bridge deck is performed according to section 3.4.

Estimated values for dimensions, densities and self-weights for the elements (see figure 3.2) are presented in the followings. The length of each elements is assumed to equal 10m, consequently estimates for the length are not presented.

### Dimension

Estimations of the dimensions for the steel and asphalt deck are made in accordance with the procedure mentioned in section 3.4. For asphalt deck, the width of the cross-section is assumed constant equal to the width of the simulated bride deck (14.5 m), while the thickness  $t$  variate. For the steel deck the cross-section of the simulated bridge deck  $A_s$ , is assumed to variate.

Distribution parameters for the variables ( $A_s, t$ ), are obtained from manuals and basis of calculation (appendix A), along with assumption stated in section 3.4. Results of the parameter estimation is stated in table 6.1.

| Deck                       | Mean value            | Standard deviation    |
|----------------------------|-----------------------|-----------------------|
| Steel (Cross-section area) | 0.5813 m <sup>2</sup> | 0.0356 m <sup>2</sup> |
| Asphalt (Thickness)        | 0.08 m                | 0.008 m               |

Table 6.1: Mean values and standard deviation for the dimension variables  $A_s$  and  $t$ .

Figure 6.1 shows histograms of the generated values for the steel cross-section and asphalt thickness, given the normal distributed parameters from table 6.1.

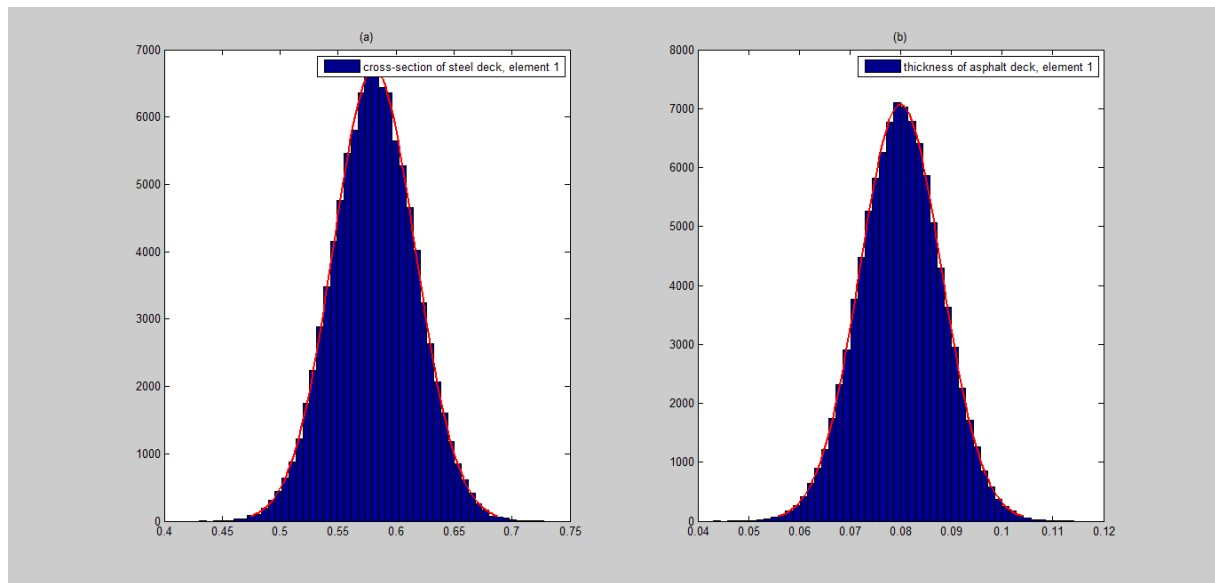
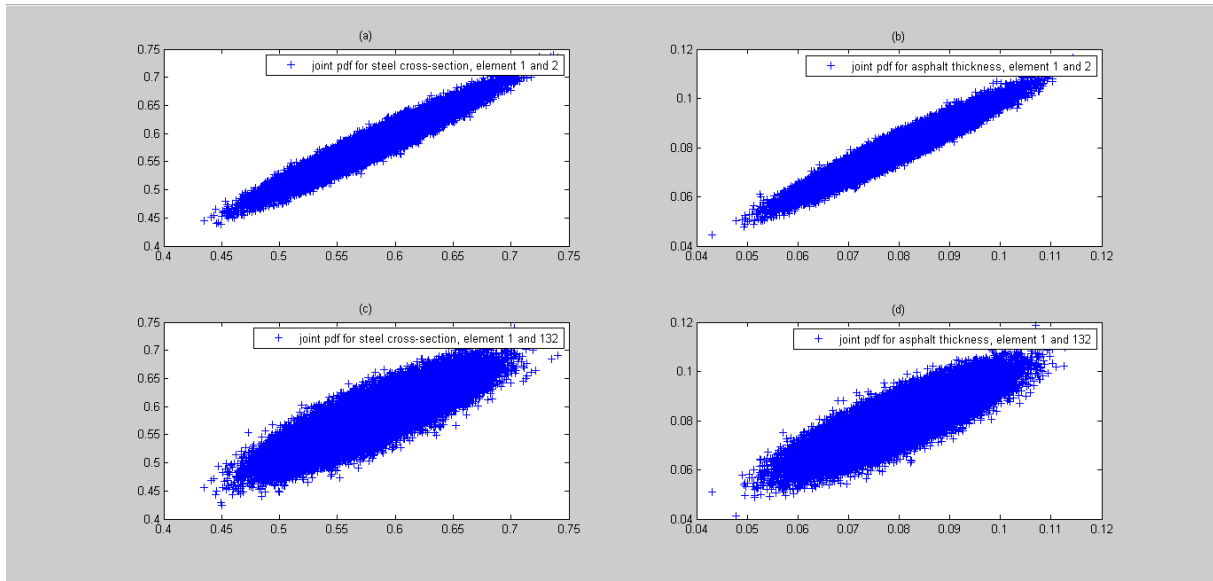


Figure 6.1: Probability density plot for (a) steel cross-section (b) asphalt thickness for element 1 (according to figure 3.2).

As expected from the tabulated data in table 6.1, most of the values for the cross-section and thickness of the steel and asphalt deck ( $A_s, t$ ) respectively, tend to become approximately equal to the mean values, i.e. little variance. The reason for this is due to the low standard deviations in the measurements.

Figure 6.2 shows bivariate density function for two adjacent elements in the simulated bridge deck and for two “far away from each other” elements. Two adjacent element have a distance

$\Delta r = 10m$ , while two “far away from each other” elements have a distance  $\Delta r = 1310m$ , as can be seen in figure 3.2.



**Figure 6.2:** Joint pdf for (a) steel deck  $\Delta r = 10m$ , (b) asphalt deck  $\Delta r = 10m$ , (c) steel deck  $\Delta r = 1310m$ , (d) asphalt deck  $\Delta r = 1310m$ .

As seen in figure 6.2, positive correlation between two adjacent elements appear in both asphalt thickness and steel cross section. For “far away from each other” elements, discrepancies between the values of the two elements increases, i.e. the dependency between the values decrease. The reason for the increasing discrepancies is most likely to originate from the assumed correlation coefficient.

The correlation coefficient for the interaction between elements within a structure are carried out by using an exponential function (3.2) and section 3.4 (dimension correlation). The exponential function give decreasing values of correlation for increasing distance  $\Delta r$ , hence increasing discrepancies between elements when  $\Delta r$  increase, given all other values remain constant.

## Densities

Estimation of the densities for the steel and asphalt deck in each element are carried out by using a multivariable distribution function and distribution parameters from table 3.1.

| Deck    | Mean value           | Standard deviation     |
|---------|----------------------|------------------------|
| Steel   | 77 kN/m <sup>3</sup> | 0.77 kN/m <sup>3</sup> |
| asphalt | 25 kN/m <sup>3</sup> | 0.75 kN/m <sup>3</sup> |

**Table 6.2:** Mean values and standard deviations of the density values for each deck.

The standard deviations are obtained from the numbers noted in table 3.1 and the formula for coefficient of variation (2.11).

Values for the densities are assumed to correlate after formula (3.2), with associated input values stated in section 3.4 (density correlation)

Figures 6.3 shows plots of the density distribution for the steel and asphalt deck.

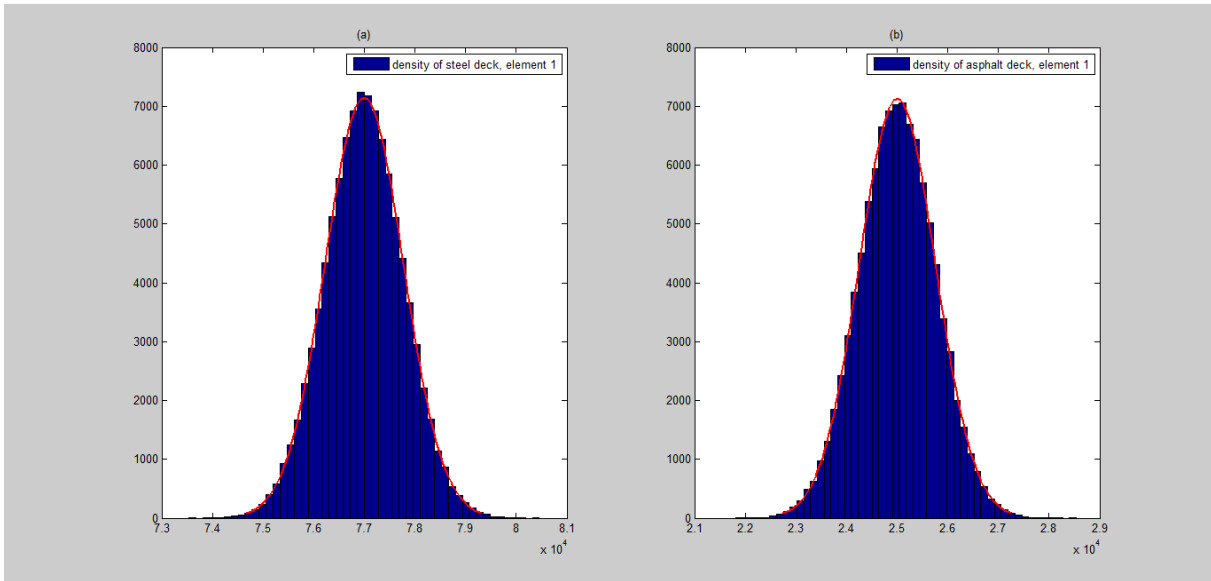


**Figure 6.3:** Probability density plot of the density for element 1 (see figure 3.2) for (a) steel deck, (b) asphalt deck.

Distribution of the density values are as for the dimensions characterized by low variation, due to low variance from the estimated distribution parameters in table 6.2.

Figure 6.4 shows plots of the joint probability distribution between different elements for both steel and asphalt deck.

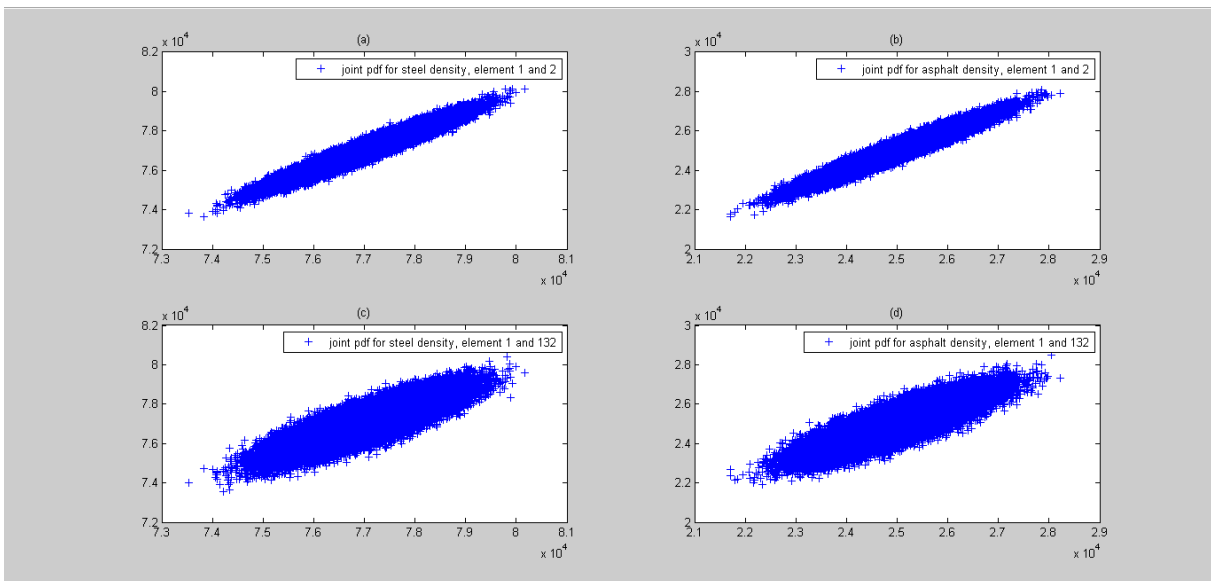


**Figure 6.4:** Joint pdf of the densities for (a) steel deck  $\Delta r = 10m$ , (b) asphalt deck  $\Delta r = 10m$ , (c) steel deck  $\Delta r = 1310m$ , (d) asphalt deck  $\Delta r = 1310m$ .

Just like the dimension values, greater scatter is obtained in the density values for the “far away from each other” elements than for adjacent elements. Reason for this is due to the identical correlation coefficient curve used for the dimensions and densities, i.e. justification for the increasing discrepancies in density values (when elements are far from each other) is the same as for the dimensions.

## Self-weight

Self-weight estimation of the steel and asphalt deck for the element are done in accordance with the method described in sections 3.4 and 5.3.1.

Plots of the self-weight distribution for the steel and asphalt deck, along with the self-weight distribution for the entire deck as well, are shown in figures 6.5 and 6.6.

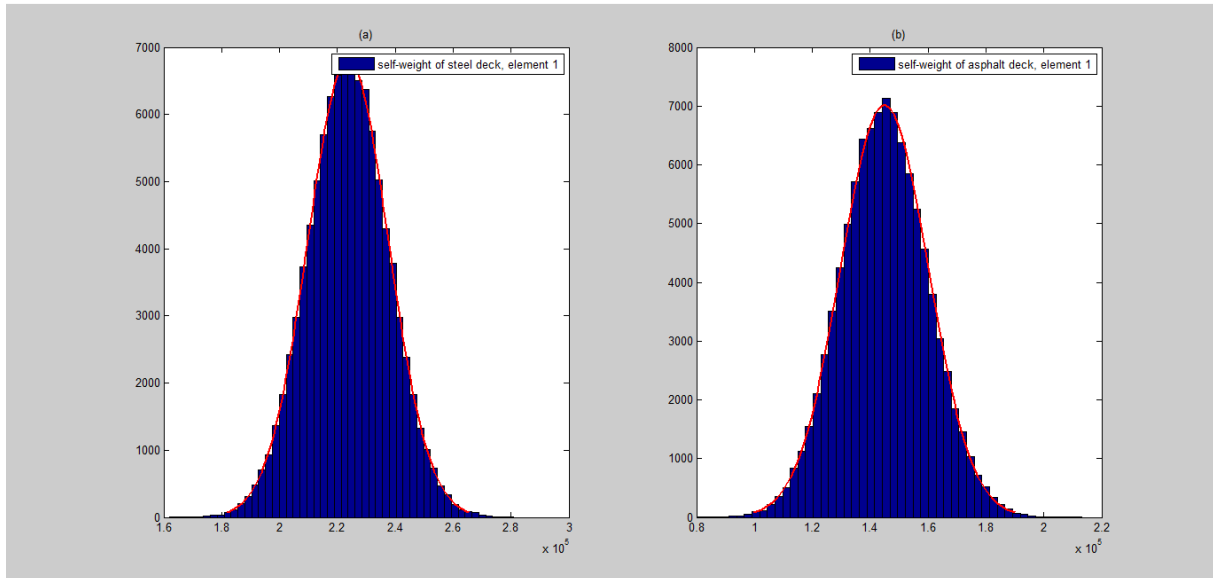


*Figure 6.5: Probability density plot for the self-weight of (a) steel deck, (b) asphalt deck. For element 1 (see figure 3.2).*

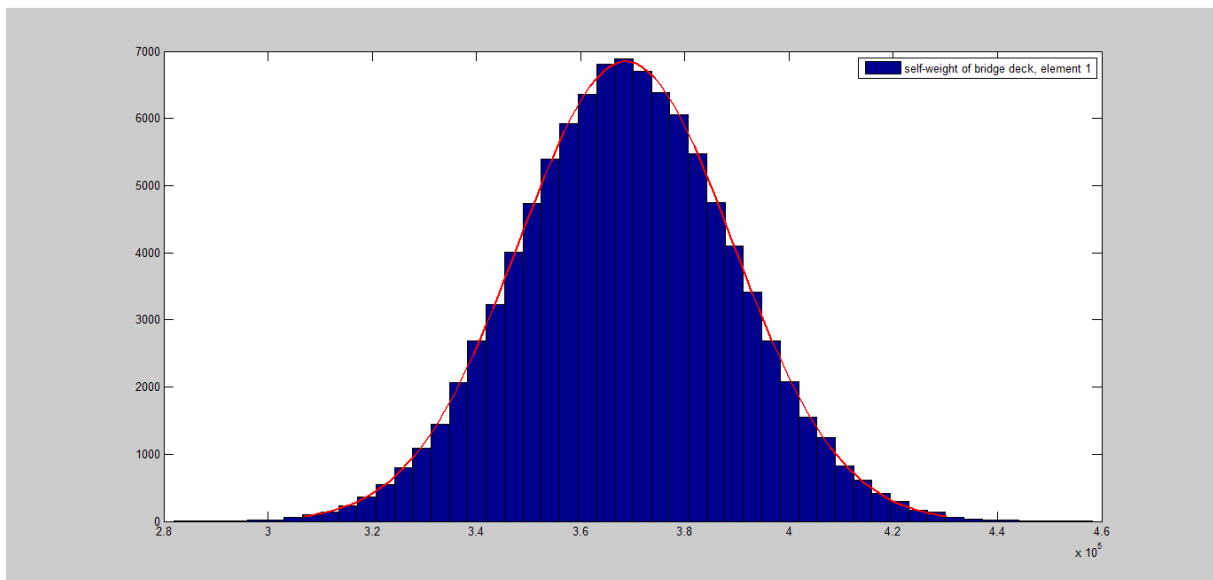


*Figure 6.6: Probability density plot for the entire bridge deck. For element 1 (see figure 3.2).*

Due to the fact that self-weight of the entire bridge deck is the sum of the two deck layer (steel and asphalt), observations and characteristics detected in the previous results is valid for the self-weight estimation as well.

One important note from this observation is the little variance in the values. As the hypothesis in the introduction states, oversizing of structures occur due to little variance in loading. The

structure considered in this thesis (Hardanger Bridge), therefore, meet the constraints stated in the hypothesis.

### 6.1.2 Component force estimation

The force calibration, with respect to the components, is performed in accordance with the procedure stated in section 5.3.1.

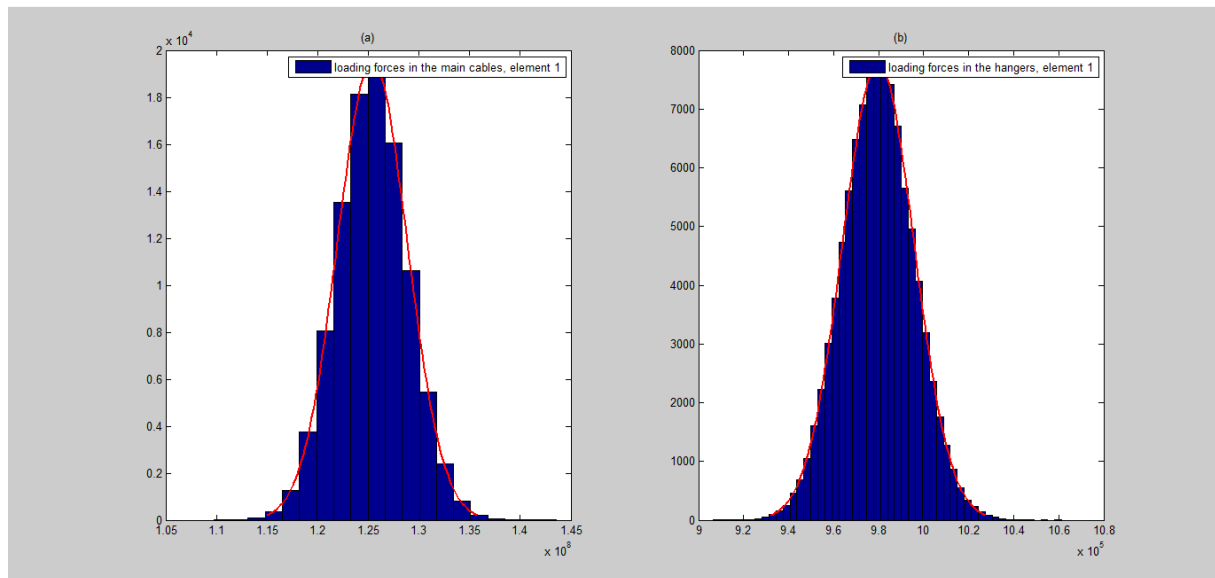
From the calibrated force values, found by using the procedure stated in section 5.3.1, normal distributed parameters for the axial loading (corresponding to each component) are estimated by using the method described in the section 5.5.1 (Loading,  $S$ ).

Table 6.3 shows mean values of the mean values and coefficients of variation for the hanger and main cable components, respectively.

| component  | Mean value | Coefficient of variation |
|------------|------------|--------------------------|
| Hanger     | 114 655 kN | 0.028                    |
| Main cable | 887 kN     | 0.043                    |

*Table 6.3: Mean values of the mean values and coefficients of variation for the axial loading in the hanger and main cable components.*

Plots of distribution of axial forces in the hangers and main cables, related to the self-weight loading is shown in figure 6.7. Notice, values for the distribution parameters, stated in table 6.3, are estimated from the distribution of forces in figure 6.7, assuming normal distribution.



*Figure 6.7: Probability density plots for the axial loading forces in component (a) 1000 (main cable), (b) 5002 (hanger). Figure 5.3 illustrate the components.*

As can be seen from the figure 6.7, values for the axial loading in the components tend to variate within a range of  $\{9.2 \cdot 10^2 kN, 10.4 \cdot 10^2 kN\}$  for the hanger (element 5002), and within a range of  $\{1.1 \cdot 10^5 kN, 1.4 \cdot 10^5 kN\}$  for the main cable (element 1000). Figure 6.7 gives higher values for the hanger loading, than the tabulated mean values in table 6.3. This

deviation may arise from the fact that the tabulated values consists of contributions from all the hanger components, while the figure only provide values for hanger component 5002.

Normal distribution, however, is assumed for both the hanger and main cable loading, which is consistent with the plot in figure 6.7.

Figure 6.8 shows plots of the dependency between different components. Number of the components are stated in table 5.1.

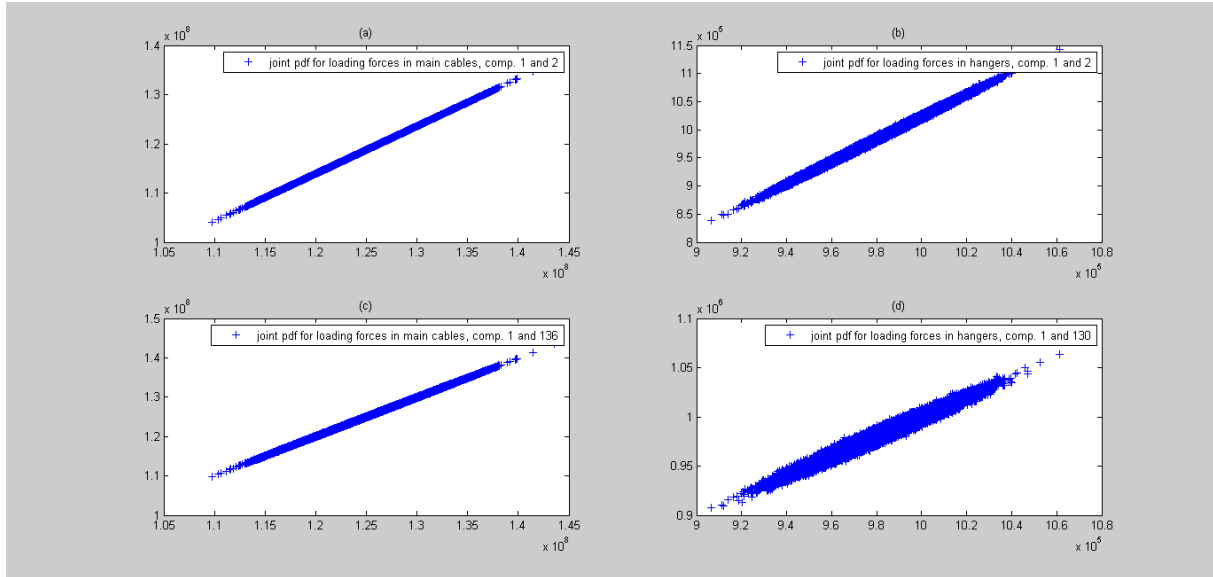


**Figure 6.8:** Joint pdf for the axial loading forces in components (a) 1000 and 1001 (main cable), (b) 5002 and 5003 (hanger), (c) 1000 and 2067 (main cable), (d) 5002 and 6066 (hanger). Figure 5.3 illustrates the components.

The plots show that the discrepancies between axial loading barely exist for the main cables, while there is a slight occurrence of discrepancies between hanger components, with increasing distance between the components. From these results, it is reasonable to believe that a higher correlation coefficient between the main cable components than for the hangers exists. The reason for this may be due to the fact that the axial loading in the main cable components are distributed into all main cable components, thus all components are assumed to carry approximately the same loading and the correlation is high. While the axial loading in the hanger components arises from loading near or close to the hanger component, hence different hangers do not carry the same loading and have a smaller correlation.

## 6.2 Resistance estimation

Estimation of the resistance capacity of the components are performed in accordance to the rules and procedure stated in chapter 4. Estimation of the hanger capacities need to be carried out by the use of codes, because of the lack of available information. Main cable capacities are estimated from tensile test data.

Values of the resistance capacities are shown in table 6.4.

## Ch. 6 Results and discussion

| Component  | Mean value (Yield stress) | Standard deviation (Yield stress) | Area of the cross-section | Coefficient of variation |
|------------|---------------------------|-----------------------------------|---------------------------|--------------------------|
| Main cable | 1686 MPa                  | 18.2 MPa                          | 0.2213 m <sup>2</sup>     | 0.011                    |
| Hanger     | 1570 MPa                  | 40 MPa                            | 0.0032 m <sup>2</sup>     | 0.025                    |

**Table 6.4:** Mean value, standard deviation, area of cross-section and coefficient of variation for the resistance capacity for the hanger and main cables components.

Density plot of the resistance capacity for components 1000 (main cable) and 5002 (hanger), are shown in figure 6.9. The different components are illustrated in figure 5.3.

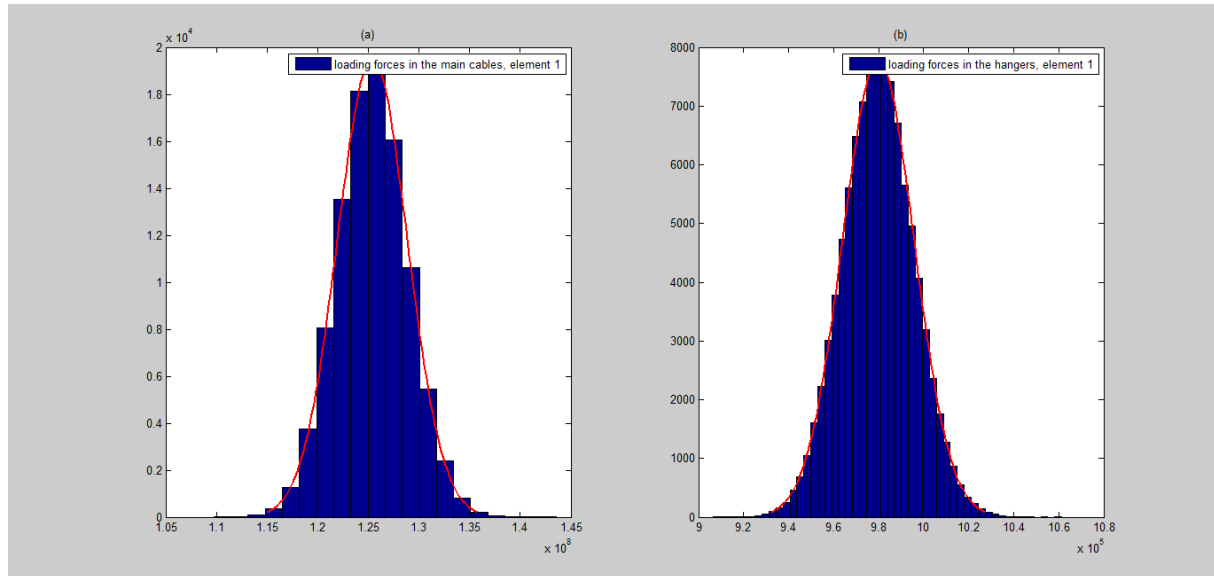


**Figure 6.9:** Probability density plot of the resistance capacity for component (a) 1000 (main cable), (b) 5002 (hanger).

Provided similar tabulated values of the material properties for the hanger and main cable components. Coefficient of variation are smaller for the main cables than the hangers. This means that the uncertainties related to the variation in capacity estimation are lower for estimates obtained from tests than from codes.

A higher mean value gives a higher resistance capacity, due to the fact that the resistance capacity is a function of the material properties  $f_{pk}$ , see (4.3) and (4.5). Hence, resistance capacities from codes tend to be smaller than capacities estimated from test data.

A lower variance and a higher mean value indicates that the estimated capacities from test data have a higher capacity and less uncertainties, while capacities estimated from codes have a lower capacity with a greater uncertainty. Hence, the resistance capacity estimated from codes tend to be undersized compared with the capacities obtained from the test data.

With a lower resistance capacities and greater variance, the area of the probability of failure becomes bigger, due to the fact that the area for overlap with the loading curve increase. Lower variance and a higher capacity decrease the area of failure, i.e. decrease the area of intersection between loading and resistance, as can be seen in figures 4.2 and 6.10. This means that the failure of probabilities will increase with the use of code estimation process, higher probability of failure lead to higher degree of dimension needed.



It is important to notice that the resistance capacity also depend on the cross-section of the component. The hanger components have smaller cross-sections than the main cables components, consequently resistance capacity in the hanger components will be less than resistance capacity in the main cable components.

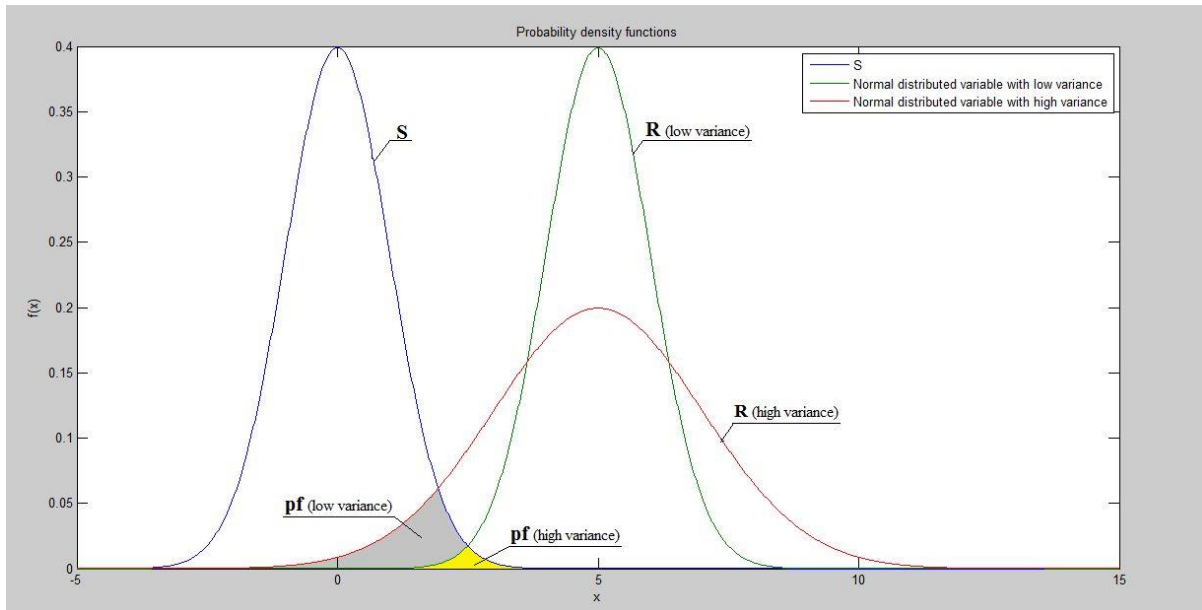


**Figure 6.10:** Curves for normal distributed variables with high and low variance and pdf for axial loading. Grey and yellow areas show the respective  $pf_f$ .

Figure 6.11 shows plots of the dependency between different components. Figure 5.3 and table 5.1 illustrate the different components.

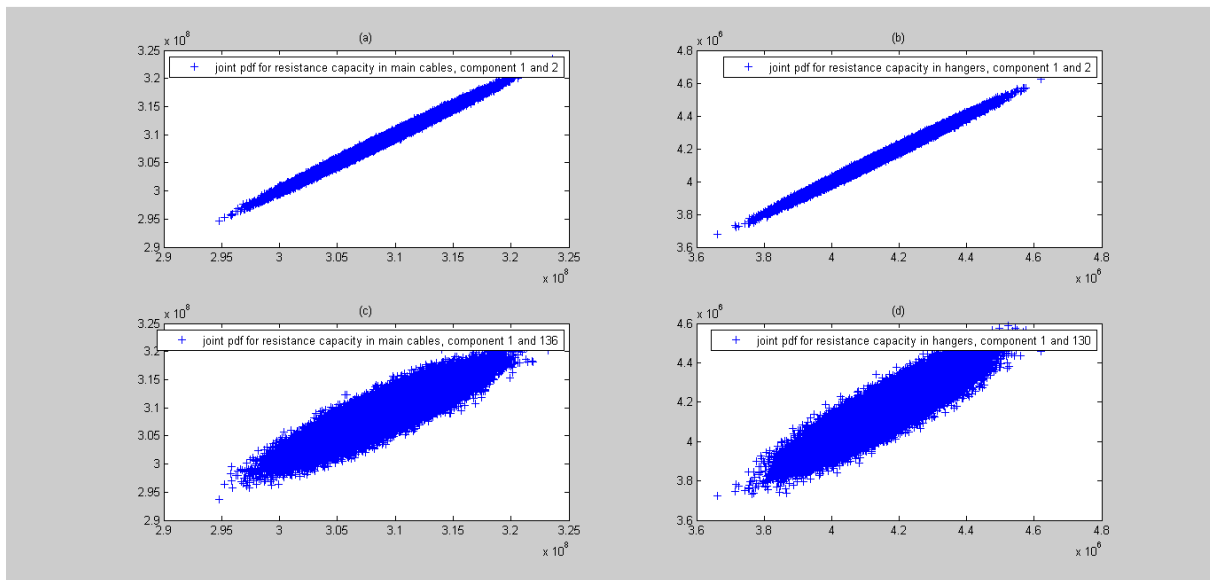


**Figure 6.11:** Joint pdf of resistance capacities between components (a) 1000 and 1001 (main cable), (b) 5002 and 5003 (hanger), (c) 1000 and 2067 (main cable), (d) 5002 and 6066 (hanger).

The plots in figure 6.11 show that the discrepancies between resistance capacities increases with increasing distance between the components. This is in agreement with the assumptions

made in section 4.3. Notice, the assumptions result in a rather low correlation between the far away from each other components, i.e. inner distance  $\Delta r = 1350 \text{ m}$  and  $\Delta r = 1290 \text{ m}$  for the main cable and hanger components, respectively. The main cable components consist of the same wires and most of the hanger components are produced by the same manufacturer, this may lead to a higher correlation coefficient than the assumed correlation coefficient in this thesis.

### 6.3 Reliability analysis

The reliability analysis was carried out according to the procedure stated in section 5.4.

Table 6.5 shows values for the reliability index, probability of failure and confidence intervals for  $n \in \{10^4, 10^5, 3 \cdot 10^5\}$  iterations of the Enhanced Monte Carlo method.

| Iterations     | $\beta$ | $p_f$                  | $C^+$                 | $C^-$                  |
|----------------|---------|------------------------|-----------------------|------------------------|
| $10^4$         | 12.46   | $5.86 \cdot 10^{-36}$  | $7.08 \cdot 10^{-30}$ | $1.30 \cdot 10^{-36}$  |
| $10^5$         | 14.36   | $4.83 \cdot 10^{-47}$  | $3.83 \cdot 10^{-41}$ | $1.65 \cdot 10^{-56}$  |
| $3 \cdot 10^5$ | 14.61   | $1.285 \cdot 10^{-48}$ | $4.83 \cdot 10^{-44}$ | $-1.40 \cdot 10^{-60}$ |

Table 6.5: Values for the reliability index, probability of failure, confidence limits for  $n$  simulations.

Figure 6.12 shows plot from the calculation process.

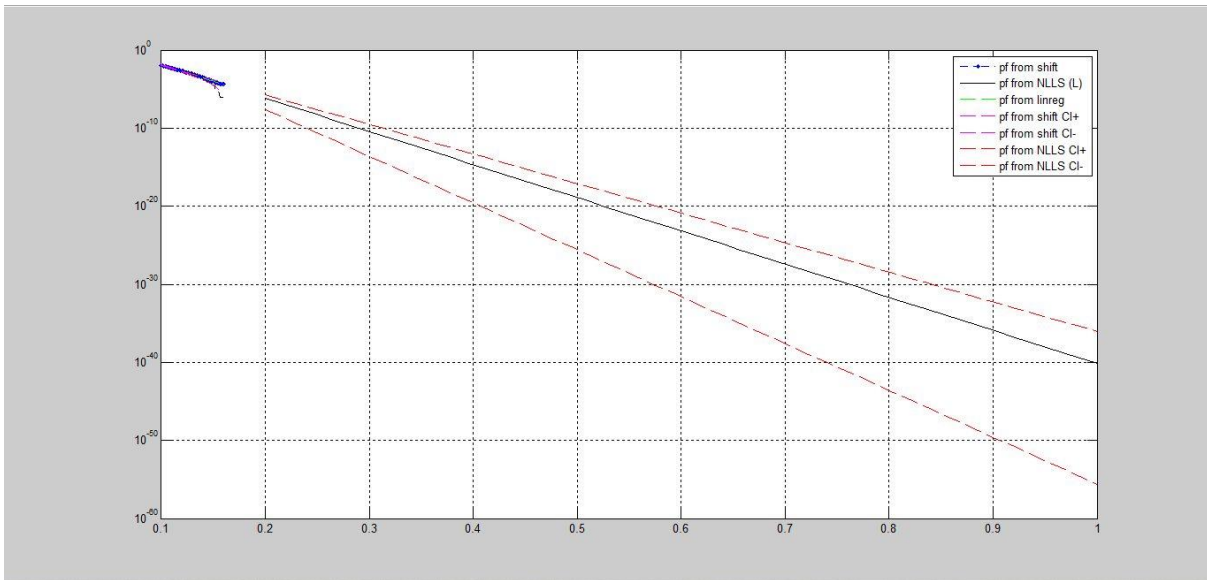


Figure 6.12: The extrapolation curve of enhanced method. Blue dots are obtained  $p_f$  from data points. Black and red curves estimate probability and confidence limit, respectively. Number of simulations,  $n = 10^5$ .

As can be seen from the figure 6.12 and table 6.5, the probability of failure  $p_f \in \{10^{-36}, 10^{-48}\}$  when  $\lambda \rightarrow 1$ . This leads to a reliability  $r = 1 - p_f \approx 1$ , which indicate that the structure satisfy the safety requirement far too well.

Even though the results state a way too high reliability, there is some uncertainties that need to be mentioned. Because of the low probability of failure, estimation of the probability of failure related to  $\lambda$  cannot be obtain for values of  $\lambda$  close to 1, i.e.  $P(\lambda_i) = NaN$  (Not a Number)  $\{\lambda \geq 0.16\}$ . Estimation of the probability of failure function, (2.106), may therefore become uncertain as follows from lack of information for  $\lambda \in \{0.16, 1.0\}$ .

The confidence interval, illustrated in figure 6.12 as dashed red lines and tabulated in table 6.5, cover a wide range of values due to the lack of obtained data  $P(\lambda_i)$  from estimations. Calculation of the confidence interval is explained in section 2.10.1 (confidence interval).

Provided assumption done in previous sections, limit state violation tend to occur in the hanger components only as  $\lambda \rightarrow 1$ . This indicate that the main cables have a higher safety level than the hangers, hence the hanger capacities need to be improved in order to obtain a higher safety level.

## 6.4 Code calibration (Second-Moment)

By using the results from section 6.1 and 6.2, along with the calibration strategy elaborated in section 5.5, calibration of the partial safety factors is possible.

Results of the partial safety factors calibrated in this master thesis for  $n = 3 \cdot 10^5$  simulations, along with partial safety factors found in codes and standards are presented in the table below.

| Partial safety factor | Calibrated from reliability analysis | Current norm of EC standards |
|-----------------------|--------------------------------------|------------------------------|
| $\gamma_R$            | 1.05                                 | 1.20                         |
| $\gamma_S$            | 1.05                                 | 1.35                         |

*Table 6.6: Partial safety factors for the resistance capacity and loading. Calibrated from the reliability analysis performed and obtained from codes [20], [24].*

Figure 6.13 shows the code calibration process.

## Ch. 6 Results and discussion

| component                    | myS [N]   | sigmaS [N] | COVs       | myR [N]   | sigmaR [N] | COVr        | Kr                   | -1,64      | beta       | $\Delta\beta$ |
|------------------------------|-----------|------------|------------|-----------|------------|-------------|----------------------|------------|------------|---------------|
| main cable north side (1000) | 125398568 | 3443286,75 | 0,02745874 | 308970525 | 3344118,03 | 0,010823421 | Ks                   | 1,64       | 5,68868989 | 0,23881781    |
|                              | 119152528 | 3329678,18 | 0,02794467 | 308970525 | 3344118,03 | 0,010823421 | $\beta$ targ         | 5,2        | 5,63526527 | 0,18945585    |
|                              | 118698992 | 3323688,03 | 0,02800098 | 308970525 | 3344118,03 | 0,010823421 | $\Sigma \Delta\beta$ | 126,058793 | 5,62916028 | 0,18417855    |
|                              | 118242240 | 3312513,14 | 0,02801463 | 308970525 | 3344118,03 | 0,010823421 | YR                   | 1,04950205 | 5,62768245 | 0,18291227    |
|                              | 117833776 | 3299786,94 | 0,02800374 | 308970525 | 3344118,03 | 0,010823421 | YS                   | 1,04950205 | 5,62886096 | 0,18392173    |
|                              | 117436664 | 3286792,3  | 0,02798779 | 308970525 | 3344118,03 | 0,010823421 | $\beta$ min          | 4,27266531 | 5,63058907 | 0,18540695    |
|                              | 117052824 | 3274114,71 | 0,02797126 | 308970525 | 3344118,03 | 0,010823421 | pf max               | 9,6575E-06 | 5,63238052 | 0,18695292    |
|                              | 116682008 | 3261950,14 | 0,0279559  | 308970525 | 3344118,03 | 0,010823421 |                      |            | 5,63404678 | 0,1883966     |
|                              | 116324296 | 3250266,28 | 0,02794142 | 308970525 | 3344118,03 | 0,010823421 |                      |            | 5,63561802 | 0,18976306    |
|                              | 115979760 | 3239017,83 | 0,02792744 | 308970525 | 3344118,03 | 0,010823421 |                      |            | 5,63713693 | 0,19108869    |
|                              | 115648464 | 3228196,25 | 0,02791387 | 308970525 | 3344118,03 | 0,010823421 |                      |            | 5,63861211 | 0,19238059    |
|                              | 115330480 | 3217754,17 | 0,02790029 | 308970525 | 3344118,03 | 0,010823421 |                      |            | 5,64008917 | 0,19367848    |
|                              | 115025880 | 3207654,84 | 0,02788638 | 308970525 | 3344118,03 | 0,010823421 |                      |            | 5,6416043  | 0,19501436    |
|                              | 114734712 | 3197969,06 | 0,02787272 | 308970525 | 3344118,03 | 0,010823421 |                      |            | 5,64309135 | 0,19632995    |
|                              | 114457048 | 3188646,58 | 0,02785889 | 308970525 | 3344118,03 | 0,010823421 |                      |            | 5,64459933 | 0,19766856    |
|                              | 114192944 | 3179704,54 | 0,02784502 | 308970525 | 3344118,03 | 0,010823421 |                      |            | 5,64611298 | 0,19901679    |
|                              | 113942464 | 3171116,48 | 0,02783086 | 308970525 | 3344118,03 | 0,010823421 |                      |            | 5,64765888 | 0,20039847    |
|                              | 113705656 | 3162911,98 | 0,02781666 | 308970525 | 3344118,03 | 0,010823421 |                      |            | 5,6492096  | 0,20178926    |
|                              | 113482576 | 3155081,74 | 0,02780235 | 308970525 | 3344118,03 | 0,010823421 |                      |            | 5,65077507 | 0,20319816    |

**Figure 6.13:** Estimation of the partial safety factors by using problem solver in excel.  $n = 3 \cdot 10^5$  simulations are performed.

The results show that the partial safety factors from standards and codes causes oversizing of the applied loading and the resistance capacity, according to (2.35) and (2.36) and section 2.11. Partial safety factors for loading gives the highest deviation between calibrated and tabulated values, as can be seen in the table 6.6. Hence, partial safety factor for loading contribute most to the oversizing.

It is important to note that the code calibration does not consider the differences between the two partial safety factors, and thus will the partial safety factors be equal. As discovered in section 6.2, codes and standards are underestimating the resistance capacities, consequently, partial safety factors from codes and standards will lead to under estimation of the resistance capacity and oversizing of the loading.

By inserting partial safety factors from codes (table 6.6) into the formula (5.3), following values for the reliability index and the probability of failure are obtained:

$$\beta = 12.64$$

$$p_f = 6.76 \cdot 10^{-37}$$

Notice, it is assumed that the system is a series system, hence minimum value of  $\beta$  is obtained in order to be conservative. The variables, however, are assumed normal distributed in order to use (2.58) for estimation of the failure probability.

The lowest values of the reliability index  $\beta$  appear in the hanger components only, low values of the reliability index result in a higher value of the failure probability, according to (2.58). This indicate that provided assumptions made in previous sections failure tend to occur in the hanger components, similar to the results from the Enhanced Monte Carlo method.

The results show that partial safety factors from codes and standard gives high reliability indexes and low failure probabilities.

## 6.5 Comparisons

By comparing the two reliability analyses of the Hardanger Bridge for  $n = 3 \cdot 10^5$  simulations, following result is obtained:

$$p_{f_{Enhanced\ MC}} < p_{f_{Second\ Moment}} \quad (6.1)$$

Hence:

$$\beta_{Enhanced\ MC} > \beta_{Second\ Moment} \quad (6.2)$$

The Enhanced Monte Carlo method provides confidence intervals with great range, due to the uncertainties related to the lack of information.

The Second-Moment method assume normal distribution of the resistance capacities and a target reliability index of 5.20, in order to obtain values for the partial safety factors and estimation of failure probability.

Failures tend to occur in the hanger components in results from both of the methods.

The components are assumed to act as a series system and simplifications of the structure in order to reduce computational effort are done.

Assumptions about the resistance capacity values for the hangers are made from obtained data and exponential function of the correlation coefficient are proposed for the resistance capacities.

In order to perform reliability analysis of the structure, assumptions and simplifications are done for both of the method, which lead to uncertainties in the results for both of the methods.

The results, however, from the two different approaches indicate that the structure is heavily oversized. Requirements for the reliability index related to structure with high amount of expected damage are equal to:

$$\beta \in \{4.30 - 5.20\} \quad (6.3)$$

Where the range in value correspond to the value of the reference period [20].

Because the estimated reliability indexes from both of the reliability analysis is way above this requirement, the analyses together state an oversizing of the structure.



---

# 7 Conclusion

In the present study, a reliability analysis of the Hardanger Bridge has been performed using two different methods:

1. Second-Moment method based on load and resistance factor design format (LRFD)
2. Enhanced Monte Carlo simulation

The analysis was separated into three main parts. Firstly, calibration of the loading, secondly estimation of the resistance and at last comparisons of the results from the two previously parts.

Results from the Second-Moment method gave partial safety factors for the resistance and loading equal to 1.05, which is much lower than the standardized partial safety factors from codes equal to {1.20, 1.35} for the resistance and loading, respectively. By taking advantage of the standardized partial safety factors, estimates for the reliability index {12.6} and failure probability { $10^{-37}$ } were obtained.

Enhanced Monte Carlo method gave estimates of the reliability index in the range {12.4, 14.6}, which corresponds to a probability of failure in the range { $10^{-36}$ ,  $10^{-48}$ }. These results involve a lot of uncertainties due to the fact lack of information when  $\lambda \rightarrow 1$ . Even though the confidence interval indicate a huge amount of uncertainties related to these results, the estimates show a significant higher safety level than required in codes and standards.

The results of the failure probability showed that hanger components tend to fail during estimation, hence the hanger components seemed to be the weakest one, i.e. ratio between capacity and loading is lower for hangers compared to main cable components. Provided consideration due to the assumptions made in previous chapters.

Both of the solution strategies show that the reliability of the bridge is widely oversized. The Second-Moment method showed that standardized partial safety factor for the loading contribute most to the oversizing of the structure. The main reason for this is due to the fact that the standardized partial safety factors ensure reliable results for all kind of structural problems. Stated in another way, to ensure reliable results for structures exposed to all kind of action forces, i.e. safety requirements are fulfilled, overestimation of the partial safety factors appears. Results from the load calibration showed that structures exposed to dead load only have a rare occurrence of large deviations, in other words dead load have a low variance. Standardized partial safety factors for loading account for high a variance, thus a high oversizing of the self-weight loading.

The conclusion of the reliability analysis is in agreement with the stated hypothesis:

*Structures, where the main loading consist of dead load, tend to be oversized due to the low variance in the loading.*

The effects of the use of codes and standard use in design calculation, in structures where self-weight is the major loading, are oversizing and inefficiency use of resources. Oversizing leads

to excessive use of materials and resources, thus the structure becomes cost inefficient and harming the environment.

In order to conduct the reliability analysis in an acceptable manner, several assumptions were made. Firstly, the limit state function was assumed to consider axial loading and resistance for the hangers and main cables only, consequently reliability analysis and code calibration were performed on the hanger and main cable components. In addition, the structure was assumed to behave as a series system.

The loading in each component was calibrated by taking advantage of an influence surface, as mentioned in sections 5.2.2 and 5.3, and by estimating the self-weight of the bridge deck chapter 3.

The resistance was estimated on behaviour of codes, manuals and available data from tensile tests. Assumptions of the correlation between the components may cause uncertainties related to the results, but within acceptable limit for the total conclusion.

Both the loading and the resistance capacities were assumed to behave normally distributed, due to the effect of the *Central-Limit-Theorem*, see Freeman and Benjamin and Cornell [11], [12].

All assumptions made in the analysis are considered to include some uncertainties. The uncertainties are assumed to be within acceptable limits of accuracy compared to the magnitude of the results, which is way above safety requirements from codes.

Further, the reliability analysis is carried out by using two different methods, both of the methods are well-known and often used methods in reliability analysis. The Second-Moment method uses the two first moments of each random variable in the limit state function to derive the reliability index, hence the name Second-Moment. In this analysis, the method uses the strength based terminology *Load and Resistance Factor Design* (LRFD) format, which compare required strength to actual strength by including several safety factors  $\gamma$  in the calculations, see [31].

The second method is a Monte Carlo method, which involve repetitive iterations. The method generate  $n$  simulations of the random variables included in the limit state function and count the occurrence of limit state violation, when the generations are applied. Due to the large number of iterations needed in order to obtain good results, the Crude Monte Carlo method tend to be too time consuming. Hence, the Enhanced Monte Carlo method was applied in order to reduce the number of iteration needed. The Enhanced Monte Carlo method is elaborated in section 2.10.3.

## 7.1 Further work

In further work, reliability analysis with more attention to reduction of the uncertainties should be performed.



As stated in the previous section, assumptions and simplifications due to reduction of the complexity of the problem were made. Considerations and investigation of following steps should be accounted for in order to increase the accuracy of the results:

- More consideration of the entire bearing system. Include contribution from pylons, bridge deck, fundamentals, etc. in the resistance and loading estimation.
- Consider taking advantage of other distribution. For instance, Gumbel distributed loading and Log-Normal distributed resistance capacity.
- Further investigation of the correlation coefficient and estimation of characteristic values for the loading and resistance capacity.
- Taking advantage of more advanced computational tools in utilization of the Enhanced Monte Carlo method, i.e. gather more data points  $(\lambda_i, p_f(\lambda_i))$ , especially for higher values of  $\lambda_i$ .

In addition, in order to increase the reliability of the analysis other steps not mentioned here should also be considered, e.g. uncertainties due to the statistical tools used, simplifications of the structure, human error, etc.

Attention of other loads acting simultaneously and cooperation of loading should be considered. In this thesis, the major loading is assumed to consist of the self-weight of the structure. Investigation and research about the validity of this assumption should be made in order to increase the reliability of the statement “...where the loading only (or nearly only) consist of self-weight...” (hypothesis). In addition, reliability analysis of similar structures, i.e. major loading consist of self-weight, should be performed in order to strengthen the credibility of the conclusion in this study.



---

# Bibliography

- [1] Statens Vegvesen. Ferjefri E39, <http://www.vegvesen.no/vegprosjekter/ferjefriE39>, May 19 2016.
- [2] G. A. Bugge. *Structural Reliability Analysis of the Hardanger Bridge using an enhanced Monte Carlo Method*. Master thesis, Norwegian University of Science and Technology (NTNU), Faculty of Engineering Science and Technology - department of Structural Engineering, Trondheim (Norge), 2014.
- [3] K. Hamang. *System identification of the Hardanger Bridge using enhanced frequency domain decomposition*, Master thesis, Norwegian University of Science and Technology (NTNU), Faculty of Engineering Science and Technology - department of Structural Engineering, Trondheim (Norge), 2015.
- [4] Statens Vegvesen. *RV. 13 Hardangerbrua*, Teknisk brosjyre Hardangerbrua, Kart over prosjektet, Brua (Bruteikning), Illustrasjoner, <http://www.vegvesen.no/vegprosjekter/Hardangerbrua>, May 23 2016.
- [5] G. Brekke. *Hardanger Bridge Information*. Norwegian Public Roads Administration, 2011.
- [6] J. Schneider. *Introduction to Safety and Reliability of Structures*, volume 5 of *Structural Engineering Documents*. Zurich: International Association for Bridge and Structural Engineering, 2nd edition, 2006.
- [7] P. Thoft-Christensen and M.-J. Baker. *Structural Reliability Theory and Its Applications*. Springer-Verlag Berlin, Heidelberg, New York, 1982.
- [8] R.E. Melchers. *Structural Reliability Analysis and Prediction*. Wiley, 2nd edition, 1999.
- [9] H.O. Madsen, S. Krenk and N.C. Lind. *Methods of Structural Safety*. DOVER PUBLICATIONS, INC. Mineola, New York, 2006.
- [10] P.-K. Larsen. *Konstruksjonsteknikk-Laster og bæresystemer*, Tapir akademisk forlag, 2nd edition, Trondheim, 2008.
- [11] H. Freeman. *An introduction to Statistical Inference*, Addison-Wesley, Reading, MA, 1963.
- [12] J.R. Benjamin and C.A. Cornell. *Probability, Statistics and Decisions for Civil Engineers*, McGraw-Hill, New York, 1970.
- [13] C.A. Cornell. A Probability-Based Structural Code, *Journal of the American Concrete Institute*, Vol. 35, No. 12, pp. 974-985, 1969.
- [14] A.M. Hasofer and N.C. Lind. Exact and Invariant Second-moment Code Format, *Journal of the Engineering Mechanics Division*, ASCE, Vol. 100 (EM1), pp. 111-121, 1974.

- [15] Lecture notes. Simulation. <http://people.hss.caltech.edu/~mshum/gradio/simulation.pdf> May 5 2016.
- [16] A. Næss et.al. System reliability analysis by enhanced monte carlo simulation. *Structural Safety*, 31(5):349–355, September 2009.
- [17] M. Papadrakakis et.al. *Computational Methods in Stochastic Dynamics*, volume 2. Springer, 2013.
- [18] P.-E. Gill, W. Murray and M.-H. Wright. *Practical Optimization*. Academic Press, London, 1981.
- [19] JCSS PROBABILISTIC MODEL CODE. Part 2: Load models, 2.1 Self Weight, 2001.
- [20] Standard Norge. NS-EN 1990:2002+A1:2005+NA2016, *Grunnlag for prosjektering av konstruksjoner*, Tabell A2.4(B), B3.1 and B3.2, January 2016.
- [21] Standard Norge, NS-EN 1993-1-1:2005+A1:2014/NA:2015, *Prosjektering av stålkonstruksjoner – Del 1-1: Allmenne regler og regler for bygninger*, 2.4.3 Dimensjonerende kapasitet, NA.6.1(1)2B, January 2015.
- [22] JCSS PROBABILISTIC CODE. Part 3: Material Properties, 3.04 Static Properties of Prestressing Steel, 2000.
- [23] Statens Vegvesen. Håndbok 410: *Kabler til hengebruer*, tekniske spesifikasjoner, June 2014.
- [24] Standard Norge. NS-EN 1993-1-11:2006/NA:2009, *Prosjektering av stålkonstruksjoner – Del 1-11: Kabler og strekkstag*, NA.3.1(1) Kapasitet av konstruksjons stål og ståltråd, NA.6.2.(2), January 2009.
- [25] M.-H. Fabera et al. Aspects of parallel wire cable reliability, *Structural Safety*, 25 (2003) 201-225, 19 August 2002.
- [26] F.-Ø. Slungård and T. Østen. *Structural performance of parallel wires*, Master thesis, Norwegian University of Science and Technology, 2015.
- [27] Statens Vegvesen. Håndbok 185: *Bruprosjektering*. Høringsutgave, November 1, 2013.
- [28] Alfasofts. Produkter, <http://www.alfasoft.com/no/produkter/matematikk/abaqus.html#info>, April 11 2016.
- [29] Dassault systems. Products & service, simulia, products, abaqus, <http://www.3ds.com/products-services/simulia/products/abaqus/>, April 11 2016.
- [30] MathWorks. Product, <http://se.mathworks.com/products/matlab/>, April 11 2016.
- [31] T.-B. Quimby (2008). Basic Design Concepts, A Beginner's Guide to the Structural Engineering, Section DC.5 ASD Vs LRFD (last revised 2014), <http://www.bgstructuralengineering.com/BGDesign/BGDesign05.htm>, April 19 2016.

---

# Appendices



---

# **Appendix A**

Basis of calculation


|  |                                      |            |           |           |                             |
|--|--------------------------------------|------------|-----------|-----------|-----------------------------|
| <br><b>Statens vegvesen</b> |                                      |            |           |           |                             |
| <b>12-2950 HARDANGERBRUA</b><br><b>BEREGNINGER</b><br><b>KAPITTEL 1: GRUNNLAG</b>                            |                                      |            |           |           |                             |
|  |                                      |            |           |           |                             |
| 5  | Til godkjenning                      | 14.11.2008 | AGK       | BI        | BI                          |
| 4  | Til teknisk delgodkjenning, supplert | 31.10.2007 | AGK       | BI        | BI                          |
| 3  | Til teknisk delgodkjenning, supplert | 13.08.2007 | AGK       | BI        | BI                          |
| 2  | Til teknisk delgodkjenning, supplert | 06.03.2007 | AGK       | GAG       | BI                          |
| 1  | Til teknisk delgodkjenning           | 16.01.2007 | AGK       | GAG       | BI                          |
| Revisjon   | Revisjonen gjelder                   | Dato       | Utarb. av | Kontr. av | Godkj. av                   |
| <b>Prosjekt:</b><br><b>12-2950 Hardangerbrua</b>   |                                      |            |           |           | <b>Revisjon</b><br><b>5</b> |

Figure A.1: Basis of Calculation.



|   |                      |       |            |
|---|----------------------|-------|------------|
| <br>Statens vegvesen | <b>Hardangerbrua</b> | SIDE  | 1-7        |
|   | Kapittel 1: Grunnlag | DATO  | 14.11.2008 |
| Teknologiavdelingen   |                      | SIGN. | AGK        |

## 1.4 Hoveddata

### 1.4.1 Geometri

|                            |           |
|----------------------------|-----------|
| Spennvidde                 | 1310 m    |
| Pilhøyde bærekabel         | 121 m     |
| Seilingshøyde              | 55 m      |
| - bredde                   | 300 m     |
| Kjørebanebredde            | 9 m       |
| Gangbanebredde             | 3,25 m    |
| Kotehøyde S-punkt Vallavik | 102,763 m |
| Kotehøyde S-punkt Bu       | 102,763 m |
| Kotehøyde T-punkt Vallavik | 187,5 m   |
| Kotehøyde T-punkt Bu       | 187,5 m   |
| Planumskote ved tårn       | 52,771 m  |
| Planumskote ved brumidte   | 63,5 m    |

|                                    |          |
|------------------------------------|----------|
| Avstand mellom kabelplan           | 14,5 m   |
| Avstand mellom S-punkter, Vallavik | 17,319 m |
| Avstand mellom S-punkter, Bu       | 17,319 m |

### 1.4.2 Stivhet

Avstivningsbærer:

$$\begin{aligned}
 A &= 0,5813 \text{ m}^2 \\
 I_x &= 0,972 \text{ m}^4 \\
 I_y &= 16,448 \text{ m}^4 \\
 I_T &= 2,460 \text{ m}^4 \\
 I_W &= 4,298 \text{ m}^6 \\
 E &= 210.000 \text{ N/mm}^2
 \end{aligned}$$

Horizontal nøytralakse:  
Vertikal nøytralakse:

- 1953 mm fra undersiden  
- tilnærmet midt i tverrsnittet

Skjærcenter:

- 1759 mm fra undersiden  
- 155 mm til side for vertikal nøytralakse

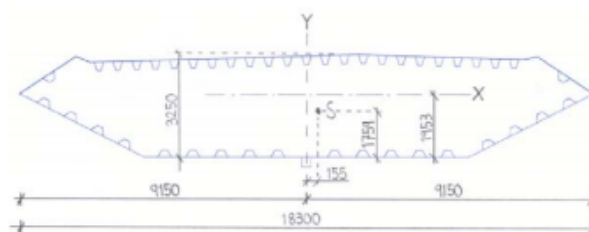


Figure A.2: Basis of Calculation.

|   |                      |       |            |
|---|----------------------|-------|------------|
| <br>Statens vegvesen | <b>Hardangerbrua</b> | SIDE  | 1-8        |
|   | Kapittel 1: Grunnlag | DATO  | 14.11.2008 |
| Teknologiavdelingen   |                      | SIGN. | AGK        |

Bærekabler:

$$A = 0,22132 \text{ m}^2 \text{ (effektivt stålareal pr. bærekabel)} \quad /K7/$$

$$E = 200.000 \text{ N/mm}^2 \quad /2/$$

Hengestenger:

$$A = 3200 \text{ mm}^2$$

$$E = 160.000 \text{ N/mm}^2$$

Merknad vedrørende E-modul for hengestenger:

På et senere tidspunkt (under produksjonen av hengestengene) skal den faktiske E-modulen fastlegges ved strekkprøving. Inntil dette er utført baseres analysene på angitt E-modul. Angitt E-modul for hengestenger er basert på resultater fra strekkprøving av lukket, spiralslått kabel til andre bruer. Det vises spesielt til rapport fra strekkprøving av bærekabler Ø97 til Lysefjordbrua.

Tåm:

Stivheten vil bli vurdert spesielt ifm. analyse og dimensjonering av tåm i hovedkapittel 4. Inntil mer detaljerte beregninger og vurderinger foreligger, kan det i globale analyser regnes med følgende øvre og nedre grense for E-modul:

$$E_{\text{curisset}} = 40\,000 \text{ N/mm}^2$$

$$E_{\text{crisset}} = 10\,000 \text{ N/mm}^2$$

Merknad:

Som det fremgår er urisset E-modul større enn betongmaterialets E-modul =  $E_{\text{ck}} = 29.764 \text{ N/mm}^2$ . Den angitte E-modul på  $40\,000 \text{ N/mm}^2$  er ment å fange virkningen av armering og i analyser regnes den effektive E-modul derfor større enn  $E_{\text{ck}}$ .

Figure A.3: Basis of Calculation.

|   |                      |       |            |
|---|----------------------|-------|------------|
| <br>Statens vegvesen | <b>Hardangerbrua</b> | SIDE  | 1-9        |
|   | Kapittel 1: Grunnlag | DATO  | 14.11.2008 |
| Teknologiavdelingen   |                      | SIGN. | AGK        |

### 1.4.3 Masse

#### i) Detaljert oppsett

|                                 |                  |               |
|---------------------------------|------------------|---------------|
| Avstivningsbærer:               |                  | /Vedlegg 1.4/ |
| Langsgående stål                | 4563 kg/m        |               |
| Ledeskovler (2 stk)             | 114 kg/m         |               |
| Tverskott                       | 1119 kg/m        |               |
| Nedre hengestangsfester         | 84 kg/m          |               |
| Rekkverk m/festeplater          | 183 kg/m         |               |
| Belegning (membran og slitelag) | 2674 kg/m        |               |
| Elektroinstallasjoner etc.      | 35 kg/m          |               |
| Transportskinne IPE 120         | 11 kg/m          |               |
| Lysmaster m/festeplater         | 5 kg/m           |               |
| Sluk                            | 3 kg/m           |               |
| Overflatebehandling             | 34               |               |
| <b>Sum</b>                      | <b>8825 kg/m</b> |               |
| Lengde avstivningsbærer         | 1 308 m          |               |
| Tonnasje i hovedspenn           | 11 543 tonn      |               |

|                               |                   |      |
|-------------------------------|-------------------|------|
| Bærekabler:                   |                   | /K7/ |
| Bærende tverrsnitt            | 1 737,4 kg/m      |      |
| Sink                          | 58,5 kg/m         |      |
| Vikletråd                     | 41,5 kg/m         |      |
| Kabelrekkverk                 | 7,0 kg/m          |      |
| Polyetylenduk                 | 6,6 kg/m          |      |
| <b>Sum (pr. bærekabel)*</b>   | <b>1 851 kg/m</b> |      |
| Lengde bærekabel i hovedspenn | 2 × 1 339,2 M     |      |
| Tonnasje i hovedspenn         | 4 958 tonn        |      |
| Tonnasje inkl. bakstag        | 6 520 tonn        |      |

\* målt pr. lengdeenhet bærekabel - ikke horisontal projeksjon.

Figure A.4: Basis of Calculation.

|   |                      |       |            |
|---|----------------------|-------|------------|
| <br>Statens vegvesen | <b>Hardangerbrua</b> | SIDE  | 1-10       |
|   | Kapittel 1: Grunnlag | DATO  | 14.11.2008 |
| Teknologiavdelingen   |                      | SIGN. | AGK        |

Hengestenger, 130 stk: /Vedlegg 1.4/

|  |                 |
|--|-----------------|
| Spiralslått tau                                  | 159,4 tonn      |
| Hengestanghoder                                  | 52,3 tonn       |
| Hengestenger 31-35 (støpejern)                   | 7,0 tonn        |
| Lagerdetaljer hengestanghoder                    | 15,1 tonn       |
| Øvre hengestangs feste                           | 165,4 tonn      |
| Tonnasje i hovedspenn                            | 399,2 tonn      |
| Fordelt langs avstivningsbærer<br>(3992000/1308) | <b>305 kg/m</b> |

Kabelklemmer bakstag: /Mat.liste D54/

|                                   |                |
|-----------------------------------|----------------|
| Totalt antall kabelklemmer        | 44 stk         |
| Vekt pr. kabelklemme inkl. bolter | 336 kg         |
| Tonnasje kabelklemmer bakstag     | 15 tonn        |
| Ekv. masse langs ett bakstag**    | <b>19 kg/m</b> |

\*\* målt pr. lengdeenhet bakstag = 15 000 / (4x191,5)

Samlet tonnasje i hovedspenn:

|                  |                    |
|------------------|--------------------|
| Avstivningsbærer | 11 543 tonn        |
| Bærekabler       | 4 958 tonn         |
| Hengestenger     | 399 tonn           |
| <b>Totalt</b>    | <b>16 900 tonn</b> |

Massetregningsmoment i hovedspenn:

|                         |                                    |
|-------------------------|------------------------------------|
| Avstivningsbærer        | 222 860 [kgm <sup>2</sup> /m]      |
| Bærekabler              | 194 586 [kgm <sup>2</sup> /m]      |
| Hengestenger            | 10 965 [kgm <sup>2</sup> /m]       |
| <b>Totalt, avrundet</b> | <b>428 411 [kgm<sup>2</sup>/m]</b> |

/Vedlegg 1.4/

#### ii) Nøkkeltall til bruk i globale analyser /K2/

|   | Teoretisk iht. oppsett over | Brukes i globale analyser i /K2/ | Avvik [%] |
|---|-----------------------------|----------------------------------|-----------|
| Masse pr. løpemeter [kg/m]:                 |                             |                                  |           |
| Avstivningsbærer                            | 8 825                       | <b>8 832</b>                     |           |
| Bærekabler inkl. alt                        | 2 × 1 851                   | <b>2 × 1 848</b>                 |           |
| Hengestenger                                | 305                         | <b>295</b>                       |           |
| <b>Totalt</b>                               | <b>12832</b>                | <b>12 823</b>                    | -0,07     |
| Massetregningsmoment [kgm <sup>2</sup> /m]: |                             |                                  |           |
| Avstivningsbærer                            | 222 860                     | <b>224 346</b>                   |           |
| Bærekabler                                  | 194 586                     | <b>194 271</b>                   |           |
| Hengestenger                                | 10 965                      | <b>9 829</b>                     |           |
| <b>Totalt</b>                               | <b>428 411</b>              | <b>428 446</b>                   | 0         |

I de globale analysene i hovedkapittel 2 benyttes mao. massedata som avviker ørlite i forhold til teoretiske verdier fra masseberegningen i vedlegg 1.4. Grunnen til dette er ørsmå justeringer som ble gjort i masseberegningen etter at de globale analysene var ferdigstilt. Avvikene har ingen praktisk betydning for analyse eller dimensjonering. Kabelgeometriregning for montasjetegning baseres på teoretiske verdier.

Figure A.5: Basis of Calculation.

|   |                      |       |            |
|---|----------------------|-------|------------|
| <br>Statens vegvesen | <b>Hardangerbrua</b> | SIDE  | 1-11       |
|   | Kapittel 1: Grunnlag | DATO  | 14.11.2008 |
| Teknologiavdelingen   |                      | SIGN. | AGK        |

## 1.5 Materialer

|   |  |      |
|---|--|------|
| Avstivningsbærer  | $f_y = 355 \text{ N/mm}^2$<br>$E = 210.000 \text{ N/mm}^2$   | /10/ |
| Bærekabler  | $f_u = 1570 \text{ N/mm}^2$<br>$E = 200.000 \text{ N/mm}^2$  | /2/  |
| Hengestenger  | $f_u = 1570 \text{ N/mm}^2$<br>$E = 160.000 \text{ N/mm}^2$  |      |
| Tårnfundament<br>Spredesadelfund.<br>Forankringskloss<br>Forankringsplate | Fasthetsklasse B35 <sup>1</sup><br>$f_{ck} = 45 \text{ N/mm}^2$<br>$f_{ock} = 35 \text{ N/mm}^2$<br>$f_{cn} = 27,3 \text{ N/mm}^2$<br>$f_{tn} = 2,00 \text{ N/mm}^2$<br>$E_{cn} = 26.968 \text{ N/mm}^2$<br>$E_{ck} = 27.602 \text{ N/mm}^2$ | /11/ |
| Tårn<br>Viadukt<br>Spredeskammer  | Fasthetsklasse B45<br>$f_{ck} = 55 \text{ N/mm}^2$<br>$f_{ock} = 45 \text{ N/mm}^2$<br>$f_{cn} = 34,3 \text{ N/mm}^2$<br>$f_{tn} = 2,30 \text{ N/mm}^2$<br>$E_{cn} = 28.879 \text{ N/mm}^2$<br>$E_{ck} = 29.764 \text{ N/mm}^2$              | /11/ |
| Understøp<br>av sadel på<br>tårntopp                                      | Fasthetsklasse B55<br>$f_{ck} = 67 \text{ N/mm}^2$<br>$f_{ock} = 55 \text{ N/mm}^2$<br>$f_{cn} = 39,8 \text{ N/mm}^2$<br>$f_{tn} = 2,55 \text{ N/mm}^2$<br>$E_{cn} = 30.197 \text{ N/mm}^2$<br>$E_{ck} = 31.611 \text{ N/mm}^2$              | /11/ |

<sup>1</sup>B35 betong:

B35 betong brukes i massive konstruksjonsdeler og utføres som spesiell lavvarmebetong for å gi redusert varmeutvikling under herding og redusert termisk opprissing i herdefasen. Betongens fasthetsegenskaper mht. dimensjonering er som for vanlig B35 betong.

Materialfaktorer:

Generelt benyttes materialfaktorer i tråd med prosjekteringsreglene og NS 3472 og NS 3473.

Materialfaktorer tårn:

For tårnene gjelder spesielt: For ordinær bruddgrensetilstand benyttes reduserte materialfaktorer for betong og armering i tråd med NS 3473 tabell 4. Under dimensjoneringen tas det hensyn til avvik i tverrsnittsdimensjoner.

Figure A.6: Basis of Calculation.



---

# **Appendix B**

Statistic tables

## Standard normalfordeling

$$\Phi(z) = P(Z \leq z)$$

| $z$  | .00   | .01   | .02   | .03   | .04   | .05   | .06   | .07   | .08   | .09   |
|------|-------|-------|-------|-------|-------|-------|-------|-------|-------|-------|
| -3.7 | .0001 | .0001 | .0001 | .0001 | .0001 | .0001 | .0001 | .0001 | .0001 | .0001 |
| -3.6 | .0002 | .0002 | .0001 | .0001 | .0001 | .0001 | .0001 | .0001 | .0001 | .0001 |
| -3.5 | .0002 | .0002 | .0002 | .0002 | .0002 | .0002 | .0002 | .0002 | .0002 | .0002 |
| -3.4 | .0003 | .0003 | .0003 | .0003 | .0003 | .0003 | .0003 | .0003 | .0003 | .0002 |
| -3.3 | .0005 | .0005 | .0005 | .0004 | .0004 | .0004 | .0004 | .0004 | .0004 | .0003 |
| -3.2 | .0007 | .0007 | .0006 | .0006 | .0006 | .0006 | .0006 | .0005 | .0005 | .0005 |
| -3.1 | .0010 | .0009 | .0009 | .0009 | .0008 | .0008 | .0008 | .0008 | .0007 | .0007 |
| -3.0 | .0013 | .0013 | .0013 | .0012 | .0012 | .0011 | .0011 | .0011 | .0010 | .0010 |
| -2.9 | .0019 | .0018 | .0018 | .0017 | .0016 | .0016 | .0015 | .0015 | .0014 | .0014 |
| -2.8 | .0026 | .0025 | .0024 | .0023 | .0023 | .0022 | .0021 | .0021 | .0020 | .0019 |
| -2.7 | .0035 | .0034 | .0033 | .0032 | .0031 | .0030 | .0029 | .0028 | .0027 | .0026 |
| -2.6 | .0047 | .0045 | .0044 | .0043 | .0041 | .0040 | .0039 | .0038 | .0037 | .0036 |
| -2.5 | .0062 | .0060 | .0059 | .0057 | .0055 | .0054 | .0052 | .0051 | .0049 | .0048 |
| -2.4 | .0082 | .0080 | .0078 | .0075 | .0073 | .0071 | .0069 | .0068 | .0066 | .0064 |
| -2.3 | .0107 | .0104 | .0102 | .0099 | .0096 | .0094 | .0091 | .0089 | .0087 | .0084 |
| -2.2 | .0139 | .0136 | .0132 | .0129 | .0125 | .0122 | .0119 | .0116 | .0113 | .0110 |
| -2.1 | .0179 | .0174 | .0170 | .0166 | .0162 | .0158 | .0154 | .0150 | .0146 | .0143 |
| -2.0 | .0228 | .0222 | .0217 | .0212 | .0207 | .0202 | .0197 | .0192 | .0188 | .0183 |
| -1.9 | .0287 | .0281 | .0274 | .0268 | .0262 | .0256 | .0250 | .0244 | .0239 | .0233 |
| -1.8 | .0359 | .0351 | .0344 | .0336 | .0329 | .0322 | .0314 | .0307 | .0301 | .0294 |
| -1.7 | .0446 | .0436 | .0427 | .0418 | .0409 | .0401 | .0392 | .0384 | .0375 | .0367 |
| -1.6 | .0548 | .0537 | .0526 | .0516 | .0505 | .0495 | .0485 | .0475 | .0465 | .0455 |
| -1.5 | .0668 | .0655 | .0643 | .0630 | .0618 | .0606 | .0594 | .0582 | .0571 | .0559 |
| -1.4 | .0808 | .0793 | .0778 | .0764 | .0749 | .0735 | .0721 | .0708 | .0694 | .0681 |
| -1.3 | .0968 | .0951 | .0934 | .0918 | .0901 | .0885 | .0869 | .0853 | .0838 | .0823 |
| -1.2 | .1151 | .1131 | .1112 | .1093 | .1075 | .1056 | .1038 | .1020 | .1003 | .0985 |
| -1.1 | .1357 | .1335 | .1314 | .1292 | .1271 | .1251 | .1230 | .1210 | .1190 | .1170 |
| -1.0 | .1587 | .1562 | .1539 | .1515 | .1492 | .1469 | .1446 | .1423 | .1401 | .1379 |
| -.9  | .1841 | .1814 | .1788 | .1762 | .1736 | .1711 | .1685 | .1660 | .1635 | .1611 |
| -.8  | .2119 | .2090 | .2061 | .2033 | .2005 | .1977 | .1949 | .1922 | .1894 | .1867 |
| -.7  | .2420 | .2389 | .2358 | .2327 | .2296 | .2266 | .2236 | .2206 | .2177 | .2148 |
| -.6  | .2743 | .2709 | .2676 | .2643 | .2611 | .2578 | .2546 | .2514 | .2483 | .2451 |
| -.5  | .3085 | .3050 | .3015 | .2981 | .2946 | .2912 | .2877 | .2843 | .2810 | .2776 |
| -.4  | .3446 | .3409 | .3372 | .3336 | .3300 | .3264 | .3228 | .3192 | .3156 | .3121 |
| -.3  | .3821 | .3783 | .3745 | .3707 | .3669 | .3632 | .3594 | .3557 | .3520 | .3483 |
| -.2  | .4207 | .4168 | .4129 | .4090 | .4052 | .4013 | .3974 | .3936 | .3897 | .3859 |
| -.1  | .4602 | .4562 | .4522 | .4483 | .4443 | .4404 | .4364 | .4325 | .4286 | .4247 |
| -.0  | .5000 | .4960 | .4920 | .4880 | .4840 | .4801 | .4761 | .4721 | .4681 | .4641 |

Table B.1: Tables of Standard Normal Probabilities for negative Z-scores.



## Standard normalfordeling

$$\Phi(z) = P(Z \leq z)$$

| $z$ | .00   | .01   | .02   | .03   | .04   | .05   | .06   | .07   | .08   | .09   |
|-----|-------|-------|-------|-------|-------|-------|-------|-------|-------|-------|
| .0  | .5000 | .5040 | .5080 | .5120 | .5160 | .5199 | .5239 | .5279 | .5319 | .5359 |
| .1  | .5398 | .5438 | .5478 | .5517 | .5557 | .5596 | .5636 | .5675 | .5714 | .5753 |
| .2  | .5793 | .5832 | .5871 | .5910 | .5948 | .5987 | .6026 | .6064 | .6103 | .6141 |
| .3  | .6179 | .6217 | .6255 | .6293 | .6331 | .6368 | .6406 | .6443 | .6480 | .6517 |
| .4  | .6554 | .6591 | .6628 | .6664 | .6700 | .6736 | .6772 | .6808 | .6844 | .6879 |
| .5  | .6915 | .6950 | .6985 | .7019 | .7054 | .7088 | .7123 | .7157 | .7190 | .7224 |
| .6  | .7257 | .7291 | .7324 | .7357 | .7389 | .7422 | .7454 | .7486 | .7517 | .7549 |
| .7  | .7580 | .7611 | .7642 | .7673 | .7704 | .7734 | .7764 | .7794 | .7823 | .7852 |
| .8  | .7881 | .7910 | .7939 | .7967 | .7995 | .8023 | .8051 | .8078 | .8106 | .8133 |
| .9  | .8159 | .8186 | .8212 | .8238 | .8264 | .8289 | .8315 | .8340 | .8365 | .8389 |
| 1.0 | .8413 | .8438 | .8461 | .8485 | .8508 | .8531 | .8554 | .8577 | .8599 | .8621 |
| 1.1 | .8643 | .8665 | .8686 | .8708 | .8729 | .8749 | .8770 | .8790 | .8810 | .8830 |
| 1.2 | .8849 | .8869 | .8888 | .8907 | .8925 | .8944 | .8962 | .8980 | .8997 | .9015 |
| 1.3 | .9032 | .9049 | .9066 | .9082 | .9099 | .9115 | .9131 | .9147 | .9162 | .9177 |
| 1.4 | .9192 | .9207 | .9222 | .9236 | .9251 | .9265 | .9279 | .9292 | .9306 | .9319 |
| 1.5 | .9332 | .9345 | .9357 | .9370 | .9382 | .9394 | .9406 | .9418 | .9429 | .9441 |
| 1.6 | .9452 | .9463 | .9474 | .9484 | .9495 | .9505 | .9515 | .9525 | .9535 | .9545 |
| 1.7 | .9554 | .9564 | .9573 | .9582 | .9591 | .9599 | .9608 | .9616 | .9625 | .9633 |
| 1.8 | .9641 | .9649 | .9656 | .9664 | .9671 | .9678 | .9686 | .9693 | .9699 | .9706 |
| 1.9 | .9713 | .9719 | .9726 | .9732 | .9738 | .9744 | .9750 | .9756 | .9761 | .9767 |
| 2.0 | .9772 | .9778 | .9783 | .9788 | .9793 | .9798 | .9803 | .9808 | .9812 | .9817 |
| 2.1 | .9821 | .9826 | .9830 | .9834 | .9838 | .9842 | .9846 | .9850 | .9854 | .9857 |
| 2.2 | .9861 | .9864 | .9868 | .9871 | .9875 | .9878 | .9881 | .9884 | .9887 | .9890 |
| 2.3 | .9893 | .9896 | .9898 | .9901 | .9904 | .9906 | .9909 | .9911 | .9913 | .9916 |
| 2.4 | .9918 | .9920 | .9922 | .9925 | .9927 | .9929 | .9931 | .9932 | .9934 | .9936 |
| 2.5 | .9938 | .9940 | .9941 | .9943 | .9945 | .9946 | .9948 | .9949 | .9951 | .9952 |
| 2.6 | .9953 | .9955 | .9956 | .9957 | .9959 | .9960 | .9961 | .9962 | .9963 | .9964 |
| 2.7 | .9965 | .9966 | .9967 | .9968 | .9969 | .9970 | .9971 | .9972 | .9973 | .9974 |
| 2.8 | .9974 | .9975 | .9976 | .9977 | .9977 | .9978 | .9979 | .9979 | .9980 | .9981 |
| 2.9 | .9981 | .9982 | .9982 | .9983 | .9984 | .9984 | .9985 | .9985 | .9986 | .9986 |
| 3.0 | .9987 | .9987 | .9987 | .9988 | .9988 | .9989 | .9989 | .9989 | .9990 | .9990 |
| 3.1 | .9990 | .9991 | .9991 | .9991 | .9992 | .9992 | .9992 | .9992 | .9993 | .9993 |
| 3.2 | .9993 | .9993 | .9994 | .9994 | .9994 | .9994 | .9994 | .9995 | .9995 | .9995 |
| 3.3 | .9995 | .9995 | .9995 | .9996 | .9996 | .9996 | .9996 | .9996 | .9996 | .9997 |
| 3.4 | .9997 | .9997 | .9997 | .9997 | .9997 | .9997 | .9997 | .9997 | .9997 | .9998 |
| 3.5 | .9998 | .9998 | .9998 | .9998 | .9998 | .9998 | .9998 | .9998 | .9998 | .9998 |
| 3.6 | .9998 | .9998 | .9999 | .9999 | .9999 | .9999 | .9999 | .9999 | .9999 | .9999 |
| 3.7 | .9999 | .9999 | .9999 | .9999 | .9999 | .9999 | .9999 | .9999 | .9999 | .9999 |

Table B.2: Tables of Standard Normal Probabilities for positive Z-scores.

**Kritiske verdier i standard normalfordelingen**

$$P(Z > z_{\alpha}) = \alpha$$

| $\alpha$ | $z_{\alpha}$ |
|----------|--------------|
| .2       | 0.842        |
| .15      | 1.036        |
| .1       | 1.282        |
| .075     | 1.440        |
| .05      | 1.645        |
| .04      | 1.751        |
| .03      | 1.881        |
| .025     | 1.960        |
| .02      | 2.054        |
| .01      | 2.326        |
| .005     | 2.576        |
| .001     | 3.090        |
| .0005    | 3.291        |
| .0001    | 3.719        |
| .00005   | 3.891        |
| .00001   | 4.265        |
| .000005  | 4.417        |
| .000001  | 4.753        |

*Table B.3: Critical values in standard normal distribution.*

---

# **Appendix C**

Tensile test data

# Appendix C

| BRIDON   |         |                                 |                            |              |               |                  |                    |                              |                             |              |
|----------|---------|---------------------------------|----------------------------|--------------|---------------|------------------|--------------------|------------------------------|-----------------------------|--------------|
| Coil Ref | Cast No | Wire Diameter (mm)              | U.T.S (N/mm <sup>2</sup> ) | Tension 100d | Reverse Bends | Zn Metal/Wt. (%) | Elong (%)          | Modulus (N/mm <sup>2</sup> ) | Adh/Duct Wrappg Pass / Fail | Date of Test |
|          |         | 5.32 Min-5.44 1570 Min-1680 Max | 1570 Min-1680 Max          | Min 8d       | 15.0mm, Min 4 | 275 Min 470 Max  | 4.0% Min 10.0% Max | 180 Min 220 Max              | 4 x 9d Pass / Fail          |              |
| W220726  | T1068   | 5.37                            | 1680                       | 30A          | 5             | 352              | 192.3              | 246.2                        | PASS                        | 13/02/10     |
| W220727  | T1068   | 5.35                            | 1680                       | 27A          | 8             | 436              | 202.0              | 197.7                        | PASS                        | 13/02/10     |
| W220840  | T1068   | 5.36                            | 1680                       | 29A          | 6             | 352              | 192.3              | 246.2                        | PASS                        | 13/02/10     |
| W220895  | T1068   | 5.37                            | 1680                       | 30A          | 7             | 358              | 197.6              | 246.2                        | PASS                        | 13/02/10     |
| W220883  | T1068   | 5.37                            | 1680                       | 29B          | 8             | 371              | 195.3              | 246.2                        | PASS                        | 13/02/10     |
| W221103  | T1068   | 5.36                            | 1700                       | 29A          | 7             | 385              | 192.3              | 246.2                        | PASS                        | 23/02/10     |
| W221341  | T1068   | 5.38                            | 1670                       | 30A          | 8             | 390              | 198.1              | 246.2                        | PASS                        | 23/02/10     |
| W221356  | T1068   | 5.39                            | 1680                       | 17B          | 8             | 355              | 192.3              | 246.2                        | PASS                        | 23/02/10     |
| W221513  | T1071   | 5.36                            | 1680                       | 28B          | 8             | 404              | 185.3              | 246.2                        | PASS                        | 23/02/10     |
| W221516  | T1071   | 5.37                            | 1680                       | 31A          | 8             | 435              | 193.8              | 246.2                        | PASS                        | 23/02/10     |
| W221433  | T1071   | 5.37                            | 1710                       | 27B          | 8             | 395              | 177.7              | 196.5                        | PASS                        | 23/02/10     |
| W221701  | T1071   | 5.36                            | 1700                       | 30A          | 8             | 366              | 199.5              | 246.2                        | PASS                        | 23/02/10     |
| W221583  | T1098   | 5.36                            | 1670                       | 30A          | 6             | 480              | 171.7              | 191.7                        | PASS                        | 06/03/10     |
| W221685  | T1070   | 5.35                            | 1700                       | 30A          | 6             | 456              | 195.7              | 246.2                        | PASS                        | 06/03/10     |
| W221697  | T1071   | 5.33                            | 1710                       | 27A          | 7             | 373              | 175.2              | 197.2                        | PASS                        | 06/03/10     |
| W221792  | T1071   | 5.37                            | 1700                       | 28A          | 8             | 346              | 164.3              | 195.7                        | PASS                        | 06/03/10     |
| W221868  | T1073   | 5.36                            | 1690                       | 11B          | 8             | 372              | 182.2              | 196.7                        | PASS                        | 06/03/10     |
| W221850  | T1073   | 5.35                            | 1680                       | 25A          | 6             | 366              | 189.9              | 193.4                        | PASS                        | 06/03/10     |
| W221873  | T1073   | 5.37                            | 1700                       | 27A          | 6             | 371              | 177.7              | 197.2                        | PASS                        | 06/03/10     |
| W221895  | T1073   | 5.36                            | 1680                       | 29A          | 7             | 371              | 166.5              | 194.9                        | PASS                        | 06/03/10     |
| W222004  | T1073   | 5.35                            | 1710                       | 27A          | 8             | 379              | 185.3              | 190.8                        | PASS                        | 06/03/10     |
| W222080  | T1073   | 5.37                            | 1680                       | 25A          | 7             | 397              | 176.6              | 192.6                        | PASS                        | 06/03/10     |
| W222231  | T1073   | 5.38                            | 1670                       | 28A          | 6             | 359              | 184.2              | 203.8                        | PASS                        | 06/03/10     |
| W222252  | T1073   | 5.35                            | 1720                       | 28A          | 8             | 398              | 183.3              | 194.9                        | PASS                        | 13/03/10     |
| W222600  | T1073   | 5.36                            | 1680                       | 21B          | 8             | 359              | 172.6              | 192.6                        | PASS                        | 13/03/10     |
| W222425  | T1073   | 5.38                            | 1700                       | 24B          | 7             | 447              | 188.2              | 198.2                        | PASS                        | 13/03/10     |
| W222401  | T1151   | 5.36                            | 1670                       | 27A          | 7             | 366              | 184.2              | 194.7                        | PASS                        | 13/03/10     |
| W222417  | T1182   | 5.34                            | 1710                       | 27A          | 7             | 392              | 198.2              | 198.2                        | PASS                        | 13/03/10     |
| W222551  | T1153   | 5.34                            | 1700                       | 27A          | 8             | 399              | 184.2              | 196.1                        | PASS                        | 23/03/10     |
| W222485  | T1153   | 5.38                            | 1670                       | 30A          | 8             | 404              | 184.2              | 196.1                        | PASS                        | 23/03/10     |

TC 10241 - Edition 1 Inspection Certificate in Accordance with EN10204 (2006) 3.2 - Project Ref 10241 Page 2 of 14

Figure C.1: Tensile test data from Bridon.

| BRIDON   |         |                                 |                            |              |               |                  |                    |                              |                             |              |
|----------|---------|---------------------------------|----------------------------|--------------|---------------|------------------|--------------------|------------------------------|-----------------------------|--------------|
| Coil Ref | Cast No | Wire Diameter (mm)              | U.T.S (N/mm <sup>2</sup> ) | Tension 100d | Reverse Bends | Zn Metal/Wt. (%) | Elong (%)          | Modulus (N/mm <sup>2</sup> ) | Adh/Duct Wrappg Pass / Fail | Date of Test |
|          |         | 5.32 Min-5.44 1570 Min-1680 Max | 1570 Min-1680 Max          | Min 8d       | 15.0mm, Min 4 | 275 Min 470 Max  | 4.0% Min 10.0% Max | 180 Min 220 Max              | 4 x 9d Pass / Fail          |              |
| W224376  | T1315   | 5.35                            | 1680                       | 28A          | 7             | 386              | 199.6              | 246.2                        | PASS                        | 06/04/10     |
| W224375  | T1315   | 5.37                            | 1710                       | 28A          | 9             | 384              | 20.1               | 198.7                        | PASS                        | 07/04/10     |
| W224754  | T1316   | 5.36                            | 1670                       | 27A          | 8             | 429              | 189.7              | 246.2                        | PASS                        | 17/04/10     |
| W224860  | T1316   | 5.36                            | 1670                       | 27A          | 8             | 417              | 189.7              | 195.2                        | PASS                        | 17/04/10     |
| W224993  | T1316   | 5.37                            | 1700                       | 27A          | 7             | 455              | 188.2              | 196.5                        | PASS                        | 17/04/10     |
| W224991  | T1316   | 5.37                            | 1680                       | 28A          | 8             | 419              | 197.2              | 197.2                        | PASS                        | 17/04/10     |
| W225483  | T1432   | 5.34                            | 1730                       | 17B          | 7             | 412              | 167.7              | 196.9                        | PASS                        | 23/04/10     |
| W225105  | T1434   | 5.36                            | 1680                       | 24B          | 8             | 385              | 182.2              | 196.5                        | PASS                        | 23/04/10     |
| W225400  | T1434   | 5.36                            | 1700                       | 29B          | 7             | 325              | 168.8              | 196.8                        | PASS                        | 23/04/10     |
| W225471  | T1434   | 5.37                            | 1700                       | 26A          | 8             | 372              | 162.4              | 192.4                        | PASS                        | 23/04/10     |
| W225478  | T1434   | 5.36                            | 1700                       | 26A          | 8             | 395              | 169.5              | 196.5                        | PASS                        | 23/04/10     |
| W225421  | T1434   | 5.36                            | 1700                       | 17B          | 8             | 327              | 166.9              | 192.2                        | PASS                        | 23/04/10     |
| W225466  | T1432   | 5.33                            | 1720                       | 25A          | 8             | 329              | 167.7              | 193.3                        | PASS                        | 07/06/10     |
| W225588  | T1434   | 5.36                            | 1700                       | 26A          | 8             | 385              | 190.0              | 206.0                        | PASS                        | 07/06/10     |
| W225436  | T1434   | 5.32                            | 1730                       | 25A          | 8             | 394              | 196.2              | 209.3                        | PASS                        | 07/06/10     |
| W225483  | T1432   | 5.35                            | 1720                       | 27A          | 8             | 469              | 209.9              | 212.7                        | PASS                        | 07/06/10     |
| W225703  | T1434   | 5.36                            | 1700                       | 26A          | 8             | 410              | 194.5              | 214.5                        | PASS                        | 07/06/10     |
| W225929  | T1434   | 5.34                            | 1720                       | 27A          | 8             | 386              | 176.2              | 201.6                        | PASS                        | 11/06/10     |
| W225982  | T1434   | 5.34                            | 1720                       | 26A          | 7             | 451              | 181.2              | 196.2                        | PASS                        | 11/06/10     |
| W226055  | T1434   | 5.36                            | 1680                       | 26A          | 8             | 459              | 185.3              | 196.2                        | PASS                        | 11/06/10     |
| W226060  | T1434   | 5.34                            | 1700                       | 26A          | 8             | 418              | 178.2              | 195.6                        | PASS                        | 11/06/10     |
| W226058  | T1434   | 5.37                            | 1700                       | 26A          | 8             | 390              | 185.3              | 196.2                        | PASS                        | 11/06/10     |
| W226071  | T1434   | 5.36                            | 1720                       | 26A          | 8             | 391              | 182.2              | 203.0                        | PASS                        | 21/06/10     |
| W226152  | T1434   | 5.38                            | 1680                       | 27A          | 8             | 403              | 187.7              | 203.7                        | PASS                        | 21/06/10     |
| W226321  | T1434   | 5.37                            | 1680                       | 27A          | 8             | 377              | 172.2              | 203.0                        | PASS                        | 21/06/10     |
| W226325  | T1434   | 5.37                            | 1650                       | 26A          | 9             | 333              | 171.0              | 200.3                        | PASS                        | 21/06/10     |
| W226317  | T1434   | 5.36                            | 1660                       | 29A          | 9             | 384              | 184.2              | 201.6                        | PASS                        | 21/06/10     |
| W226261  | T1434   | 5.36                            | 1660                       | 29A          | 9             | 422              | 183.2              | 201.6                        | PASS                        | 21/06/10     |
| W226280  | T1434   | 5.35                            | 1670                       | 28A          | 9             | 410              | 169.9              | 201.4                        | PASS                        | 21/06/10     |
| W226335  | T1434   | 5.36                            | 1680                       | 28A          | 8             | 385              | 184.2              | 204.6                        | PASS                        | 21/06/10     |

TC 10241 - Edition 1 Inspection Certificate in Accordance with EN10204 (2006) 3.2 - Project Ref 10241 Page 4 of 14

Figure C.2: Tensile test data from Bridon.

| BRIDON   |         |                                 |                            |              |               |                  |                    |                              |                             |              |
|----------|---------|---------------------------------|----------------------------|--------------|---------------|------------------|--------------------|------------------------------|-----------------------------|--------------|
| Coil Ref | Cast No | Wire Diameter (mm)              | U.T.S (N/mm <sup>2</sup> ) | Tension 100d | Reverse Bends | Zn Metal/Wt. (%) | Elong (%)          | Modulus (N/mm <sup>2</sup> ) | Adh/Duct Wrappg Pass / Fail | Date of Test |
|          |         | 5.32 Min-5.44 1570 Min-1680 Max | 1570 Min-1680 Max          | Min 8d       | 15.0mm, Min 4 | 275 Min 470 Max  | 4.0% Min 10.0% Max | 180 Min 220 Max              | 4 x 9d Pass / Fail          |              |
| W228256  | T1664   | 5.35                            | 1680                       | 16B          | 8             | 379              | 179.2              | 202.8                        | PASS                        | 21/08/10     |
| W228277  | T1664   | 5.34                            | 1730                       | 25B          | 9             | 328              | 167.7              | 202.9                        | PASS                        | 21/08/10     |
| W228498  | T1664   | 5.33                            | 1680                       | 18B          | 9             | 373              | 183.2              | 202.5                        | PASS                        | 21/08/10     |
| W228473  | T1664   | 5.35                            | 1680                       | 27A          | 7             | 392              | 199.7              | 207.6                        | PASS                        | 01/09/10     |
| W228155  | T1664   | 5.34                            | 1720                       | 27A          | 5             | 398              | 185.3              | 203.6                        | PASS                        | 01/09/10     |
| W228546  | T1664   | 5.34                            | 1720                       | 26B          | 8             | 341              | 181.2              | 201.5                        | PASS                        | 01/09/10     |
| W228929  | T1664   | 5.35                            | 1680                       | 21B          | 7             | 391              | 181.2              | 205.3                        | PASS                        | 01/09/10     |
| W228928  | T1664   | 5.34                            | 1720                       | 29A          | 5             | 380              | 173.2              | 206.6                        | PASS                        | 01/09/10     |
| W228931  | T1664   | 5.35                            | 1710                       | 16B          | 7             | 341              | 178.8              | 205.0                        | PASS                        | 01/09/10     |
| W228862  | T1664   | 5.34                            | 1710                       | 18B          | 7             | 373              | 184.2              | 203.2                        | PASS                        | 01/09/10     |
| W228982  | T1665   | 5.35                            | 1690                       | 27A          | 8             | 359              | 180.2              | 207.4                        | PASS                        | 01/09/10     |
| W228999  | T1665   | 5.36                            | 1680                       | 28A          | 8             | 455              | 189.9              | 206.8                        | PASS                        | 01/09/10     |
| W228967  | T1665   | 5.35                            | 1680                       | 27A          | 8             | 328              | 181.2              | 206.5                        | PASS                        | 01/09/10     |
| W228917  | T1665   | 5.38                            | 1660                       | 28A          | 7             | 404              | 184.2              | 204.6                        | PASS                        | 06/09/10     |
| W228843  | T1668   | 5.35                            | 1660                       | 15B          | 6             | 437              | 182.2              | 203.7                        | PASS                        | 06/09/10     |
| W228962  | T1665   | 5.34                            | 1710                       | 26A          | 7             | 393              | 170.8              | 204.4                        | PASS                        | 06/09/10     |
| W228923  | T1665   | 5.36                            | 1710                       | 27A          | 7             | 430              | 182.2              | 205.7                        | PASS                        | 13/09/10     |
| W228956  | T1668   | 5.35                            | 1700                       | 26A          | 7             | 353              | 184.2              | 204.3                        | PASS                        | 13/09/10     |
| W229160  | T1665   | 5.33                            | 1720                       | 27A          | 6             | 406              | 185.3              | 201.6                        | PASS                        | 13/09/10     |
| W229253  | T1750   | 5.34                            | 1680                       | 28A          | 8             | 351              | 185.3              | 203.8                        | PASS                        | 13/09/10     |
| W229242  | T1750   | 5.34                            | 1670                       | 29A          | 8             | 366              | 182.2              | 203.6                        | PASS                        | 13/09/10     |
| W229013  | T1665   | 5.37                            | 1680                       | 28A          | 8             | 399              | 185.3              | 203.2                        | PASS                        | 13/09/10     |
| W229262  | T1665   | 5.37                            | 1680                       | 28A          | 8             | 390              | 182.2              | 202.3                        | PASS                        | 13/09/10     |
| W229175  | T1750   | 5.38                            | 1680                       | 28A          | 8             | 383              | 181.2              | 205.1                        | PASS                        | 20/09/10     |
| W229462  | T1750   | 5.35                            | 1680                       | 25A          | 8             | 373              | 183.2              | 204.6                        | PASS                        | 20/09/10     |
| W229467  | T1750   | 5.36                            | 1680                       | 28A          | 8             | 385              | 185.3              | 204.1                        | PASS                        | 20/09/10     |
| W229563  | T1750   | 5.38                            | 1660                       | 28A          | 8             | 454              | 185.3              | 204.6                        | PASS                        | 20/09/10     |
| W229505  | T1869   | 5.35                            | 1670                       | 19B          | 8             | 353              | 176.2              | 207.7                        | PASS                        | 27/09/10     |
| W229750  | T1750   | 5.36                            | 1680                       | 28A          | 8             | 398              | 182.2              | 205.6                        | PASS                        | 27/09/10     |
| W229490  | T1750   | 5.35                            | 1680                       | 29A          | 8             | 398              | 185.3              | 205.0                        | PASS                        | 27/09/10     |

TC 10241 - Edition 1 Inspection Certificate in Accordance with EN10204 (2006) 3.2 - Project Ref 10241 Page 6 of 14

Figure C.3: Tensile test data from Bridon.

| BRIDON   |         |                    |                            |              |               |                    |                     |                              |                   |          |              |             |                   |  |
|----------|---------|--------------------|----------------------------|--------------|---------------|--------------------|---------------------|------------------------------|-------------------|----------|--------------|-------------|-------------------|--|
| Coil Ref | Cast No | Wire Diameter (mm) | U.T.S (N/mm <sup>2</sup> ) | Torsion 3000 | Reverse Bonds | In Metal Wt. (g/m) | Elong (%)           | Modulus (N/mm <sup>2</sup> ) | Adh/Duct          | Wires    | Date of Test | BRIDON      |                   |  |
|          |         | 1.32 Min 1.44 Max  | 1570 Min 1830 Max          | M18 B8       | 15.0mm, Min 4 | 275 Min 470 Max    | 4.00% Min 20.0% Max | 180 Min 220 Max              | 4 x B Pass / Fail |          |              | Pass / Fail | 4 x B Pass / Fail |  |
| W211153  | T1864   | 5.37               | 1670                       | 21A          | 8             | 359                | 8.11                | 205.3                        | PASS              | 25/10/10 |              |             |                   |  |
| W211155  | T1970   | 5.37               | 1680                       | 21A          | 8             | 359                | 8.85                | 206.0                        | PASS              | 09/11/10 |              |             |                   |  |
| W211549  | T1970   | 5.36               | 1670                       | 21A          | 8             | 371                | 8.85                | 206.2                        | PASS              | 09/11/10 |              |             |                   |  |
| W211342  | T1970   | 5.35               | 1700                       | 21B          | 8             | 437                | 6.56                | 203.5                        | PASS              | 09/11/10 |              |             |                   |  |
| W211259  | T1970   | 5.33               | 1710                       | 21B          | 7             | 374                | 6.38                | 205.0                        | PASS              | 09/11/10 |              |             |                   |  |
| W211215  | T1978   | 5.36               | 1680                       | 21B          | 6             | 378                | 6.82                | 204.0                        | PASS              | 09/11/10 |              |             |                   |  |
| W2115918 | T1977   | 5.34               | 1700                       | 21A          | 6             | 406                | 8.37                | 208.7                        | PASS              | 09/11/10 |              |             |                   |  |
| W2113397 | T1977   | 5.37               | 1700                       | 21A          | 7             | 429                | 5.89                | 209.5                        | PASS              | 09/11/10 |              |             |                   |  |
| W2113123 | T1977   | 5.34               | 1710                       | 21A          | 8             | 326                | 6.02                | 205.9                        | PASS              | 09/11/10 |              |             |                   |  |
| W2113128 | T1978   | 5.35               | 1680                       | 21A          | 5             | 418                | 8.41                | 207.7                        | PASS              | 09/11/10 |              |             |                   |  |
| W2113513 | T1978   | 5.34               | 1700                       | 21A          | 7             | 380                | 6.45                | 205.2                        | PASS              | 09/11/10 |              |             |                   |  |
| W2113558 | T1977   | 5.34               | 1700                       | 21A          | 8             | 425                | 7.30                | 205.8                        | PASS              | 09/11/10 |              |             |                   |  |
| W2114554 | T1977   | 5.34               | 1700                       | 21A          | 5             | 399                | 6.07                | 204.8                        | PASS              | 09/11/10 |              |             |                   |  |
| W2114811 | T1978   | 5.34               | 1700                       | 21A          | 6             | 367                | 6.63                | 207.3                        | PASS              | 09/11/10 |              |             |                   |  |
| W2115130 | T1970   | 5.36               | 1680                       | 21B          | 8             | 404                | 6.82                | 203.3                        | PASS              | 09/11/10 |              |             |                   |  |
| W2115120 | T1970   | 5.36               | 1680                       | 21A          | 5             | 378                | 7.84                | 205.6                        | PASS              | 09/11/10 |              |             |                   |  |
| W2115112 | T1977   | 5.34               | 1720                       | 21A          | 6             | 361                | 7.65                | 209.6                        | PASS              | 09/11/10 |              |             |                   |  |
| W2115143 | T1978   | 5.36               | 1680                       | 21A          | 7             | 441                | 7.08                | 209.8                        | PASS              | 09/11/10 |              |             |                   |  |
| W2115886 | T1977   | 5.32               | 1710                       | 21A          | 7             | 315                | 7.56                | 208.8                        | PASS              | 09/11/10 |              |             |                   |  |
| W2115869 | T1978   | 5.36               | 1700                       | 21A          | 6             | 391                | 7.08                | 206.4                        | PASS              | 09/11/10 |              |             |                   |  |
| W2117923 | T1977   | 5.35               | 1680                       | 21A          | 7             | 334                | 7.19                | 204.7                        | PASS              | 09/11/10 |              |             |                   |  |
| W2116118 | T1977   | 5.36               | 1700                       | 21B          | 7             | 430                | 6.51                | 207.6                        | PASS              | 09/11/10 |              |             |                   |  |
| W2116234 | T1978   | 5.37               | 1680                       | 21A          | 5             | 340                | 6.61                | 207.1                        | PASS              | 09/11/10 |              |             |                   |  |
| W2116466 | T1977   | 5.37               | 1680                       | 21B          | 6             | 404                | 6.83                | 207.7                        | PASS              | 09/11/10 |              |             |                   |  |
| W2116539 | T1978   | 5.37               | 1680                       | 21A          | 6             | 385                | 6.20                | 206.6                        | PASS              | 09/11/10 |              |             |                   |  |
| W2116643 | T1978   | 5.39               | 1670                       | 21A          | 6             | 333                | 6.43                | 207.9                        | PASS              | 09/11/10 |              |             |                   |  |
| W2116611 | T1978   | 5.36               | 1680                       | 21A          | 5             | 354                | 6.42                | 205.1                        | PASS              | 09/11/10 |              |             |                   |  |
| W2116187 | T2068   | 5.36               | 1680                       | 30A          | 6             | 347                | 7.75                | 205.7                        | PASS              | 15/11/10 |              |             |                   |  |
| W2117255 | T2068   | 5.38               | 1680                       | 29A          | 7             | 384                | 6.72                | 209.7                        | PASS              | 15/11/10 |              |             |                   |  |

Figure C.4: Tensile test data from Bridon.

| BRIDON   |         |                    |                            |              |               |                    |                     |                              |                   |          |              |             |                   |  |
|----------|---------|--------------------|----------------------------|--------------|---------------|--------------------|---------------------|------------------------------|-------------------|----------|--------------|-------------|-------------------|--|
| Coil Ref | Cast No | Wire Diameter (mm) | U.T.S (N/mm <sup>2</sup> ) | Torsion 3000 | Reverse Bonds | In Metal Wt. (g/m) | Elong (%)           | Modulus (N/mm <sup>2</sup> ) | Adh/Duct          | Wires    | Date of Test | BRIDON      |                   |  |
|          |         | 1.32 Min 1.44 Max  | 1570 Min 1830 Max          | M18 B8       | 15.0mm, Min 4 | 275 Min 470 Max    | 4.00% Min 20.0% Max | 180 Min 220 Max              | 4 x B Pass / Fail |          |              | Pass / Fail | 4 x B Pass / Fail |  |
| W2123679 | T2060   | 5.33               | 1670                       | 21B          | 8             | 397                | 25.0                | 205.0                        | PASS              | 29/11/10 |              |             |                   |  |
| W2123410 | T2064   | 5.35               | 1680                       | 24B          | 7             | 405                | 1.03                | 205.5                        | PASS              | 29/11/10 |              |             |                   |  |
| W2123667 | T2066   | 5.36               | 1650                       | 30A          | 8             | 417                | 8.22                | 203.8                        | PASS              | 15/11/10 |              |             |                   |  |
| W2123625 | T2064   | 5.37               | 1680                       | 21B          | 8             | 378                | 2.27                | 204.7                        | PASS              | 15/11/10 |              |             |                   |  |
| W2123656 | T2064   | 5.36               | 1680                       | 21A          | 8             | 413                | 7.68                | 205.6                        | PASS              | 15/11/10 |              |             |                   |  |
| W2123110 | T2060   | 5.35               | 1700                       | 21A          | 8             | 334                | 8.20                | 206.6                        | PASS              | 15/11/10 |              |             |                   |  |
| W2123608 | T2060   | 5.36               | 1680                       | 21B          | 7             | 353                | 6.81                | 205.3                        | PASS              | 15/11/10 |              |             |                   |  |
| W2123380 | T2060   | 5.36               | 1680                       | 21A          | 8             | 378                | 6.81                | 205.3                        | PASS              | 15/11/10 |              |             |                   |  |
| W2123406 | T2064   | 5.36               | 1680                       | 21A          | 8             | 346                | 2.06                | 206.6                        | PASS              | 15/11/10 |              |             |                   |  |
| W2124008 | T1978   | 5.33               | 1680                       | 21A          | 8             | 342                | 6.93                | 204.4                        | PASS              | 15/11/10 |              |             |                   |  |
| W2124110 | T2066   | 5.37               | 1680                       | 27A          | 7             | 422                | 4.00                | 203.4                        | PASS              | 15/11/10 |              |             |                   |  |
| W2124462 | T2066   | 5.36               | 1680                       | 21B          | 8             | 450                | 6.22                | 204.0                        | PASS              | 15/11/10 |              |             |                   |  |
| W2125240 | T2064   | 5.34               | 1670                       | 21A          | 9             | 361                | 5.74                | 205.4                        | PASS              | 15/11/10 |              |             |                   |  |
| W2125218 | T2064   | 5.33               | 1710                       | 21A          | 7             | 361                | 6.70                | 205.1                        | PASS              | 15/11/10 |              |             |                   |  |
| W2126155 | T2060   | 5.36               | 1680                       | 21A          | 6             | 434                | 6.16                | 204.1                        | PASS              | 15/11/10 |              |             |                   |  |
| W2125505 | T2060   | 5.35               | 1700                       | 21A          | 8             | 418                | 6.18                | 205.2                        | PASS              | 15/11/10 |              |             |                   |  |
| W2125974 | T2060   | 5.37               | 1650                       | 21A          | 8             | 416                | 5.85                | 203.4                        | PASS              | 15/11/10 |              |             |                   |  |
| W2126338 | T2068   | 5.36               | 1680                       | 21B          | 8             | 411                | 6.15                | 206.1                        | PASS              | 15/11/10 |              |             |                   |  |
| W2127187 | T2068   | 5.36               | 1680                       | 31A          | 8             | 442                | 7.91                | 210.5                        | PASS              | 15/11/10 |              |             |                   |  |
| W2127900 | T2064   | 5.37               | 1680                       | 21A          | 9             | 430                | 8.14                | 205.4                        | PASS              | 15/11/10 |              |             |                   |  |
| W2127488 | T2064   | 5.36               | 1680                       | 21B          | 8             | 423                | 6.84                | 204.5                        | PASS              | 15/11/10 |              |             |                   |  |
| W2127755 | T2060   | 5.36               | 1680                       | 21B          | 7             | 418                | 7.09                | 203.9                        | PASS              | 15/11/10 |              |             |                   |  |
| W2128114 | T2060   | 5.35               | 1680                       | 21B          | 8             | 446                | 7.18                | 202.2                        | PASS              | 15/11/10 |              |             |                   |  |
| W2128184 | T2060   | 5.36               | 1680                       | 21B          | 8             | 334                | 6.50                | 203.9                        | PASS              | 15/11/10 |              |             |                   |  |
| W2128223 | T1977   | 5.35               | 1740                       | 31A          | 8             | 450                | 8.30                | 209.0                        | PASS              | 15/11/10 |              |             |                   |  |
| W2128101 | T1806   | 5.36               | 1740                       | 31A          | 7             | 353                | 6.15                | 203.3                        | PASS              | 15/11/10 |              |             |                   |  |
| W2128017 | T1806   | 5.36               | 1680                       | 31A          | 7             | 359                | 5.83                | 208.4                        | PASS              | 15/11/10 |              |             |                   |  |
| W2128847 | T2060   | 5.33               | 1670                       | 32A          | 8             | 418                | 5.67                | 203.7                        | PASS              | 23/11/10 |              |             |                   |  |
| W2129444 | T2060   | 5.36               | 1680                       | 21B          | 8             | 353                | 6.23                | 203.8                        | PASS              | 23/11/10 |              |             |                   |  |
| W2129444 | T2060   | 5.35               | 1680                       | 21A          | 6             | 334                | 6.61                | 204.9                        | PASS              | 23/11/10 |              |             |                   |  |

Figure C.5: Tensile test data from Bridon.

| BRIDON   |         |                    |                            |              |               |                    |                     |                              |                   |          |              |             |                   |  |
|----------|---------|--------------------|----------------------------|--------------|---------------|--------------------|---------------------|------------------------------|-------------------|----------|--------------|-------------|-------------------|--|
| Coil Ref | Cast No | Wire Diameter (mm) | U.T.S (N/mm <sup>2</sup> ) | Torsion 3000 | Reverse Bonds | In Metal Wt. (g/m) | Elong (%)           | Modulus (N/mm <sup>2</sup> ) | Adh/Duct          | Wires    | Date of Test | BRIDON      |                   |  |
|          |         | 1.32 Min 1.44 Max  | 1570 Min 1830 Max          | M18 B8       | 15.0mm, Min 4 | 275 Min 470 Max    | 4.00% Min 20.0% Max | 180 Min 220 Max              | 4 x B Pass / Fail |          |              | Pass / Fail | 4 x B Pass / Fail |  |
| W2124242 | T2190   | 5.34               | 1720                       | 21A          | 7             | 398                | 7.64                | 208.3                        | PASS              | 11/01/11 |              |             |                   |  |
| W2124214 | T2190   | 5.33               | 1720                       | 21A          | 6             | 387                | 8.19                | 208.6                        | PASS              | 11/01/11 |              |             |                   |  |
| W2124321 | T2190   | 5.34               | 1680                       | 21A          | 5             | 380                | 8.08                | 207.5                        | PASS              | 11/01/11 |              |             |                   |  |
| W2124322 | T2190   | 5.36               | 1680                       | 27A          | 4             | 410                | 7.64                | 206.8                        | PASS              | 11/01/11 |              |             |                   |  |
| W2124376 | T2190   | 5.35               | 1700                       | 27A          | 7             | 360                | 8.29                | 206.4                        | PASS              | 11/01/11 |              |             |                   |  |
| W2124412 | T2190   | 5.35               | 1680                       | 21A          | 7             | 409                | 6.15                | 201.5                        | PASS              | 11/01/11 |              |             |                   |  |
| W2124624 | T1817   | 5.37               | 1670                       | 21A          | 7             | 430                | 6.00                | 203.5                        | PASS              | 07/02/11 |              |             |                   |  |
| W2124625 | T1817   | 5.37               | 1650                       | 21A          | 6             | 416                | 5.76                | 203.7                        | PASS              | 07/02/11 |              |             |                   |  |
| W2124632 | T1817   | 5.36               | 1680                       | 21A          | 6             | 353                | 6.54                | 204.2                        | PASS              | 07/02/11 |              |             |                   |  |
| W2124771 | T1817   | 5.37               | 1680                       | 21A          | 6             | 397                | 6.26                | 207.4                        | PASS              | 07/02/11 |              |             |                   |  |
| W2125075 | T2190   | 5.36               | 1680                       | 21A          | 7             | 395                | 8.89                | 204.5                        | PASS              | 14/01/11 |              |             |                   |  |
| W2125084 | T2190   | 5.38               | 1670                       | 27A          | 7             | 332                | 6.37                | 203.6                        | PASS              | 14/01/11 |              |             |                   |  |
| W2125111 | T2190   | 5.37               | 1700                       | 21A          | 8             | 324                | 7.85                | 207.9                        | PASS              | 14/01/11 |              |             |                   |  |
| W2125165 | T2190   | 5.34               | 1700                       | 14B          | 8             | 339                | 7.51                | 205.1                        | PASS              | 14/01/11 |              |             |                   |  |
| W2125246 | T2190   | 5.34               | 1700                       | 21A          | 7             | 393                | 7.58                | 202.0                        | PASS              | 14/01/11 |              |             |                   |  |
| W2125300 | T2190   | 5.36               | 1680                       | 21B          | 9             | 410                | 7.03                | 202.6                        | PASS              | 14/01/11 |              |             |                   |  |
| W2125415 | T2190   | 5.37               | 1670                       | 30A          | 7             | 403                | 6.67                | 206.6                        | PASS              | 14/01/11 |              |             |                   |  |
| W2125674 | T2190   | 5.35               | 1710                       | 21A          | 8             | 334                | 7.47                | 206.3                        | PASS              | 14/01/11 |              |             |                   |  |
| W2125682 | T2190   | 5.34               | 1700                       | 21A          | 7             | 335                | 7.23                | 205.9                        | PASS              | 14/01/11 |              |             |                   |  |
| W2125727 | T4111   | 5.35               | 1700                       | 21A          | 6             | 386                | 6.78                | 207.5                        | PASS              | 14/01/11 |              |             |                   |  |
| W2125721 | T4111   | 5.37               | 1680                       | 21A          | 8             | 390                | 6.73                | 206.9                        | PASS              | 14/01/11 |              |             |                   |  |
| W2125791 | T4111   | 5.35               | 1680                       | 21A          | 8             | 411                | 6.06                | 209.5                        | PASS              | 07/04/11 |              |             |                   |  |
| W2125771 | T2064   | 5.34               | 1680                       | 21B          | 8             | 348                | 6.76                | 203.7                        | PASS              | 07/04/11 |              |             |                   |  |
| W2125798 | T4111   | 5.38               | 1680                       | 11B          | 8             | 358                | 8.33                | 207.2                        | PASS              | 07/04/11 |              |             |                   |  |
| W2125807 | T4111   | 5.37               | 1680                       | 27A          | 7             | 448                | 8.53                | 207.0                        | PASS              | 07/04/11 |              |             |                   |  |
| W2126027 | T4111   | 5.37               | 1710                       | 21A          | 8             | 454                | 7.51                | 207.3                        | PASS              | 07/04/11 |              |             |                   |  |
| W2126089 | T4111   | 5.36               | 1670                       | 27A          | 8             | 417                | 7.67                | 203.4                        | PASS              | 07/04/11 |              |             |                   |  |
| W2126119 | T4111   | 5.37               | 1680                       | 21B          | 9             | 416                | 8.76                | 209.2                        | PASS              | 14/01/11 |              |             |                   |  |
| W2126286 | T4111   | 5.36               | 1710                       | 27A          | 7             | 430                | 8.40                | 210.0                        | PASS              | 14/01/11 |              |             |                   |  |
| W2126306 | T4111   | 5.34               | 1730                       | 21A          | 7             | 386                | 7.53                | 210.1                        | PASS              | 14/01/11 |              |             |                   |  |

Figure C.6: Tensile test data from Bridon.

## Appendix C

|    | A    | B    | C    | D    | E    | F    | G    | H    | I    | J    | K    | L    |
|----|------|------|------|------|------|------|------|------|------|------|------|------|
| 1  | 1680 | 1680 | 1680 | 1650 | 1680 | 1700 | 1700 | 1680 | 1670 | 1680 | 1720 | 1690 |
| 2  | 1690 | 1700 | 1710 | 1700 | 1730 | 1690 | 1690 | 1680 | 1690 | 1690 | 1720 | 1720 |
| 3  | 1690 | 1680 | 1670 | 1680 | 1690 | 1680 | 1680 | 1680 | 1650 | 1710 | 1680 | 1680 |
| 4  | 1680 | 1700 | 1670 | 1670 | 1680 | 1710 | 1710 | 1660 | 1680 | 1670 | 1690 | 1690 |
| 5  | 1680 | 1660 | 1700 | 1680 | 1730 | 1660 | 1660 | 1700 | 1680 | 1670 | 1700 | 1680 |
| 6  | 1700 | 1690 | 1690 | 1710 | 1720 | 1690 | 1690 | 1660 | 1700 | 1690 | 1690 | 1690 |
| 7  | 1670 | 1670 | 1730 | 1660 | 1690 | 1690 | 1690 | 1650 | 1690 | 1670 | 1670 | 1700 |
| 8  | 1690 | 1670 | 1680 | 1680 | 1720 | 1660 | 1660 | 1660 | 1690 | 1650 | 1650 | 1680 |
| 9  | 1690 | 1700 | 1700 | 1670 | 1710 | 1700 | 1700 | 1670 | 1660 | 1690 | 1690 | 1680 |
| 10 | 1690 | 1670 | 1700 | 1650 | 1710 | 1690 | 1690 | 1710 | 1690 | 1680 | 1680 | 1690 |
| 11 | 1710 | 1696 | 1730 | 1660 | 1690 | 1690 | 1690 | 1650 | 1690 | 1710 | 1690 | 1690 |
| 12 | 1700 | 1696 | 1700 | 1670 | 1680 | 1690 | 1690 | 1690 | 1680 | 1680 | 1670 | 1690 |
| 13 | 1670 | 1707 | 1720 | 1670 | 1680 | 1690 | 1690 | 1650 | 1670 | 1700 | 1700 | 1700 |
| 14 | 1700 | 1670 | 1700 | 1670 | 1660 | 1700 | 1700 | 1680 | 1710 | 1690 | 1700 | 1700 |
| 15 | 1710 | 1670 | 1730 | 1690 | 1660 | 1680 | 1680 | 1680 | 1660 | 1720 | 1700 | 1680 |
| 16 | 1700 | 1690 | 1720 | 1680 | 1710 | 1680 | 1680 | 1670 | 1700 | 1700 | 1690 | 1690 |
| 17 | 1690 | 1680 | 1720 | 1650 | 1710 | 1690 | 1690 | 1650 | 1650 | 1700 | 1670 | 1680 |
| 18 | 1680 | 1700 | 1720 | 1670 | 1700 | 1670 | 1670 | 1680 | 1660 | 1700 | 1710 | 1660 |
| 19 | 1700 | 1690 | 1720 | 1670 | 1720 | 1690 | 1690 | 1680 | 1680 | 1650 | 1700 | 1690 |
| 20 | 1690 | 1690 | 1690 | 1680 | 1680 | 1690 | 1690 | 1690 | 1690 | 1690 | 1700 | 1700 |
| 21 | 1710 | 1710 | 1690 | 1660 | 1670 | 1670 | 1670 | 1710 | 1690 | 1670 | 1690 | 1690 |
| 22 | 1680 | 1690 | 1700 | 1700 | 1680 | 1700 | 1700 | 1710 | 1690 | 1670 | 1680 | 1700 |
| 23 | 1670 | 1670 | 1720 | 1710 | 1680 | 1700 | 1700 | 1690 | 1670 | 1700 | 1690 | 1710 |
| 24 | 1720 | 1680 | 1680 | 1680 | 1680 | 1690 | 1690 | 1700 | 1660 | 1680 | 1680 | 1680 |
| 25 | 1700 | 1660 | 1680 | 1700 | 1680 | 1680 | 1680 | 1670 | 1740 | 1680 | 1680 | 1720 |
| 26 | 1700 | 1680 | 1650 | 1680 | 1680 | 1660 | 1660 | 1680 | 1710 | 1690 | 1710 | 1690 |
| 27 | 1670 | 1680 | 1660 | 1700 | 1660 | 1690 | 1690 | 1670 | 1690 | 1650 | 1670 | 1690 |
| 28 | 1710 | 1690 | 1670 | 1700 | 1670 | 1660 | 1660 | 1710 | 1670 | 1620 | 1660 | 1660 |
| 29 | 1700 | 1690 | 1670 | 1690 | 1680 | 1660 | 1660 | 1710 | 1660 | 1650 | 1710 | 1690 |
| 30 | 1670 | 1680 | 1680 | 1670 | 1680 | 1670 | 1670 | 1680 | 1680 | 1670 | 1730 |      |

Figure C.7: Excel script of obtained tensile test data from Bridon.

|    | A                                     | B                         | C           | D                    | E                   | F | G                  | H |
|----|---------------------------------------|---------------------------|-------------|----------------------|---------------------|---|--------------------|---|
| 1  | <b>tensile strength test (hanger)</b> |                           |             |                      |                     |   |                    |   |
| 2  | fy [Mpa]                              | $\Delta(x-\text{mean})^2$ |             | sum of fy            | 605259              |   |                    |   |
| 3  | 1680                                  | 35,50035304               | 35,50035304 | <b>mean pr. tråd</b> | <b>1686 MPa</b>     |   | <b>6488,328 kN</b> |   |
| 4  | 1690                                  | 16,33600763               | 16,33600763 | sum of $\Delta$      | 119296,4            |   |                    |   |
| 5  | 1690                                  | 16,33600763               | 16,33600763 | <b>VAR pr. tråd</b>  | <b>333 MPa</b>      |   | <b>1282,42 kN</b>  |   |
| 6  | 1680                                  | 35,50035304               | 35,50035304 | <b>Areal tråd</b>    | 3848,451            |   |                    |   |
| 7  | 1680                                  | 35,50035304               | 35,50035304 | <b>STD pr. tråd</b>  | <b>18,25459 MPa</b> |   |                    |   |
| 8  | 1700                                  | 197,1716622               | 197,1716622 |                      |                     |   |                    |   |
| 9  | 1670                                  | 254,6646984               | 254,6646984 |                      |                     |   |                    |   |
| 10 | 1690                                  | 16,33600763               | 16,33600763 |                      |                     |   |                    |   |
| 11 | 1690                                  | 16,33600763               | 16,33600763 |                      |                     |   |                    |   |
| 12 | 1690                                  | 16,33600763               | 16,33600763 |                      |                     |   |                    |   |
| 13 | 1710                                  | 578,0073168               | 578,0073168 |                      |                     |   |                    |   |

Figure C.8: Statistical interpretation of the obtained tensile test data.